MARTIN MARIETTA ENERGY SYSTEMS LIBRARIES
3 4456 0361488 1

CENTRAL RESEARCH LIBRARY
DOCUMENT COLLECTION

ORNL-2935
UC-81 - Reactors-Power

FISSION-PRODUCT RELEASE FROM UO_2

W. B. Cottrell J. L. Scott
H. N. Culver M. M. Yarosh

CENTRAL RESEARCH LIBRARY
DOCUMENT COLLECTION
LIBRARY LOAN COPY
DO NOT TRANSFER TO ANOTHER PERSON
If you wish someone else to see this document, send in name with document and the library will arrange a loan.

OAK RIDGE NATIONAL LABORATORY
operated by
UNION CARBIDE CORPORATION
for the
U.S. ATOMIC ENERGY COMMISSION

Printed in USA. Price $2.50. Available from the

Office of Technical Services
Department of Commerce
Washington 25, D.C.

LEGAL NOTICE

This report was prepared as an account of Government sponsored work. Neither the United States, nor the Commission, nor any person acting on behalf of the Commission:

A. Makes any warranty or representation, expressed or implied, with respect to the accuracy, completeness, or usefulness of the information contained in this report, or that the use of any information, apparatus, method, or process disclosed in this report may not infringe privately owned rights; or

B. Assumes any liabilities with respect to the use of, or for damages resulting from the use of any information, apparatus, method, or process disclosed in this report.

As used in the above, "person acting on behalf of the Commission" includes any employee or contractor of the Commission, or employee of such contractor, to the extent that such employee or contractor of the Commission, or employee of such contractor prepares, disseminates, or provides access to, any information pursuant to his employment or contract with the Commission, or his employment with such contractor.

ORNL-2935

Reactors—Power
TID-4500 (15th ed.)

Contract No. W-7405-eng-26

REACTOR PROJECTS DIVISION

FISSION-PRODUCT RELEASE FROM UO_2

W. B. Cottrell
H. N. Culver
J. L. Scott
M. M. Yarosh

DATE ISSUED

SEP 13 1960

OAK RIDGE NATIONAL LABORATORY
Oak Ridge, Tennessee
operated by
UNION CARBIDE CORPORATION
for the
U. S. ATOMIC ENERGY COMMISSION

MARTIN MARIETTA ENERGY SYSTEMS LIBRARIES

3 4456 0361488 1

TABLE OF CONTENTS

Foreword v

Abstract vi

1. Introduction 1

2. Model for Fission-Product Release 3

   2.1. Isothermal Conditions Without Decay 5

   2.2. Nonisothermal Conditions Without Decay 7

   2.3. Isothermal Conditions With Decay 10

   2.4. Limitations of the Model 12

3. Variables Affecting Rate of Fission-Gas Release 20

   3.1. Thermal Conductivity 20

   3.2. Porosity and Grain Growth 27

   3.3. Surface Area and Density 33

   3.4. Oxygen-to-Uranium Ratio 36

   3.5. Discontinuities 38

4. Procedures for Experimental Studies of Fission-Gas Release from UO_2 44

   4.1. Release Measured During Irradiation 46

      4.1.1. Experiments Based on Pressure Buildup 46

      4.1.2. Experiments Based on Activity Release 47

   4.2. Release Measured After Irradiation 48

      4.2.1. Puncture Tests 48

      4.2.2. Residual Fission-Product Content 48

   4.3. Postirradiation Annealing Experiments 49

   4.4. Measurement of Released Fission Products 50

5. Results of Fission-Product-Release Experiments 52

   5.1. Percentage Release and Diffusion Coefficients 52

   5.2. Activation Energy 56

   5.3. Discussion of Experimental Results 57

6. Release of Fission Products from EGCR Fuel Elements 63

   6.1. Basis for Calculations 63

   6.2. Effect of Fuel Location on Fission-Gas Release 66

6.3. Effect of Gap Between UO_2 and Cladding 68
6.4. Effect of Cladding Temperature 73
6.5. Requirements of EGCR Fuel 74
6.6. Activity Release from EGCR Fuel 76
7. The ORNL Experimental Fuel-Irradiation Program 82
7.1. Description of Fuel-Irradiation Program 82
7.1.1. LITR Irradiations 83
7.1.2. ORR and ETR Irradiations 85
7.2. Puncture Tests of LITR-Irradiated Capsules 86
7.2.1. Calculational Procedure 86
7.2.2. Calculated Diffusion Constants 91
7.3. Annealing Tests of LITR-Irradiated Capsules 93
8. Current and Proposed Research Programs 96
8.1. Determination of D′ 97
8.2. The Study of Grain Growth 98
8.3. Studies of the UO_2-Capsule Interface 100
8.4. Effects of Porosity 100
8.5. Temperature Structure During Irradiation 101
8.6. Pressure Measurements on Irradiated Capsules 101
8.7. Additional Considerations 102
9. Summary and Conclusions 103
Appendix: Calculation of Fission-Product Release from EGCR Fuel Elements 110
A.1. Temperature Distribution in the Fuel 110
A.2. Fission-Gas Release 114
A.3. Pressure Buildup in Fuel Elements 122
A.4. Partial Pressure Due to Cesium 129
References 131

Foreword

This report on fission-product release from UO_2 was written during the summer and fall of 1959 following an extensive study of existing literature and after discussions on the subject with personnel at various atomic energy installations. At the time of writing this report, it became clear that a significant amount of work on fission-gas release from UO_2 was currently under way and that much additional work was planned in existing programs. The effort to that time had served to identify the problem for subsequent experimental programs designed to obtain useful information. This report deals in particular with the identification of the problem, and, since it was completed in the fall of 1959, it does not contain the more recent information developed with the past year. Recent data on fission-product release and information on the application of this data to the Experimental Gas-Cooled Reactor may be obtained from the ORNL project literature, including both topical and progress reports.

Abstract

The information available, as of the fall of 1959, on the release of fission products from UO_2 has been studied and correlated in order to present a comprehensive and consistent interpretation of the experimental data. A discussion of the mechanism for fission-gas release, the analytical model for predicting release, the model limitations, and the parameters affecting release are included. These considerations are necessary for the prediction of the total pressure buildup in a clad UO_2 fuel element and the prediction of the activity release from a defective or unclad UO_2 fuel element.

The fuel-irradiation program of the Oak Ridge National Laboratory is reviewed, and a number of parametric studies bearing on the performance of the fuel element for the Experimental Gas-Cooled Reactor are described. For this report the emphasis has been placed on fuel elements operated at higher surface temperatures and lower external pressures than those for pressurized-water systems. Most of the experimental data have been obtained for pressurized-water systems, however, and the analytical extrapolations of these data to other conditions remain to be verified experimentally.

FISSION-PRODUCT RELEASE FROM UO_2

W. B. Cottrell* J. L. Scott***
H. N. Culver** M. M. Yarosh*

1. INTRODUCTION

Shortly after the establishment of a sizable gas-cooled reactor program in this country, the AEC delegated to the Oak Ridge National Laboratory the responsibility for much of the research and development required by this program. After an initial design study, it was concluded[1] that the first U. S. gas-cooled reactor should be a helium-cooled, graphite-moderated reactor with stainless-steel-clad, slightly enriched UO_2 fuel. Inasmuch as a fuel element of this type has not been operated at the conditions specified for this reactor, and because of the importance of the fuel element to the success of the entire program, a considerable portion of the Laboratory's research and development program is concerned directly with the fuel element. The aspect of the fuel element program which is of special concern in this report is the release of fission products from the UO_2.

The work on this problem prior to this time was centered principally at the Westinghouse Bettis Plant and the Canadian Chalk River Plant and was concerned with fuel elements for use in pressurized-water reactors. Thus, with few exceptions, investigations were concerned with fuel which operated in-pile at relatively low surface temperatures (~400°C) and with cladding materials which were designed for relatively high (up to 2000 psi) external pressures. Both of these conditions are significantly different in a gas-cooled reactor.

In its program on gas-cooled reactor fuel elements, the Oak Ridge National Laboratory is undertaking an extensive materials research and development program. The principal purpose of the report is to summarize

---

*Reactor Projects Division

**On assignment from Tennessee Valley Authority

***Metallurgy Division

the current status of the knowledge of fission-product release from UO_2. In carrying out this objective the authors have reviewed the literature pertinent to fission-product release from UO_2 and have formed opinions as to the validity of various data and their applicability to gas-cooled reactor fuel elements. A second purpose is to ascertain a reasonable basis upon which to estimate the fission-product release from UO_2 fuel elements in gas-cooled reactors in general and the EGCR in particular. A third purpose of this report is to review the current ORNL experimental fuel-irradiation program and to evaluate this program.

This report describes the analytical models which have been found useful in calculating fission-product release and discusses in detail the important variables which affect the release rate. A number of different experiments by which release rates have been measured are described. These experiments serve to illustrate the principal techniques for obtaining information on fission-product release. The report also includes an analytical evaluation of the release of fission products in the EGCR fuel elements based upon intuitive extrapolations of existing data. Finally, the report summarizes the current ORNL experimental program and discusses its limitations as well as the necessary extension of this program in order to provide sufficient information for the evaluation of fission-product release from UO_2 in gas-cooled reactors.

2. MODEL FOR FISSION-PRODUCT RELEASE

An acceptable model for the release of fission products from bulk UO_2 must be consistent with the following three critical observations. First, the rate of release of Xe^{133} from sintered UO_2 under isothermal conditions has been found[2] to be independent of the size of the fragments for materials of densities up to ~95% of theoretical. Second, it has been observed by several investigators[2-4] that the rate of release increases markedly with increasing temperature. Third, it has been noted that the rate of release increases at constant temperature as the density of the sintered UO_2 decreases.[2]

Three mechanisms of fission-gas release which have been proposed are fuel comminution, release by recoil, and release by diffusion.[3] Critical observations at temperatures above about 1500°F have indicated, however, that only release by diffusion is significant. No comminution is observed in fuel pellets after the initial thermal cracking, although fission-product release continues. Release by recoil contributes to the over-all rate of release, but this mechanism is not affected by temperature or by the density of the UO_2 compact. In instances in which the UO_2 is dispersed in a matrix material, the release is predominantly by recoil, which is a function of the particle size.[5] On the other hand, when dealing with solid UO_2 compacts, the recoil release is determined in relation to the geometric surface area. The diffusion mechanism is thus the only one that will account for the experimental observations, and, as will be shown in subsequent chapters of this report, the diffusion model describes the observed data rather well under most conditions.

The fact that the rate of fission-product release from bulk UO_2 is independent of the sample size indicates that there are interconnected pores within pellets of densities up to 95% of theoretical. That this is indeed the case has been amply demonstrated by comparisons of the bulk and immersion densities of pellets and by surface area measurements.[3] The total surface areas of pellets measured by the Brunauer, Emmett, and Teller (BET) adsorption method was found to exceed the geometric

surface areas by an order of magnitude, even for 95%-dense material.[3] Surface area measurements of UO_2 fuel bodies fabricated by different techniques at the Oak Ridge National Laboratory (see Sec. 4.2) have shown that the ratio of the total surface area to the geometric surface area varies between 4 and 120 for pellets of 95% theoretical density. The reason for the variation is not known, but the data indicate that in some pellets, at least, there are open pores.

A two-stage process has been proposed by both Booth[6] of Chalk River and Lustman[7] of Westinghouse to explain known facts concerning the rate of release of fission products from sintered UO_2 bodies. According to this process the rate-controlling step is activated diffusion from the oxide lattice to the open pores. It is assumed that the rate of permeation through the pore structure is sufficiently rapid to be ignored in considerations of the release rate. This process is now generally accepted as the most reasonable model for the release of fission products from UO_2.

The model has been treated mathematically[6,7] by assuming that a UO_2 pellet or powder can be represented by uniform spheres of theoretical density with the same total surface area-to-volume ratio as that of the pellet. The equivalent sphere of radius a (cm) for a pellet of total surface area S (cm^2/cm^3), whose density is the fraction d of the theoretical density, is described by the equation

$$a = \frac{3d}{S} \quad . \tag{1}$$

Thus mathematical solutions of Fick's second law[8] for a sphere of radius a, with appropriate boundary conditions, should represent the rate of release of fission products from UO_2 with equivalent physical properties. An implicit assumption in the model is that no closed pores exist within the pellets.

The mathematical solutions for several cases are of importance. In all cases it is assumed that the fission-product concentration is zero at the surface of the sphere. This assumption is in agreement with

experimental data[3] which indicate that argon, krypton, and xenon are not soluble in UO_2.

2.1. Isothermal Conditions Without Decay

Experiments for investigating the release of fission products under isothermal or nearly isothermal conditions may be conducted in two ways. One method is to irradiate the fuel material at a low temperature (less than 1000°F) i.e., a temperature at which the loss by diffusion is negligible, and then to anneal the material at elevated temperatures out of pile. The fission products which escape are collected, and the rates of fission-product release are measured at different temperatures. The second method is to irradiate a sample at an elevated temperature and to measure the rates of release of the different fission products during irradiation. Approximately isothermal conditions are achieved during irradiation by means of auxiliary heaters and low neutron-flux densities or by use of very thin samples of UO_2. Although the second method is the more direct, it is also more difficult to use because of the inherent difficulties of in-pile temperature measurement and control.

The equation which describes the rate of release of a given fission product from UO_2 during a high-temperature out-of-pile anneal following low-temperature irradiation is based on the assumption that the initial concentration of the fission product throughout the specimen is uniform. In this case the general diffusion equation is

$$\frac{\partial C}{\partial t} = D\left(\frac{\partial^2 C}{\partial r^2} + \frac{2}{r}\frac{\partial C}{\partial r}\right) , \qquad (2)$$

where C is the concentration of the fission product at radius r at time t, and D is the diffusion coefficient. This equation may be solved to determine C as a function of r and t. The fraction f of the given fission product which has been released in time t is determined by integrating the amount passing through the surface and dividing by the amount initially present. The result is given by the expression[2]

$$f = 1 - \frac{6}{\pi 2} \sum_{n=1}^{\infty} \frac{1}{n^2} \exp\left(-n^2\pi^2 Dt/a^2\right) \quad . \tag{3}$$

In Eq. (3), a is the radius of the equivalent sphere.

For values of fractional release of less than 0.7, corresponding to values of

$$\frac{\pi^2 Dt}{a^2} \leq 1 \quad ,$$

the value of f may be expressed by

$$f = 6\left(\frac{Dt}{\pi a^2}\right)^{1/2} - \frac{3Dt}{a^2} \quad . \tag{4}$$

The second term on the right is negligible for values of

$$\frac{\pi^2 Dt}{a^2} < 0.01 \quad ,$$

corresponding to values of f of ~0.10. Thus the rate of release of fission products from UO_2 under isothermal conditions should be proportional to the square root of the time for low fractional releases.

It might be concluded from Eq. (4) that the rate of fission-product release could be obtained by taking values of D from the literature and determining the radius a by a surface area measurement. Unfortunately, presently reported values of D show several orders of magnitude of scatter (see Sec. 5). There is also some question with regard to the validity of an equivalent radius obtained by a surface area measurement. Because of these uncertainties it is most convenient to determine the quantity D' (= D/a^2) as a function of temperature from data obtained in fission-product-release experiments for each batch of pellets of UO_2. Such D′ values may then be used to characterize the UO_2.

The second mathematical solution of interest is based on the assumption that the fission product under study is being generated at a constant rate B

at the time the release is occurring. In this instance, the general differential equation for diffusion is

$$\frac{\partial C}{\partial t} = D\left(\frac{\partial^2 C}{\partial r^2} + \frac{2}{r}\frac{\partial C}{\partial r}\right) + B \quad . \tag{5}$$

From the solution to Eq. (5) the amount of fission products passing through the surface up to time t is obtained by integration. When this result is divided by the total amount generated up to time t, the fraction released, f, is[6]

$$f = 1 - \frac{6a^2}{90Dt} + \frac{6a^2}{\pi^4 Dt}\sum_{n=1}^{\infty}\frac{1}{n^4}\exp\left(-n^2\pi^2 Dt/a^2\right) \quad . \tag{6}$$

For values of the fractional release f of less than 0.57, corresponding to values of

$$\frac{\pi^2 Dt}{a^2} \leq 1 \quad ,$$

the value of f is given by the approximation

$$f = 4\left(\frac{Dt}{\pi a^2}\right)^{1/2} - \frac{3Dt}{2a^2} \quad . \tag{7}$$

Again, the second term is negligible for values of

$$\frac{\pi^2 Dt}{a^2} < 0.01 \quad ,$$

and the fractional release rate is proportional to the square root of time.

2.2. Nonisothermal Conditions Without Decay

The irradiation of fuel in a nuclear reactor results in temperature gradients in the fuel both in the radial and longitudinal directions.

Therefore the equations previously discussed for estimating fission-gas release for the isothermal case are not directly applicable for the case of fuel at varying temperatures.

There are two important conditions which may be treated with regard to the temperature distribution in the fuel in an operating reactor, i.e., one in which it changes with time and one in which it does not change with time. The mathematical models for each case are discussed here.

The case in which the temperature distribution in the fuel does not change with time would exist if there were no gap between the UO_2 and the cladding. Since there would be constant power generation in the fuel, the temperature gradient in the fuel would remain constant. For this case the problem of estimating the fission-gas release consists of determining the temperature distribution in the fuel and then subdividing the fuel according to the temperature distribution and summing up the results of the solution of the isothermal problem. The equations and steps to solve this problem are:

1. Determine the flux distribution along the particular channel of interest in the reactor and, from these data, determine the heat rating or power generation in the fuel element of interest. The particular rod may then be subdivided into q smaller lengths for greater accuracy of solution of the isothermal problems. The number of subdivisions selected depends on the variation of the flux in the particular rod.

2. Determine the temperature of the cladding inner surface along the rod. For the case with no gap this also represents the UO_2 outer surface temperature.

3. Compute the temperature distribution in a radial direction in each length of rod using the information from steps 1 and 2 and the following expression if the UO_2 fuel material is in the form of a hollow cylinder:

$$\int_{T_r}^{T_b} k(T)\,dT = \frac{H}{2\pi}\left[\frac{r^2 - b^2}{2(b^2 - a^2)} + \frac{a^2}{b^2 - a^2}\ln\frac{b}{r}\right], \qquad (8)$$

where

T_r = UO_2 temperature at radial point r,

T_b = UO_2 surface temperature,

H = heat rating, Btu/hr·ft,

k(T) = thermal conductivity of UO_2, Btu/hr·ft·°F,

b = outside radius of UO_2, in.,

a = inside radius of UO_2, in.,

r = distance from center of fuel rod, in.

4. Divide the pellet into m number of shells, and compute the temperature in each shell using Eq. (8). The significance of the integral, $\int k(T)dT$, in defining the condition of the fuel in lieu of precise knowledge of the temperature structure was first discussed by Lewis.[9] Robertson and his co-workers of Chalk River subsequently elaborated on this method in a paper[10] which defines the integral for several geometries of interest.

5. Compute the fission gas released from each shell in each pellet f_{sp}, using the equations developed for the isothermal case, i.e.,

$$f_{sp} = 1 - \frac{6}{90D'_{sp}t} + \frac{6}{\pi 4D'_{sp}t} \sum_{n=1}^{\infty} \frac{1}{n^4} \exp\left(-n^2\pi^2 D'_{sp}t\right) \quad . \qquad (9)$$

The number of atoms, n, of a particular species escaping from a shell in a given pellet is then

$$n_{sp} = f_{sp}g_{sp} \quad , \qquad (10)$$

where g_{sp} is the number of atoms generated in the shell of a given pellet. The atoms released, N, in the entire fuel rod are therefore

$$N = \sum_{s=1}^{m} \sum_{p=1}^{q} f_{sp}g_{sp} \quad , \qquad (11)$$

or the fractional release, f, from the rod is

$$f = \frac{\sum_{s=1}^{m} \sum_{p=1}^{q} f_{sp} g_{sp}}{\sum_{s=1}^{n} \sum_{p=1}^{q} g_{sp}} \quad . \tag{12}$$

The case in which the temperature distribution in the fuel changes with time would exist if there were a gas-filled gap between the UO_2 and the cladding. For this case the temperature profile in the UO_2 would be similar to that for the case described above, but, in addition, there would be an appreciable temperature differential across the gap because the thermal conductivity of the gas mixture would be low. The composition of the gas mixture would change with time as xenon and krypton were released from the fuel, and such release would cause a decrease in the thermal conductivity of the gas or an increase in the temperature in the UO_2 as the exposure time increased.

For these conditions it is necessary to solve the problem as a function of time. The solution may be obtained by dividing the exposure time into smaller time intervals and solving for the fission-gas release during each interval; the release in each interval is then used to determine a new temperature distribution which, in turn, is used to compute the fission-gas release in the following time interval. The total fission gas release is then obtained by summing the release values for the smaller time intervals. The equations needed for calculations by this method are described in detail by Rosenthal.[11]

2.3. Isothermal Conditions with Decay

The model for release of radioactive fission products from fuel material is based on the diffusion model discussed above for stable fission products, with a term λC added to account for decay of radioactive species with decay constant λ. The general diffusion equation, not including burnup, is:

$$\frac{\partial C}{\partial t} = D\left(\frac{\partial^2 C}{\partial r^2} + \frac{2}{r}\frac{\partial C}{\partial r}\right) + B - \lambda C \quad , \tag{13}$$

The solution to Eq. (13) has been reported by both Eichenberg et al.[3] and Booth[12] and is given by

$$N_i = 4\pi a^3 B \left\{ \left[\frac{D'}{\lambda} \coth \left(\frac{\lambda}{D'}\right)^{1/2} - \frac{D'}{\lambda}\right] \frac{1 - e^{-\lambda t}}{\lambda} - \right.$$

$$\left. - \frac{2}{\pi^2} e^{-\lambda t} \sum_{n=1}^{\infty} \frac{1 - e^{-n^2\pi^2 D' t}}{n^2(n^2\pi^2 D' + \lambda)} \right\} , \tag{14}$$

where

$D' = D/a^2$,

a = radius of equivalent sphere,

N_i = total number of atoms external to the equivalent sphere.

The number, n, of spheres of radius a per cubic centimeter of fuel is

$$n = \frac{1}{\frac{4}{3}\pi a^3} \quad .$$

Therefore the number of atoms released from 1 cm^3 of fuel is

$$N(t) = nN_i = 3B\left\{\left[\frac{D'}{\lambda} \coth \left(\frac{\lambda}{D'}\right)^{1/2} - \frac{D'}{\lambda}\right] \frac{1 - e^{-\lambda t}}{\lambda} - \right.$$

$$\left. - \frac{2}{\pi^2} e^{-\lambda t} \sum_{n=1}^{\infty} \frac{1 - e^{-n^2\pi^2 D' t}}{n^2(n^2\pi^2 D' + \lambda)} \right\} . \tag{15}$$

If the fractional release of radioactive species is defined as the ratio of the number of atoms external to the fuel at a particular time to the number which would exist in the fuel at that time if there were no diffusion, then:

$$f(t) = \frac{N(t)}{\left(\frac{B}{\lambda}\left(1 - e^{-\lambda t}\right)\right)} = \frac{N(t)\lambda}{B\left(1 - e^{-\lambda t}\right)} \quad . \tag{16}$$

Therefore, combining Eqs. (15) and (16):

$$f(t) = 3\left\{\left[\left(\frac{D'}{\lambda}\right)^{1/2} \coth\left(\frac{\lambda}{D'}\right)^{1/2} - \frac{D'}{\lambda}\right] - \right.$$

$$\left. - \frac{2\lambda e^{-\lambda t}}{\pi^2(1 - e^{-\lambda t})} \sum_{n=1}^{\infty} \frac{1 - e^{-n^2\pi^2 D' t}}{n^2(n^2\pi^2 D' + \lambda)}\right\} \tag{17}$$

or at equilibrium:

$$f = 3\left(\frac{D'}{\lambda}\right)^{1/2}\left[\coth\left(\frac{\lambda}{D'}\right)^{1/2} - \left(\frac{D'}{\lambda}\right)^{1/2}\right] \text{for } \left(\frac{\lambda}{D'}\right)^{1/2} > 10. \tag{18}$$

Equation (18) may be approximated by

$$f \cong 3\left(\frac{D'}{\lambda}\right)^{1/2} \quad . \tag{19}$$

2.4. Limitations of the Model

Questions can be raised concerning the diffusion model both with regard to the validity of the assumptions and the experimental applicability. The validity of the assumptions is related to the density of the UO_2, being more questionable as the density of the UO_2 increases. The model is probably accurate for powder material and for low-density pellets, except that it ignores the surface oxidation usually associated with these materials, but its use is open to question for pellets with densities above 90% of theoretical. At higher densities the actual geometry and the closed porosity play more important roles in the release mechanism. For pellets with

densities greater than 97% of theoretical, a diffusion model based on the geometry of the pellet is probably more exact than the use of the equivalent sphere, but the differences in predicted release rates would be small. Since this innovation also ignores the closed porosity, little would be gained by its introduction.

Some of the factors leading to the inexactness of the diffusion model for 95%-dense UO_2 pellets are illustrated by the microstructure of Fig. 2.1, which shows a UO_2 pellet manufactured from UO_2 powder prepared by the ammonium diuranate process.[13] The density of this pellet is 10.40 g/cm^3 and the BET surface area is 34.3 cm^2/g. This surface area corresponds to an equivalent-sphere diameter of 2 mils, which may

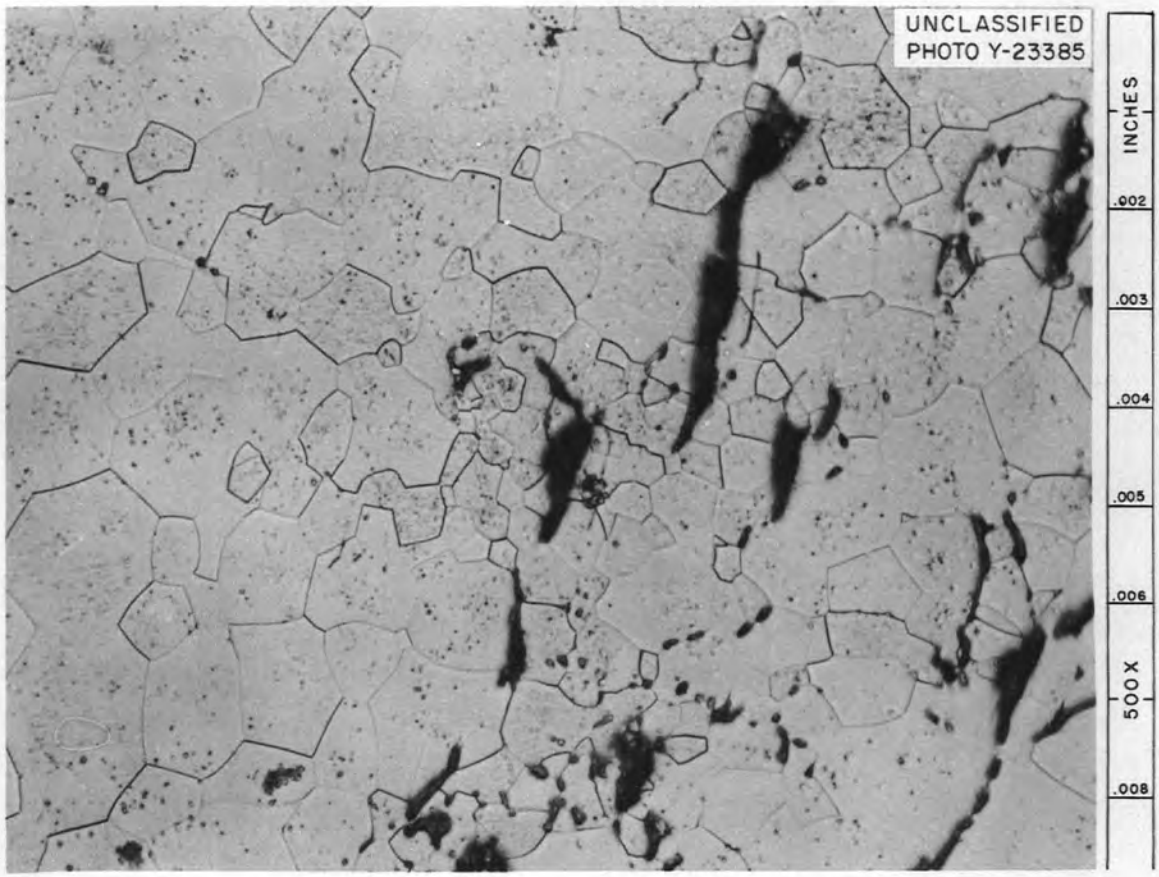

Fig. 2.1. Microstructure of a 94.8%-Dense UO_2 Pellet.

be compared with the scale associated with the photomicrograph. As may be observed, there are open pores (large dark areas) that are nonuniformly distributed and very fine closed pores that are randomly distributed throughout the grains. The average grain diameter is of the order of 1 mil. As a result of the shapes and distribution of the open pores and the existence of closed pores, it may be concluded that the diffusion model is only a rough approximation to the actual structure of a 95%-dense pellet. The existence of grain boundaries may also invalidate the model, because these grain boundaries may represent sites of accelerated diffusion and release. The effects of grain boundaries have not been studied to date.

Rosenthal[14] made calculations to evaluate the error introduced by the fuel not being made up of spherical particles, as postulated in the model, in which he assumed that the fuel bodies were composed of long cylinders in one case and flat plates in another. His calculations show that for low fractional release values, there would be no differences between the release rates for the different geometries, since under these conditions all the geometries are approximately semi-infinite diffusion-wise. For high fractional releases the amount of gas actually released from long cylinders or flat plates would be somewhat higher than predicted by the model. The differences are small, however, and it may be concluded that the geometry assumed in the model is of secondary importance.

A more significant factor that is neglected in the model is the presence of closed pores. The closed pores are important because fission products diffusing out of the UO_2 can be expected to go into the closed pores as well as the open pores. Since the closed pores are not interconnected, the fission gas that goes into closed pores will not contribute to the over-all capsule pressure. The fission gas in the closed pores could, however, create localized pressure and might cause plastic deformation of the UO_2, along with swelling, if the temperature and pressure were sufficiently high. The amount of gas within the closed pores may possibly be limited by the existence of high-resistance flow paths, such as grain boundaries, or by re-entry of the fission products into the lattice by "knock-on" events.

The error introduced in predicting fractional release values by ignoring the closed porosity has also been studied by Rosenthal.[14] The error was determined by comparing the fractional release calculated from the diffusion model with the release calculated by assuming closed porosity and including in the calculation the release to the closed pores. The results, presented in Fig. 2.2, show that the fractional release values are the same for the initial part of the exposure, but that for longer irradiation times the release estimated by ignoring closed porosity is higher than that which would actually occur. Thus a design based on an analysis which ignores closed porosity would be conservative if structural and composition changes did not also occur.

Another effect not considered in the model is the re-entry of gaseous fission products into the UO_2 by collisions with recoil atoms. This mechanism was first proposed by Lewis[15] and the events were called "knock-ons." Since the mechanism is the opposite of the release mechanism, it would serve to limit the pressure buildup within clad UO_2 fuel elements. While it is obvious that such a mechanism exists, the quantitative magnitude of the effect is uncertain. Recent evidence obtained by Davies and Kelley[16] indicates that the process might limit the pressure in a fuel element to approximately 100 atm. If this figure is correct, the mechanism may be disregarded in the design of fuel elements for gas-cooled reactors.

Another factor the diffusion model ignores is the effect of composition changes in the UO_2 as a result of the accumulation of solid fission products. These composition changes would be expected to cause changes in the diffusion coefficients of gaseous fission products. In order for the model to be correct, the concentration dependence of the diffusion coefficients should be considered. To date, however, few attempts have been made to compare release rates from UO_2 with high burnup with the release from low-burnup material. Some work of this type has been scheduled in the EGCR program.

In addition to the factors discussed above that relate to the assumptions associated with the model, there are also several important limitations associated with the way in which the model is used. The

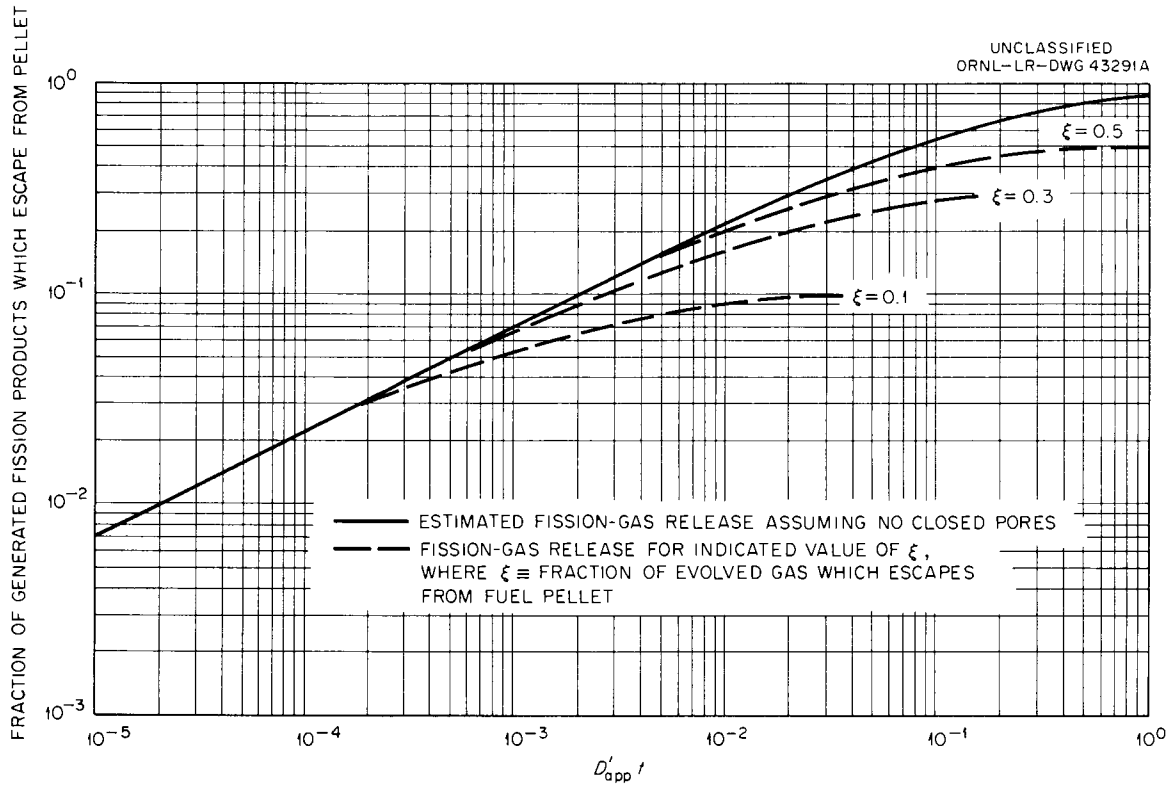

Fig. 2.2. Effect of Closed Porosity on Fission-Gas Release from UO_2.

common usage has been to make a series of measurements of the physical properties of UO_2 samples prior to irradiation or to measure release rates at very low burnups and to assume that the physical properties or the release rates do not change during irradiation to high burnups. It has already been mentioned that the release rates would be expected to change as a result of composition changes. In addition, it would be expected that the physical properties and release rates would be affected by the structural changes that would occur during irradiation. While it is possible to irradiate UO_2 at low enough temperatures for no structural changes to occur, except cracking of the UO_2 bodies, such irradiation conditions would not be of interest in a power reactor. In systems of practical importance the central temperatures in the UO_2 bodies will be above the sintering temperature (approximately 1500°C). The portions of the fuel that are at temperatures above the sintering temperature will probably undergo density increases which, in turn, will affect the ratio of open to closed pores and the total surface area. Because of temperature gradients, these structural changes will not be uniform throughout the bodies; rather, they will vary with the temperature. The diffusion model might be made applicable to those regions where sintering occurs if the proper relationship between the equivalent radius a and time were known at each temperature. Such data are not, however, available.

A qualitative picture of what happens when UO_2 undergoes sintering is given by the data of Belle and Lustman,[17] which indicate that, as sintering occurs, the density of UO_2 increases. The densification is very slow in out-of-pile sintering, but the rate may be markedly increased by the presence of a neutron flux. Associated with the density increase are changes in open porosity, closed porosity, and grain size, as shown in Fig. 2.3. Although these data apply to only one kind of oxide, the relationships are qualitatively correct for other oxides as well. For EGCR pellets, which have a density range of 94 to 96% of theoretical, both the open and closed porosity will decrease as sintering proceeds, and grain growth will occur. The decrease in open porosity will result in a decrease in the total surface area and thus a decrease

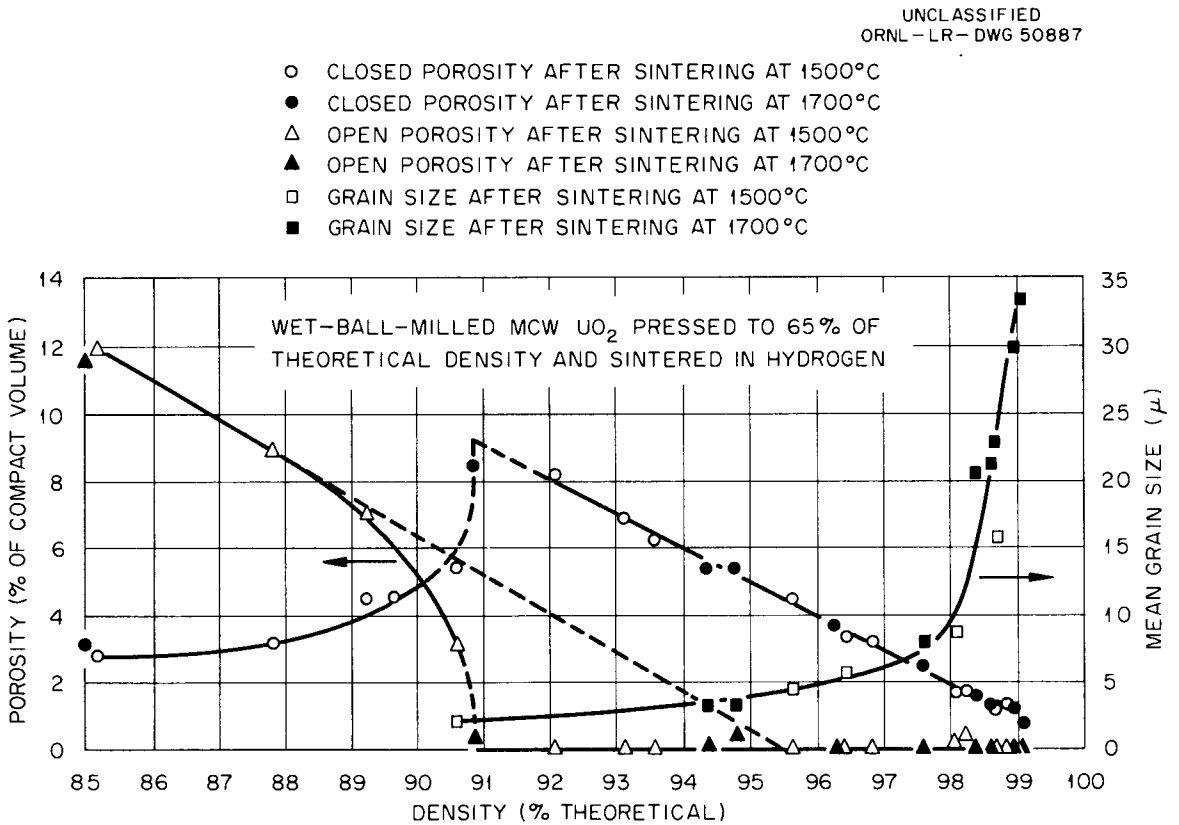

Fig. 2.3. Effect of Sintering on Porosity and Grain Size of UO_2 (From ref. 17, p. 105).

in the rate of fission-product release. The decrease in the closed porosity will be beneficial or detrimental depending on the mechanism of removal of closed pores. Grain growth may be detrimental while it is occurring because of the short-circuit diffusion of fission products along grain boundaries; however, the fission-product release rates for coarse-grained UO_2 may be expected ultimately to be the same or lower than those for fine-grained UO_2. The magnitudes of these effects are unknown, and the rates of these processes are unknown under reactor conditions.

3. VARIABLES AFFECTING RATE OF FISSION-GAS RELEASE

Application of the mathematical diffusion model described in Chapter 2 to predict the rate of release of fission products from UO_2 under reactor conditions requires specific knowledge of the physical properties of UO_2 under those conditions. The thermal conductivity of the material must be known in relation to the oxygen-to-uranium ratio, and the effect of irradiation on the thermal conductivity must be determined. Since the porosity of the material and grain growth under irradiation affect fission-product retention, these variables must be studied, and measurements of surface area and density must be made. The available information on these physical properties is discussed here.

3.1. Thermal Conductivity

The postulation that a diffusion mechanism is responsible for the release of fission products makes the value of the diffusion coefficient of prime importance. The strong temperature dependence of the diffusion process suggests the importance of accurate knowledge of the temperature at all positions within the oxide fuel. The temperature structure will, in general, be quite dependent on the thermal conductivity of the material.

A short theoretical discussion of the variation of thermal conductivity with temperature and of the theory of heat transfer in UO_2 has been given by Tennery.[18] As noted by Tennery, some of the effects of temperature on thermal conductivity are not, as yet, amenable to theoretical treatment, and, in general, values for the thermal conductivity of UO_2 have been determined by experimental methods.

An excellent discussion of the various techniques employed in making the experimental measurements has been presented by Ross,[19] and the data obtained by a number of investigators are presented in Fig. 3.1. The data were adjusted on a linear basis to represent 95%-dense material. It may be seen in Fig. 3.1 that the data of Kingery et al.[20] are well above those obtained by other investigators and that the data of Hedge

and Fieldhouse[21] are in the low range of the data presented. It has been suggested that the Hedge and Fieldhouse data are somewhat low because the UO_2 used in the conductivity determinations was cracked. Hedge and Fieldhouse obtained their data from steady-state radial-heat-flow measurements, whereas Kingery and his co-workers obtained their data by using a steady-state comparative linear-heat-flow method. The fabrication methods employed in obtaining the UO_2 specimens were also dissimilar. Scott of Harwell[22] obtained his data by measuring the radial heat loss and radial temperatures of a resistance-heated cylinder of UO_2. His measurements unfortunately covered only a narrow temperature range. He estimated the accuracy of the data at ±10%. Data obtained in a joint program by Battelle Memorial Institute[23] and Hanford Atomic Power Operations[24] are also presented in Fig. 3.1.

The spread of the values given in Fig. 3.1 can be explained by the difficulties encountered in making such measurements, the variations in the techniques used, the differences in sample fabrication methods, and the effects of variables that were, perhaps, not carefully controlled. One such variable would be the oxygen-to-uranium ratio of the UO_2 sample.

Information has been obtained at Chalk River[25,26] on the variation of thermal conductivity with the oxygen-to-uranium ratio, and data showing this variation are given in Fig. 3.2. It may be seen that the effect of the oxygen-to-uranium ratio is pronounced, at least at the low temperatures at which the measurements were made.

The reports of Hedge and Fieldhouse[21] and Kingery et al.[20] do not give values for the oxygen-to-uranium ratios of the materials they tested. Scott[22] gives a ratio of 2.00 ± 0.005 for his test specimens. The data of Nichols,[27] which were obtained at 60°C, show the thermal conductivity of material with an oxygen-to-uranium ratio of 2.16 to be only 37% of that of material with an oxygen-to-uranium ratio of 2.00. This reduction is comparable in magnitude to the reductions indicated by the Chalk River data.[25,26] Whether these reductions in thermal conductivity noted at low temperatures (approximately 60°C) would be as large at higher temperatures is not known. The effects noted here of the oxygen-to-uranium

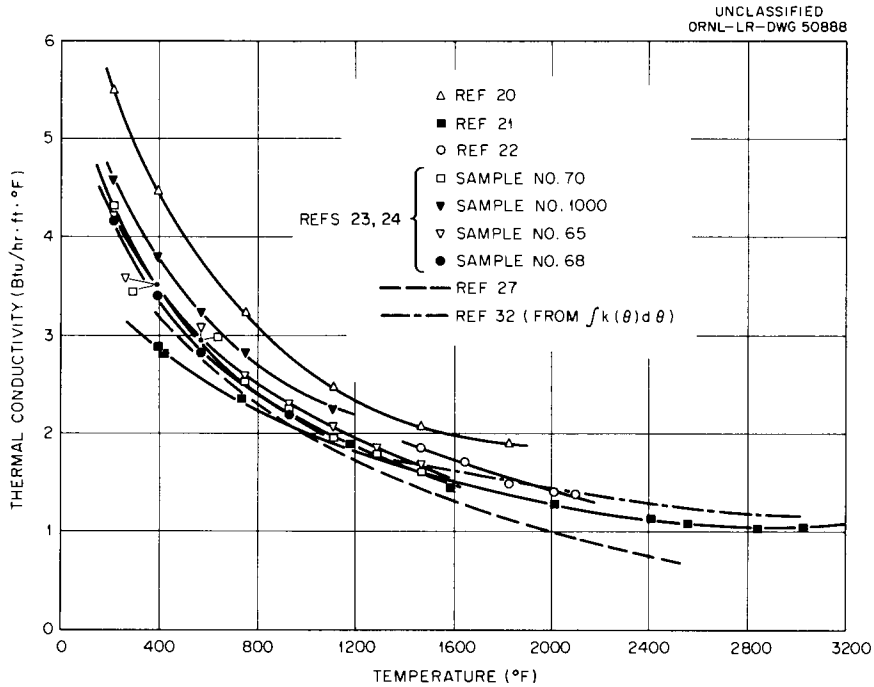

Fig. 3.1. Thermal Conductivity Data of Several Investigators for 95%-Dense UO_2. Conductivity at measured densities adjusted to conductivity for 95%-dense material on a linear basis.

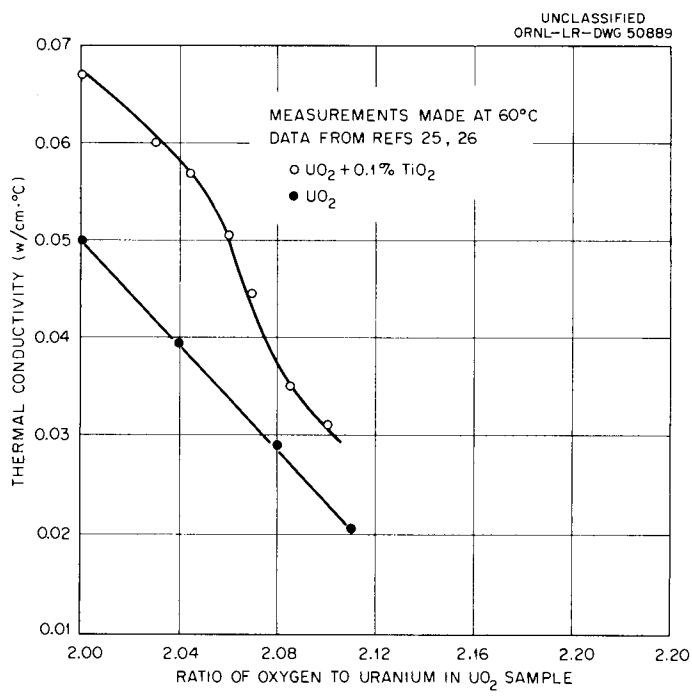

Fig. 3.2. Effect of Oxygen-to-Uranium Ratio on Thermal Conductivity of UO_2.

ratio on thermal conductivity offer, however, a strong incentive for controlling the production to obtain stoichiometric material.

The method of fabrication of the UO_2 also appears to affect the thermal conductivity. Ross at Chalk River has reported[28] a value for the conductivity of a sample of steam-sintered hydrogen-cooled stoichiometric UO_2 that is 25% lower than the conductivity of a sample of stoichiometric UO_2 which was hydrogen-sintered and cooled at 1400°C. The thermal conductivity tests carried out at Battelle[23] on a number of UO_2 specimens fabricated by Hanford also showed variations in conductivity (see Fig. 3.1) that are believed to be attributable to differences in the techniques used for fabricating the specimens. On the other hand, changes in the thermal conductivity with variations in the sintering procedures used on specimens with essentially identical oxygen-to-uranium ratios and fabrication histories are not understood. The possible effects of grain size on thermal conductivity are being investigated.[29]

Studies of the effects of irradiation on the thermal conductivity of UO_2 have been reported by Eichenberg[30] and by Chalk River.[28] The data reported by Eichenberg are "effective" in-pile conductivity values for the reactor fuel element complex employed in the test. The values include the effects of a possible gap between the cladding and the fuel, the effects of cracks in the fuel, and the effects of temperature and irradiation. The initial conductivity data reported by Eichenberg[30] for a capsule assembled with a 0.0035-in. diametral clearance between the cladding and the UO_2 indicate lower values, by a factor of ~2, than those given in a later Westinghouse report[31] for capsules having initial UO_2-to-cladding clearances of 0.0015 in. The effect of the gap on the measured thermal conductivity is being studied further (see sec. 3.5).

Conductivity data for UO_2 irradiated at temperatures estimated to be less than 500°C have been reported by Chalk River.[28] The measurements were made on the irradiated material at approximately 60°C. The data, presented in Fig. 3.3, indicate a rapid reduction in thermal conductivity to approximately 75% of the value for unirradiated material and then no further significant changes in conductivity over the irradiation range covered.

The effect of high-temperature annealing on the thermal conductivity of previously irradiated UO_2 has also been investigated at Chalk River. In these studies, the irradiated samples were annealed for 1 hr at temperatures from 400 to 1000°C, and the thermal conductivity was measured for each condition.[28] The results were expressed in terms of a recovery factor,

$$R = 100 \frac{k_{annealed} - k_{irradiated}}{k_{unirradiated} - k_{irradiated}} ,$$

which is plotted as a function of irradiation dose and annealing temperature in Fig. 3.4.

The following conclusions were drawn from the data by Chalk River personnel: (1) as the annealing temperature was increased, the fractional recovery of thermal conductivity increased for a given irradiation dose; (2) for a given annealing temperature, the fractional recovery decreased as the irradiation dose increased. Studies of the effect of the length of the annealing period and the relation of the rate of recovery to the annealing temperature and irradiation dose have not been reported. In addition, there is uncertainty as to the extent of the effect on conductivity of irradiation at temperatures in the range of annealing temperatures. It seems probable that the decrease of thermal conductivity with neutron irradiation may be less rapid at high operating temperatures and that the annealing effect of such temperatures may result in the recovery of a significant fraction of the thermal conductivity loss due to irradiation alone. In-pile and out-of-pile studies are required to resolve these uncertainties.

Scott[22] has predicted on the basis of general considerations that the effect of irradiation on thermal conductivity will not be large. He suggests an equation for the thermal conductivity of UO_2 under irradiation that yields values 20% below comparable out-of-pile values. Thermocouple measurements on a specimen being used in-pile in a fission-gas-release experiment being carried out at ORNL have shown a decrease of approximately 15% in thermal conductivity over a two-month irradiation period.

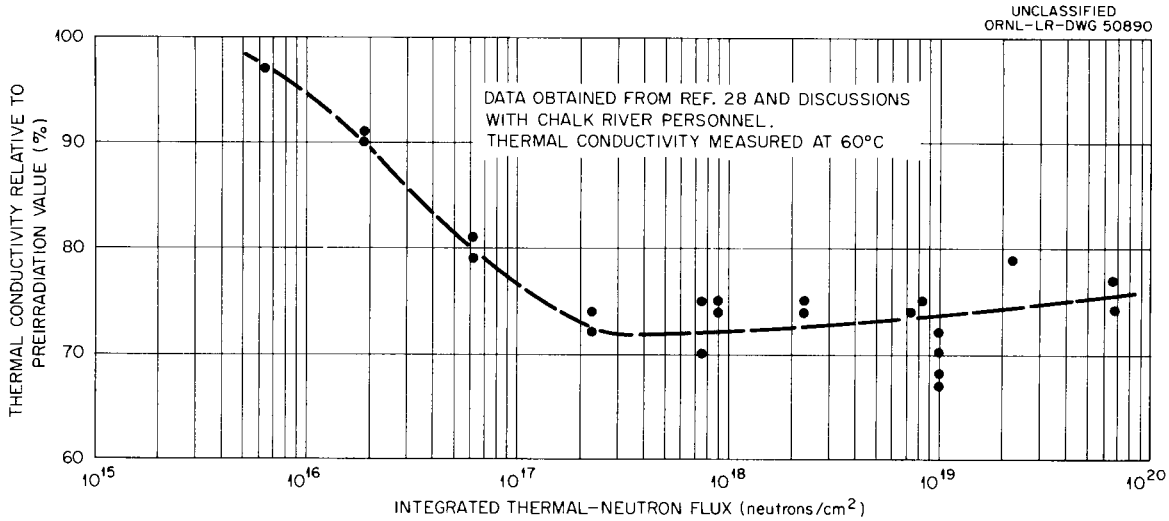

Fig. 3.3. Effect of Irradiation on Thermal Conductivity of UO_2.

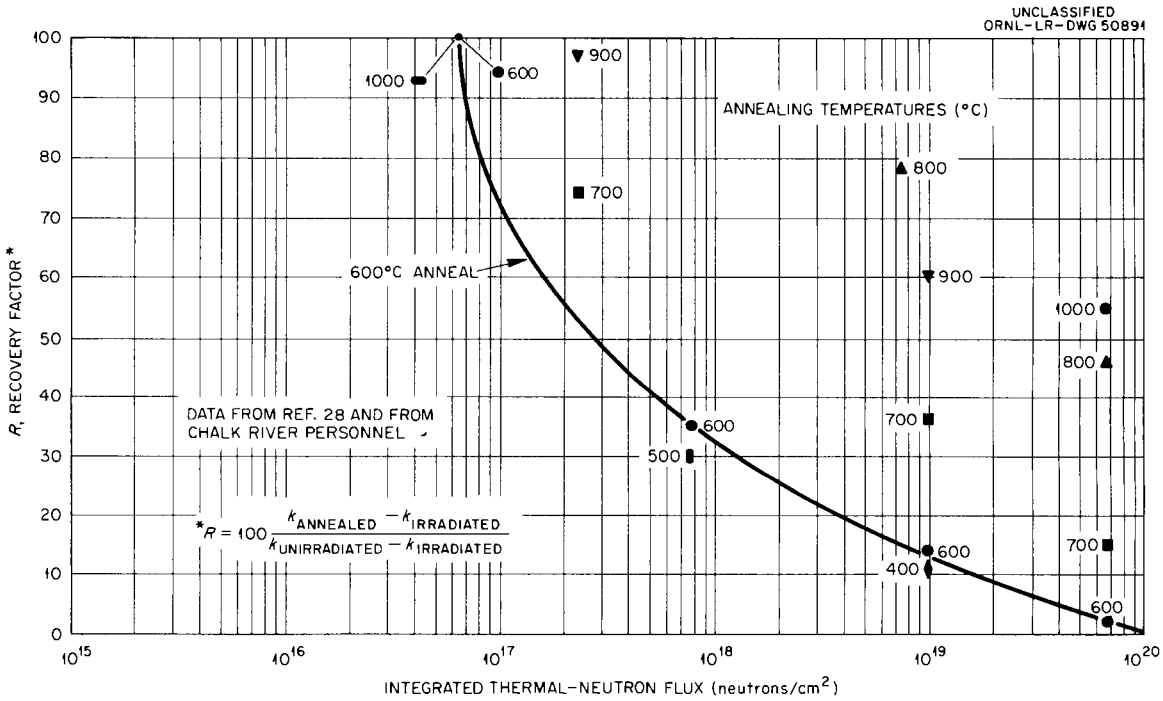

Fig. 3.4. Effect of Postirradiation Annealing on Thermal Conductivity of UO_2.

In order to avoid some of the uncertainties in determining the thermal conductivity and the temperature of UO_2 fuel, investigators at Chalk River utilize the concept of an integrated thermal conductivity.[9,32] In this concept the heat loading on a solid fuel pellet with uniform heat generation is expressed as:

$$\int_{t_u}^{t_b} k\,dt = \frac{q}{4\pi} \quad ,$$

where

t_u = UO_2 surface temperature,

t_b = central UO_2 temperature,

q = heat load per ft of length.

Similarly, for a hollow pellet with uniform heat generation,

$$\int_{t_u}^{t_b} k\,dt = \frac{q}{4\pi} - \frac{qb^2}{2\pi(a^2 - b^2)} \ln \frac{a}{b} \quad ,$$

where

a = outer radius of pellet,

b = inner radius of pellet.

Since the heat loading can be measured, the value of the effective conductivity integral can be determined. The value of the integral is a function of the heat loading on the fuel. In order to determine a value for the thermal conductivity it is necessary to establish the value of the integral for known values of the limits of integration. Personnel at Chalk River established for their geometry at a measured surface temperature the value of the integral for a melting temperature at the pellet center, for an assumed grain-growth temperature, and for a condition in which the UO_2 temperature was measured by a thermocouple. This established the relation

$$\int_{\theta_1}^{\theta_2} k(\theta)d\theta \text{ vs } \theta \quad ,$$

and from this relation the value of $k(\theta)$ could be determined. The results of such a determination are plotted on Fig. 3.1 as data from ref. 32. The data agree reasonably well with some of the other conductivity values established by direct measurement.

It is interesting to note that the use of $\int k(\theta)d\theta$ to establish a function from which the thermal conductivity can be determined assumes a continuous conductivity function across the test element. Actually, an effective conductance is determined and thence the conductivity across the material under actual in-pile conditions. The fact that the results of such a determination agree reasonably well with out-of-pile conductivity measurements suggests that no serious deterioration of the conductance of the material under reactor conditions occurs; that is, the combined effects of neutron irradiation, high temperatures, and pellet fracture do not materially affect the gross conductivity. The variance of this conclusion with the results of early effective conductivity studies reported by Westinghouse may be reduced when additional data become available.

The variations of the data obtained in out-of-pile conductivity measurements are more difficult to reconcile than are the differences between out-of-pile conductivity data and in-pile effective conductivity data. When it is considered that irradiation may change the conductivity on the order of 25%, that annealing may effect recovery of up to 100%, and that the effects of cracks and gaps in the test element are unknown, the degree of agreement indicated in Fig. 3.1 between the out-of-pile and the effective in-pile conductivity data is surprising. Additional thermal conductivity measurements on irradiated UO_2 are being carried out at BMI, but no data are available at present.

3.2. Porosity and Grain Growth

The mathematical model of Chapter 2 for diffusion of fission products from sintered UO_2 postulated an oxide lattice with extensive open pores. It was theorized that the open pores would permit rapid fission-gas release after relatively slow diffusion from the oxide lattice.

Examinations of sintered UO_2 have shown that closed pores or voids may also exist within the fuel body; electron micrographs have been obtained of such closed pores.[33] The changes in the open and closed porosity with the increases in density that occur during sintering were illustrated for a particular batch of UO_2 in Fig. 2.3 of chapter 2. The total volume of the closed pores may be computed from the difference between the immersion density and the theoretical density of the material.

As mentioned above, the postulated mathematical model for diffusion does not take into account the possible effect of closed porosity on the rate of release of fission gases. In order to study the effect of the closed pores as sinks for fission products, investigators at Chalk River have performed a series of crushing experiments on UO_2 material.[34,35] Pellets of the material were irradiated without heating and then subsequently ground or crushed to particles less than 1 μ in size. During the crushing operation, the fractional release of Xe^{133} was measured as a function of crushing time.

Crushing experiments were also performed on similarly irradiated pellets which had been annealed at 1400°C for periods of 1 to 72 hr. The amount of gas released upon crushing the annealed pellets was then compared with the gas released when the unannealed pellets were crushed to determine the effect of the annealing step. The results of some of the crushing experiments are shown in Fig. 3.5.

The gas that is released during the crushing operation emanates not only from the closed pores, but also from cleavage planes opened up by the crushing. The difference between the gas release from the annealed and unannealed samples should, however, represent only the diffusion of fission gas into the closed pores during annealing. The observations and conclusions from these experiments were summarized as follows:[35]

1. Gas movement to the closed pores is essentially complete after annealing for approximately 1 hr.

2. The difference curve representing the gas that diffuses into the closed pores reaches a maximum after about 100 min of crushing and

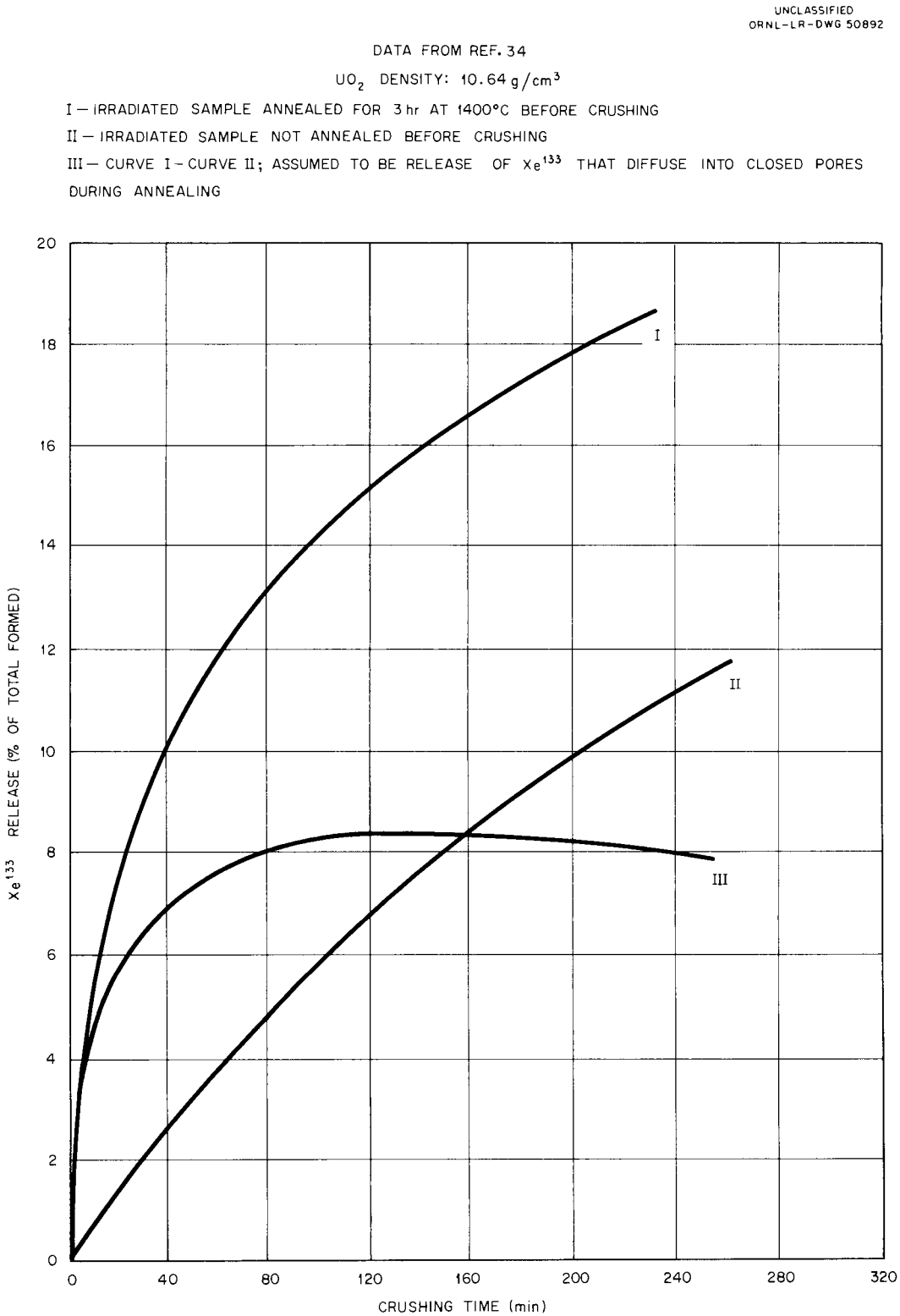

Fig. 3.5. Release of Xe^{133} Upon Crushing of Irradiated Sintered

remains approximately constant with further crushing time. The maximum difference value is approximately 10%. [The 10% value includes data not included in Fig. 3.5.]

3. The crushing operation continues to release gas both from the annealed and unannealed samples for as long as crushing has been continued in these experiments, that is, 4 hr.

4. Gas release from the irradiated material during annealing amounts to less than 2% of that generated.

There exists some difficulty in reconciling results of the above crushing experiments with analytical predictions and with results from certain of the Chalk River puncture tests.[36] It has been pointed out[35] that if the value of D' is taken to be 2.6×10^{-14} at 1400°C and it is assumed that closed pores as small as 1 μ were broken into by crushing, movement of gas to such pores should have been 80% complete after an annealing time of 2 to 3 hr, in essential agreement with the experimental results. Since the maximum gas release from the closed pores amounted to only about 10% of that generated, regardless of annealing or crushing time, it was hypothesized that a substantial fraction of the fission gas was immobilized, presumably almost immediately on formation, in pores smaller than those opened by the crushing technique used, and thus most of the fission gas remained in the fuel.

Robertson et al.[36] have discussed the differences between the results of the crushing experiments and the results of certain of the Chalk River puncture experiments. The total gas evolution from open and closed pores during long anneals (72 hr) and subsequent crushing never exceeded more than one-third of the gas present in the oxide, whereas capsules such as CRIV-X-2-r when punctured released approximately 25% of the fission gas after burnups of only 1500 Mwd/T. It is suggested[36] that the oxide material may be more effective in the trapping of fission gas during annealing than during irradiation.

Since the conductivity integral for the Chalk River puncture specimens was high, approximately 50 w/cm, the D' values in the central regions of the pellets were probably quite high, and thus the gas

evolution from the central region could be expected to be high. It seems probable that the annealing period at 1400°C would have had to cover many decades in time before the D't value in an annealing experiment would be equivalent to that of an in-pile test. Perhaps a comparison of the results for equivalent D't values would not lead to anomolies.

The low values of gas evolution from closed pores indicate that the release of fission gas from UO_2 during short-term irradiations is a weak function of the closed porosity of the material. A partial substantiation of this is the fact that reasonably close approximations of the fractional release can be calculated using a model which does not take closed porosity into consideration. Such release values are normally based on the results of short-term annealing experiments from which the diffusion coefficients are calculated and applied to the determination of the fractional release from irradiated fuel with the use of the no-closed-porosity model.

It should be noted that a diffusion coefficient obtained from an annealing experiment that does not include crushing is actually only an apparent diffusion coefficient since it ignores diffusion into closed pores. The measured D' values will be lower than the actual D' values, and, as mentioned previously, when the diffusion coefficients are applied to reactor conditions the effect of porosity is again ignored. As shown by Rosenthal,[14] the net effect of this, for short-term irradiation, is negligible, but, for long-term irradiations, the resulting prediction of gas evolution is conservative.

The role of closed pores as holdup volumes for fission gases can be investigated further by irradiation of single crystals of UO_2 and subsequent annealing and crushing experiments similar to those described above. This would permit a comparison of the gas evolved upon crushing of a sintered compact with that evolved upon crushing a single crystal containing no closed pores. Such experiments would yield additional information on the importance of closed pores and lattice defects in fission-gas evolution.

A major difficulty in evaluating the importance of closed pores in fission-gas release under reactor conditions originates from the

possibility that the porosity will change during irradiation. In work reported by Belle and Lustman,[33] variations of closed-pore volume and distribution with density changes were indicated. In general, electron micrographs showed the persistence of large pores located on grain boundaries and a reduction in smaller pore clusters located within the grains when wet-ball-milled MCW UO_2 was sintered at various temperatures. If the behavior under irradiation is similar, the volume and distribution of closed pores may be expected to change with irradiation time. The principal importance of the closed pores may lie in their relationship to grain size in the material. Runnalls[37] suggests that the large pores found along grain boundaries may serve as anchor points for the grain boundaries. A justification for this hypothesis is indicated in the grain growth and closed-porosity studies at Westinghouse. In the sintering studies carried out at Westinghouse,[38] little change in grain size occurred until the extrapolated open-porosity curve (see Fig. 2.3, chap. 2) reached zero and further densification occurred as a result of reduction in the closed porosity. During the period of reduction of the closed porosity, the grain size increased rapidly as the closed porosity decreased.

The existence of factors affecting grain growth are of particular importance because of the apparently significant effect of grain growth on fission-gas release. Data obtained at Chalk River[34] have shown that, in areas where substantial grain growth occurs, there is marked depletion of fission products. This indicates a high rate of fission-product diffusion from these areas. In addition, other studies on material of various grain sizes have shown a possible dependence of thermal conductivity on grain size.[29] British experience has indicated a dependence of grain growth on the oxygen-to-uranium ratio (see section 3.4), and this finding has been substantiated by work of other investigators.

The data of Belle and Lustman[33] on grain size as a function of sintering time have shown that the expression

$$D = Kt^n$$

in which D is the mean grain diameter, K is the temperature-dependent constant, t is time, and n is a characteristic of the material, describes the grain growth during isothermal sintering at 1500°C of the MCW oxide investigated.

The time-temperature dependence of the grain size of sintered UO_2 must be established for material of known fabrication history and known initial grain size. Determinations of the grain sizes of fabricated pellets may aid in initial characterizations of the material.

The sharply increased fission-gas release in regions of grain growth is not well understood. It has been suggested[36] that this is the effect of grain-boundary movement which in some manner forces out the gas. Whether subsequent gas release rates would be significantly higher for regions where grain growth had occurred as a result of temporary high-temperature transients is not clear. If gas release from regions of grain growth is a function of the grain-boundary movement, it might be expected that fission gas generation in large-grained areas would not be greater than in areas of small grains. The concurrent effects on gas release of changes in open porosity and density during grain-growth periods must also be considered. The need for much additional study of these relations is evident.

3.3. Surface Area and Density

Surface-area measurements of UO_2 are commonly made by using the Brunauer, Emmett, Teller (BET) method, with either nitrogen or krypton as the adsorbed gas.[39] For measurements on the pellets used in the EGCR fuel-irradiation program, krypton adsorption has been employed. The pressure sensitivity of the apparatus used for these measurements has a minimum limit that determines the minimum sample size required for accurate measurements of surface areas. For high-density material, where the ratio of actual (or BET) area to the geometric area is low, the required sample size (that is, number of pellets) is greater than for low-density material.

The variation of the ratio of actual to geometric area as a function of density is illustrated in Fig. 3.6. It may be seen that the available data for 95%-dense material vary by an order of magnitude for different pellets. If such variation is real for pellets of this density, it would be expected that the fission-gas release rates for such samples would vary approximately with the square root of the variation in the surface area. If the affect of closed pores is slight, as suggested above, the variations in surface area for a given density will be directly reflected in variations in the D' values obtained in annealing experiments.

Thus comparisons of release rates must take into account the surface areas of the pellets involved. Wide variations in D' values for sintered UO_2 of given density have been reported[2] and have been attributed to differences in fabrication history and character of the material. The rapid change in surface area with density, as indicated in Fig. 3.6 for some ORNL samples, is essentially in agreement with published data.[2,3]

In the diffusion model the diffusion path length, a, may be described in terms of one-half the distance between open pores. The value of a is determined from surface area measurements on the material. The sensitive relationship of surface area to density at approximately the 95%-dense level suggests that even slight increases in density above 95% may effect substantial improvements in D' values. Since changes in both bulk density and immersion density may occur during the fuel irradiation and since, as mentioned above, such changes may decrease the open porosity, there may be a resultant increase in the length of the diffusion path.

The effect of the pellet fracture may also be significant, particularly for high-density material. The available information[40] indicates the possibility of fracture as a result of thermal stresses that will be set up by temperature transients caused by rapid changes in the reactor power level. Such transients can be caused, for example, by a reactor scram. It is likely that such rapid power-level changes will occur early in the life of a fuel element, and thus for the effective life of the fuel element the surface areas of the UO_2 pellets will be those produced by the initial cracking. For material with an initially low ratio of BET

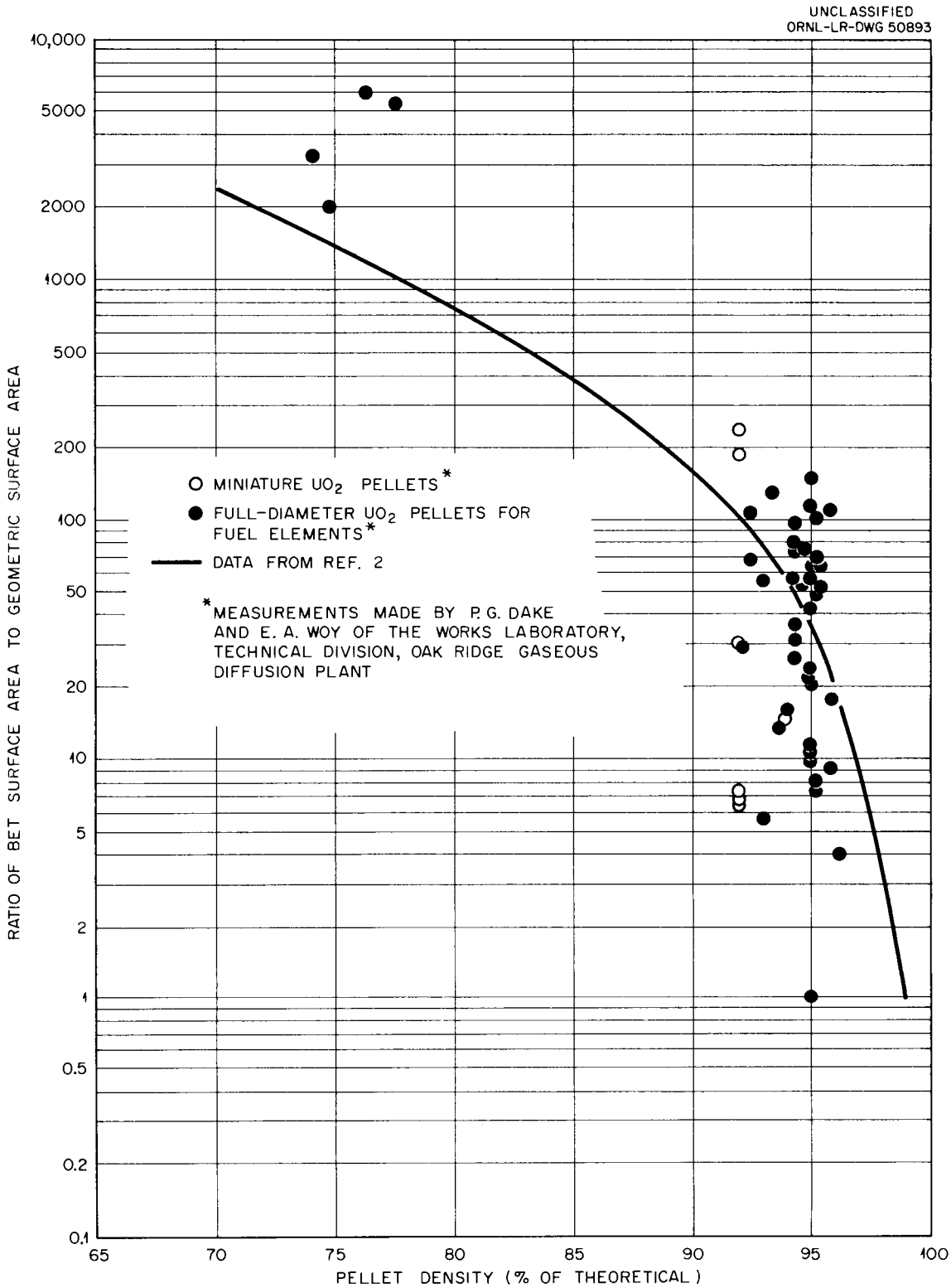

Fig. 3.6. Surface Areas of UO_2 Pellets as a Function of Density.

area to geometric area a substantial change in the ratio may occur upon cracking. Surface area measurements of irradiated samples would contribute substantially to an understanding of the effect of pellet breakup on fission-gas release.

Density measurements of UO_2 pellets are made at ORNL by the CCl_4 immersion technique and by direct weighing of the sample. The CCl_4 is presumed to penetrate the open pores. The difference between the immersion density and the bulk density obtained by weighing the sample permits a determination of the open porosity. The measurements in CCl_4 do not, however, give the real density or the total volume of the open pores. As discussed by Belle,[38] density measurements by the helium displacement techniques give higher open porosity values and lower bulk densities.

3.4. Oxygen-to-Uranium Ratio

The effects of excess oxygen on UO_2 have been studied by several investigators. In addition to the effect on thermal conductivity discussed above, it has been noted that UO_2 can usually be sintered to higher densities at lower temperatures in oxidizing atmospheres than in reducing atmospheres. Following sintering, cooling in hydrogen is required to obtain the stoichiometric oxide. It is generally believed that the higher oxygen ion mobility accounts for the improved density upon sintering in an oxidizing atmosphere.

British experience[41] has indicated that grain growth proceeds at lower temperatures in a nonstoichiometric oxide than in stoichiometric material and that, in regions where grain growth has occurred, fission-gas release is substantially increased. These findings are in agreement with those reported by Chalk River,[10,42] which show that for equivalent heating rates the fission-gas release from oxides having higher than stoichiometric oxygen-to-uranium ratios is 100 to 200 times higher than for oxides with near stoichiometric ratios. Since excess oxygen decreases the thermal conductivity, part of the increase in fission-gas release may be due to a difference in temperature structure in the material.

Lindner and Matzke[4] determined in an investigation of the diffusion of fission products from uranium oxide powders that the diffusion constant for Xe^{133} was markedly sensitive to the oxygen content of the material; for example, the diffusion constant was higher for U_3O_8 than for UO_2. In related experiments, they introduced air at 1100°C to one fuel specimen and found that the release of xenon from the specimen was higher by a factor of 50 than from a similar specimen to which air was not admitted. This result gave a difference of three orders of magnitude in the diffusion constants for the two specimens.

Excess oxygen has also been found to have a significant effect on the plasticity of UO_2. British work[41,43] indicates that material with higher than a stoichiometric oxygen-to-uranium ratio exhibits substantially greater plasticity than stoichiometric material at comparable temperatures. The plasticity of $UO_{2.06}$ at 800°C was reported to be equivalent to that of $UO_{2.0}$ at 1100°C. The effects of plastic deformation of the UO_2 on the position and migration of the fuel within the cladding are, of course, of importance in fission-gas release studies and in studies of fuel integrity in general.

Murray et al.[44] have suggested that a distillation process in which excess oxygen acts as a carrier may occur in fuel having a high oxygen-to-uranium ratio. The hot central portions of the oxide fuel tend to volatilize the higher oxides of uranium, such as UO_3, and the volatile products condense on the colder sections of the element or cladding and disassociate into UO_2 and oxygen. The oxygen rapidly diffuses into the center of the element and the process is repeated. Such a process is postulated to explain the occurrence of a central void in elements in which melting is believed not to have occurred.

Bates and Roake[45] have reported gross physical movement of UO_2 powder within irradiated fuel containers. One of the mechanisms postulated to explain powder movement was a vaporization-deposition cycle operating from the hot to the cold sections of the fuel can.

In many of the annealing experiments to date it has been noted that there is an initial large release of fission gas followed by release at

a decreasing rate; the rate becomes linear with the square root of time. Thus the graph of fractional release versus square root of time appears not to pass through zero.[2] It has been suggested that the large initial release comes from the existing very fine open pores or from fine pores opened during the initial stages of annealing. An alternate suggestion is that the initial release may be due to high oxygen-to-uranium ratios near the surface of the material.[34] In studies at Westinghouse,[46] it has been determined that oxygen is adsorbed by oxides of uranium and that the adsorption is time and temperature dependent. Thus if the material near the surface adsorbs additional oxygen, the release of fission gases from this area may be increased.

In order to determine the effects of such oxidation on diffusion coefficients, investigators at Chalk River exposed samples of UO_2 to air for times varying from 15 min to 16 days and then irradiated the samples in a vacuum.[34] Higher values of the diffusion coefficients by one to two orders of magnitude were obtained for the samples exposed to air for 10 and 16 days before irradiation than for the sample exposed for only 15 min. A sample exposed only to an atmosphere of CO_2 prior to irradiation had a D' value an order of magnitude lower than that for the sample exposed to air for 15 min.

In Westinghouse experiments the rapid release of fission gas during the initial stage of the annealing cycle did not recur in subsequent heating cycles. This fact tends to lend credence to the rapid release being a result of higher diffusion rates from oxidized areas of the sample.[46] At Chalk River, however, experiments showed that the burst releases recurred at successively higher temperatures.[35] If the initial release of fission products amounted to 20 to 30% of the total release in a 3-hr anneal, as has been the case, a D' value computed from the fractional release including the initial burst would be high by as much as a factor of 2.

3.5. Discontinuities

When stainless-steel-clad UO_2 fuel elements are fabricated, the inside diameter of the tube of cladding material is made enough larger

than the outside diameter of the UO_2 pellets for the pellets to be inserted into the tube with relative ease. The difference in the diameters results in a radial gap between the UO_2 and the cladding material, and, during irradiation, heat is transferred across the gap by radiation and conduction. One of the uncertainties associated with predicting fuel element performance is due to this gap; the existence of the gap will cause an increase of the temperature in the UO_2 and the increased temperature will lead to greater gas evolution and higher pressure buildup.

Although the initial width of the gap may be appreciable (>1 mil), several factors will tend to reduce the gap during irradiation. The temperature gradient in the fuel will be such that the resultant thermal stresses will cause the UO_2 to crack and expand. Although the coefficient of thermal expansion of stainless steel is somewhat greater than that of UO_2, the UO_2 will be at a sufficiently higher temperature for the total expansion of the UO_2 relative to that of the stainless steel to cause a decrease in the gap width. Furthermore, at high temperatures, stainless steel cladding will creep as a result of the initial pressure differential across it. It is important in the design of fuel capsules that the initial clearance between the UO_2 and cladding be small enough to prevent wrinkling[47] when the cladding collapses onto the UO_2. To ensure uniform collapse of the cladding onto the UO_2 in EGCR fuel elements, it is planned to precollapse the cladding prior to use in the reactor. Until appreciable quantities of fission gases have been released from the fuel, the cladding will probably remain collapsed onto the UO_2.

One of the major areas of uncertainty in the prediction of the effects of fission-gas release from UO_2 is the actual gap width and its effectiveness during the lifetime of the fuel element. For the EGCR calculations described in Chapter 5, various gap widths were assumed, and the thermal conductivity was considered to be a function of the composition of the gas in the capsule.

When the cladding is collapsed onto the UO_2, the effective interface resistance must be considered. The effective conductance across such mating surfaces has been studied by Cetinkale and Fishenden,[48] as well

as by others, in order to determine the contact resistance as a function of surface roughness, pressure, and medium surrounding the contacting surfaces. Use of the equations proposed by Cetinkale and Fishenden requires, however, knowledge of interface pressures, surface conditions, and other information not readily determinable for many reactor fuel element designs.

In general, interfacial resistance in a clad element of the EGCR type will be a function of (1) the relative expansion of the fuel and the cladding material, (2) the initial gap width before collapse of the cladding, (3) the surface roughness of the cladding and of the fuel material, (4) the fluid medium between the cladding and the fuel, and (5) the relative internal and external pressures on the element. Changes of the physical properties of the materials as functions of temperature and irradiation will also have an effect. Further, high temperatures within the fuel region may cause part of the UO_2 to operate in the region where plastic deformation can occur.[43]

In a recent Canadian report,[36] data are cited that indicate an increase in the central UO_2 temperature when the initial diametral clearance exceeds 2% of the fuel diameter and the normal central UO_2 temperature is 2200 to 2500°C. When the initial diametral clearance is below 2% of the fuel diameter for similar irradiation temperatures, the central temperatures will presumably be held down by interfacial contact that will reduce the contact resistance or gap effect. Reference is made to data to be published which indicate in a similar way a dependence of the central temperature on interfacial pressures and, for certain specimens, a relative dependence of the fuel temperature on the composition of the gas in the element. It should be pointed out that the data referred to were obtained in a pressurized-water loop at 100 psi and that the relative sheath and fuel temperatures in these tests would not be similar to those for a gas-cooled element.

The conclusion that the diametral clearance must be equal to 2% or more of the fuel diameter before an effect of the gap on the central temperature can be detected may be interpreted in terms of thermal

expansion of the UO_2 to 1.02 times the initial diameter. The calculated uniform temperature required for such expansion was 1700°C for central temperatures of 2200 to 2500°C. This value appears to be quite high and could be indicative of circumferential gaps in the fuel element that might give apparent expansions in excess of the actual expansion or an indication of radial cracks and outward movements of the oxide. The effect on the central UO_2 temperature will, of course, be dependent on the relative position of any circumferential gaps within the fuel element.

Canadian experiments have indicated that initial fuel-to-cladding gap widths from 0.003 to 0.014 in. have no effect on the surface temperatures of solid fuel pellets 0.67 in. in diameter. Further, a sheathed pellet with a 0.017-in. gap had a measured surface temperature approximately 100°C higher than that of a specimen with an initial gap of only 0.005 in.[42] Data such as these have led to suppositions that the cracked oxide segments move out and contact the cladding and that the interfacial temperature drop then becomes dependent on interfacial pressure and the properties of the contacting surfaces.[10] Thus the predicted temperatures based on the initial clearance do not appear to be realistic unless the initial gap is large (approximately 2% of the initial fuel diameter). It should again be pointed out that these data were obtained in a pressurized-water loop and therefore cannot be directly extrapolated to other environmental conditions for the fuel element.

Measurements of effective thermal conductivities for various initial gap widths are being carried out at Westinghouse (see sec. 3.1).[46] Initial results indicate a substantial effect of gap width in disagreement with Chalk River results referred to above. Westinghouse personnel plan to investigate gap widths of 0 to 0.0035 in. using xenon and krypton atmospheres in the capsules in order to determine the sensitivity of the effective conductivity to gap widths and to gas composition.

Data obtained in early irradiation experiments in the LITR at ORNL were examined for indications of the existence and effects of gaps at operating temperatures. Design calculations indicated that gaps of 0.001 in. to 0.004 in. would exist at operating temperatures. The initial

gap required to obtain the final desired operating gap was determined by a trial and error solution using the best values available for the physical properties of UO_2 and by assuming that no pellet fractures would occur. It was found in the LITR experiments, however, that pellet fractures did occur and that the effect was a decrease in the central UO_2 temperature.

In capsules filled with helium and maintained at a constant surface temperature, there should be a detectable increase in the central UO_2 temperature as the initial helium gas becomes diluted with xenon and krypton fission gases during long burnup experiments. A report by Morrison[49] indicates that the effect of xenon and krypton on helium conductivity is sufficiently great that, even with low fission-gas release rates, a temperature effect should be detectable. Unfortunately, in most of the LITR experiments, the deterioration of the internal thermocouple with time was sufficient to mask any effect of gas composition on the UO_2 temperature.[50] The initial central pellet temperatures measured in the LITR have generally indicated the actual effect of the gap on the central UO_2 temperature to be less than that calculated by assuming a uniform continuous gap. This error is in a direction that is in agreement with the data presented in Section 6.3. The uncertainties of the temperature measurements, however, necessarily reflect on the validity of the conclusions.

Murray et al.[44] have hypothesized that cracks in the oxide material caused by thermal stresses provide additional paths for gas release and that on subsequent reactor cycling many of the old cracks resinter and new cracks form in other areas. It is thought that the release of fission gases from cracked areas probably reduces the internal stresses and that therefore any new cracking is most likely to occur in areas where fission gases have not been released. This postulated mechanism implys that thermal cycling of the fuel element may have a pumping effect on the fission gases that causes release of trapped gas through thermal cracking. The effectiveness of such a mechanism may be conveniently studied by comparing the fission-gas release from an irradiated specimen thermally

cycled out-of-pile with the fission-gas release from an identical specimen heated isothermally. Evidence exists that gross cracking of sintered UO_2 cannot be repaired by resintering of the fuel body out of pile under normal conditions; however, under irradiation, cracks have repaired in UO_2 specimens known to possess cracks. The repair process is not yet understood.[51]

4. PROCEDURES FOR EXPERIMENTAL STUDIES OF FISSION-GAS RELEASE FROM UO_2

Most experimental determinations of the release of fission products from fuel materials have involved compromises of some conditions which may be important in the release process. For example, in postirradiation annealing experiments on fuel that has been irradiated at low temperatures, the radiation environment is not present during the release and the temperatures at which such experiments can be conducted are limited. Further, this type of experiment does not introduce the temperature gradient that would exist during reactor irradiation. An experiment conducted in an experimental facility in a radiation field in which the fuel attained the desired temperature structure would overcome the objections to the annealing experiments, but such experiments would introduce additional problems. The most significant of the problems are (1) the determination of the actual temperature distribution in the fuel, (2) the evaluation of possible changes in the diffusion properties of the fuel during the irradiation, and (3) the measurement of the released fission products.

A few in-pile experiments have been conducted in which the evolved fission products were continuously monitored and the thermal gradient across the UO_2 was minimized by the use of thin UO_2 specimens or low power densities. In most in-pile irradiation experiments, however, UO_2 fuel geometries which approximate those of interest to power reactors have been used, as well as flux levels comparable to or higher than those anticipated in service. The fission-product evolution has, in general, been measured after the test specimen has been removed from the reactor. In such experiments there is a substantial temperature gradient in the fuel during irradiation, which, in most instances, cannot be determined directly but must be calculated from other experimental data.

The determination of the temperature distribution is difficult because of the inadequacy of the available temperature-measuring devices at temperatures much above 2000°F and because of uncertainties with respect to the

thermal conductivity and physical condition of the material. As a result of these uncertainties, a calculated fuel temperature distribution based on measured values of the fuel-surface temperatures is tenuous at best. The Canadian experimenters[10] have resolved this problem, to a certain extent, by the assignment of a unique temperature, 1500°C, as the lower limit for discernible grain growth in UO_2 specimens. While this may permit an approximation of the fuel temperature, the usefulness of the result is limited because grain growth is a function of time, temperature, and type of UO_2.[42,52]

Thermocouples are not presently available that will give reliable measurements of internal UO_2 temperatures at much above 2000°F, but considerable effort is being expended at ORNL[53] and elsewhere on the development of thermocouples to measure central UO_2 pellet temperatures. To date, Chromel-Alumel, platinum-platinum-rhodium, and tungsten-rhenium thermocouples have been employed with various degrees of success, and it is hoped that with some further developmental work the tungsten-rhenium thermocouple will be useful up to 4000°F.[54]

It is well known that the physical properties of the fuel change under irradiation at normal reactor conditions. Postirradiation photomicrographs have shown that cracking, grain growth, and, in more extreme instances, melting, migration by vaporization, and condensation of the UO_2 may occur. Furthermore, sintering of low-density UO_2 may be expected. None of these effects have been correlated with the release of fission products, although it is reasonable to expect that one or more may have an important bearing on the release rate.

Experiments for determining the evolution of fission products may be divided into various categories: (1) direct measurement of release during irradiation at temperature, (2) postirradiation measurement of release following irradiation at temperature, and (3) measurement of release from postirradiation annealing following irradiation at low temperature. Each of these measurement techniques has advantages and disadvantages, as discussed below. Furthermore, there are several variations of each technique which attempt to surmount one or another of the numerous experimental difficulties which surround such experiments.

With the exception of the direct measurement of capsule pressure, all experiments depend upon isotopic analysis to determine release. There are numerous variations of fission-product measurement techniques which are independent of the particular experiment in question. These techniques are also described below.

4.1. Release Measured During Irradiation

The evolution of fission products during the irradiation of an encapsulated UO_2 specimen may be observed by measurement of the pressure buildup in the capsule and by identification of the activity in the gas. At the present time, both these techniques have serious limitations; the information obtained is of value only insofar as it supplements other data on the release of fission products.

4.1.1. Experiments Based on Pressure Buildup

Capsule pressures may be calculated from (1) the quantity and amount of each gaseous or volatile fission product evolved from the fuel, (2) the temperature of the gas within the capsule, and (3) the void volume within the capsule. Since the determination of each of these quantities is hampered by uncertainties, the determination of capsule pressure on the basis of these quantities is even more uncertain. The only alternative is direct measurement of the pressure in the capsule during irradiation, since postirradiation measurements of the capsule pressure would be subject to some uncertainty, even if the capsule were heated to the operating cladding temperature, inasmuch as the UO_2 temperature distribution and volume expansion would not be simulated. In order to interpret the measured pressures, the volumes of the gas space in the capsule and in the capillary and pressure transducer must be determined. Furthermore, the temperature of the capillary and transducer must be maintained above the coldest cladding temperature in order to prevent deposition of volatile materials which would otherwise contribute to the pressure. Such pressure measurements will have more significance in the

determination of the stress in a particular fuel capsule than in the determination of diffusion coefficients of fission products.

An attempt was made by members of the Chemistry and Metallurgy Division of the Chalk River Laboratory to measure the pressure in an aluminum sheath containing 1-in.-diam cylindrical UO_2 pellets during irradiation. The apparatus is briefly described in progress reports.[55,56] In order to measure the pressure in the sheath, the inside of the sheath was connected by capillary tubing to a pressure transducer at the top of the rod. At least two separate attempts[56,57] to measure the pressure during irradiation with this device were unsuccessful because of the development of system leaks after the irradiation had begun. In the first attempt, before a leak developed, the pressure increased from an initial value of 70 to 110 psi in 2 hr. These attempts to measure pressure were subsequently discontinued in deference to other experimental work, since capsule pressure was not of prime concern in pressurized-water systems. In view of the importance of capsule pressures in gas-cooled reactor systems, however, consideration has been given to such experiments, both by ORNL and by Nuclear Development Associates, Inc., although no experiments of this type are presently scheduled.[58]

4.1.2. Experiments Based on Activity Release

The activity which diffuses from UO_2 fuel material during irradiation may be vented, purged, or swept out of the capsule, collected in some fashion, and counted. Such experiments have been employed with moderate success for determining the evolution of the noble fission-product gases. These experiments are not usually designed, however, for measuring the particulate or volatile constituents which will condense or deposit on the tubing between the capsule and the collector. Another requirement of the experiment is that the fuel geometry and temperature be such that the release by recoil does not mask the release by diffusion. Experiments of this type have been conducted at Chalk River,[34,35,57,59-62] Westinghouse,[52] and ORNL.[63-65]

4.2. Release Measured After Irradiation

Although postirradiation measurements of the amount of fission-product release are subject to interpretation, most measurements of release are made after irradiation because they can be made simply and more reliably than corresponding in-pile measurements. The amount of fission-product release may be determined either from the direct measurement of the fission products released or from measurements of the residual fission products in the UO_2. Diffusion coefficients may be determined from the fraction lost. Both these techniques, (1) postirradiation puncture tests and (2) determinations of the fission-product content of irradiated fuels, have provided pertinent information on the mechanism of release of fission products from UO_2.

4.2.1. Puncture Tests

Postirradiation puncture tests are commonly employed[10,52,63-65] for determining gas content within a fuel capsule. It is assumed that the fission products found were evolved from the UO_2 during irradiation and that D' may be calculated as described in Section 2. In a typical experiment,[63-65] irradiated capsules are taken to a hot cell, where they are punctured with a tube-piercing valve. The gas from the capsule is then allowed to flow into an evacuated system from which an aliquot is valved off into a glass bulb. The aliquot is subsequently analyzed by a gamma-ray spectrometer.

4.2.2. Residual Fission-Product Content

If the residual fission-product content of the irradiated UO_2 specimen can be determined, it may be subtracted from the quantity of fission products generated during irradiation in order to determine the amount of fission-product release. This information, together with the temperature distribution, may then be employed to determine diffusion coefficients as a function of temperature.

Although experiments of this type have not been extensive enough to provide diffusion coefficients, experimenters at Chalk River have for

some time been concerned with the determination of the distribution of fission products in irradiated UO_2[34,35,57,59-62] in connection with burnup studies. In these experiments the fuel capsule is evacuated to remove gases from the open pores of the UO_2. Selected portions of the fuel are then dissolved in nitric acid, and the gases which evolve from the solution are collected, purified, and measured. Results of such experiments reveal that the noble gases and the volatile fission products, such as cesium, are depleted from the high-temperature regions. Experiments of this type (see also sec. 3.2) have not, as yet, produced any quantitative diffusion data.

4.3. Postirradiation Annealing Experiments

In the annealing experiments, the fuel material is irradiated at some low temperature and, after removal from the radiation flux, is subjected to a thermal anneal at the elevated temperatures of interest. The fission products evolved are collected and measured, either during or following the anneal. It is implicit in such tests that the irradiation temperature be significantly lower than the annealing temperature so that the fission-product release during irradiation will not contribute significantly to the release during annealing. If the quantity of gas evolved during irradiation is significant, the fuel capsule may be evacuated before the annealing experiment is conducted. Although the fraction of fission products released during irradiation may be independently determined from a puncture test, as mentioned above, if it were necessary to puncture the capsule before the annealing experiment, all the uncertainties associated with the puncture test would be superimposed on the results of the annealing experiment. Further, it is imperative that in the various steps of the experiment the significant physical properties, such as the oxygen-to-uranium ratio, remain unchanged, since the changes could significantly affect the subsequent release.

Annealing experiments are widely employed[10,52,66] because thermal annealing may be conducted under closely monitored conditions and the

evolved fission products may be collected continuously. Temperatures in the neighborhood of 1400°C will release measurable quantities of gas from most fuel materials within reasonable annealing times (a few hours).

4.4. Measurement of Released Fission Products

The existence of fission products in the gas phase surrounding the UO_2 material may be indicated by (1) an increase in the pressure of an enclosed volume surrounding the fuel (or a gas-sampling system), (2) the activity either in or external to the fuel, and (3) the composition of the surrounding gas. Pressure measurements of the enclosed volume, as mentioned above (see sec. 4.1.1), do not provide data on the diffusion of specific elements, but the pressure of fission-product gas desorbed from charcoal adsorbers in the sampling system has provided a quantitative measure of the gas volume. Measurements of the composition of the gas are frequently made with a mass spectrometer if the fuel has been irradiated under conditions which would produce an adequate gas sample. Because of the limitations of these techniques, measurements of specific activities have been most extensively employed for quantitative determinations of the fission products evolved.

There are significant deviations in the detailed procedures employed at various installations when making fission-product measurements in accordance with the general experimental techniques discussed above. For example, the source of the activity in one measurement may be the gas evolved continuously from the fuel during irradiation, and, in another, it may be the residual gas released when the fuel is dissolved. The procedures and techniques used by various experimenters are summarized in Table 4.1.

Table 4.1. Techniques of Collecting and Measuring Fission-Product Gases

Experimenter	Reference	Date	Experimental Technique	Fission-Product Source	Carrier Gas	Gas Removal	Gas Sampling	Trapping Device	Method of Gas Analysis	Principle Isotopes Found
Markowitz et al.	67	July 1957	In-pile measurements at temperature	Evolved gas	Helium	Continuous	Periodic	Charcoal	Gamma-ray spectrometer	Kr^{87}, Xe^{135}
Booth et al.	68	October 1957	Postirradiation puncture test	Evolved gas	Helium	Once	Once	Charcoal	Volumetric mass spectrometer	Xe isotopes, Kr^{85}
Booth et al.	57	February 1959	In-pile measurements at temperature	Evolved gas	None	Periodic	Periodic	Capillary	Gamma-ray spectrometer	All isotopes
Stubbs and Walton	69		In-pile measurements at temperature	Evolved gas	Helium	Continuous	Periodic	Fixed volume	Gamma-ray spectrometer	Xe^{133}, Xe^{135}, Kr^{85m}
			Postirradiation annealing	Evolved gas	Helium	Once	Once	Fixed volume	Gamma-ray spectrometer	Xe^{133}, Xe^{135}, Kr^{85m}
Bostrom	52	October 1957	Adsorbed gas measurements	Residual gas					Mass spectrometer	
Bostrom	52		Postirradiation annealing	Evolved gas					Mass spectrometer	
Bates and Peake	45	April 1959	Postirradiation puncture test	Evolved gas					Mass spectrometer	Xe^{131}, Kr^{94}
Morgan and Hart	59	May 1958	Postirradiation dissolution of UO_2	Residual gas	Helium	Once	Once		Mass spectrometer	Xe, Cs isotopes
	35	July 1959		Residual gas	None	Once	Once	Charcoal	Pressure	All gaseous isotopes
	61	1958		Residual gas		Once	Once		Gamma-ray spectrometer	Xe
Sisman et al.	63	May 1959	Postirradiation puncture test	Evolved gas	None	Once	Once	Fixed volume	Gamma-ray spectrometer	
Sisman et al.	63	May 1959	In-pile measurements at temperature	Evolved gas	Helium	Continuous	Continuous	Fixed volume	Total activity	
							Periodic	Charcoal	Gamma-ray spectrometer	
Sisman et al.	64	August 1959	Postirradiation annealing	Evolved gas	Helium	Once	Once	Charcoal	Gamma- and beta-ray spectrometer	
Robertson et al.	10	June 1958	Postirradiation puncture test	Evolved nongases	None	Once	Once	Surface deposition	Gamma- and beta-ray spectrometer	
Auskern	52			Evolved gas		Once	Once			
Lindner and Matzke	4	1958	Postirradiation puncture test	Evolved gas	None	Once	Once	Fixed volume	Gamma-ray spectrometer	Xe^{133}

5. RESULTS OF FISSION-PRODUCT-RELEASE EXPERIMENTS

Experiments of the type described in Section 4 have yielded, as might have been expected, a wide range of values for both diffusion coefficients and activation energies. Inasmuch as the many parameters which affect fission-product release (sec. 3) have only recently been described qualitatively, the experimental data have not yet defined all these parameters quantitatively. Data are presented here which summarize the results of the more definitive investigation in this field.

The diffusion results are frequently expressed in terms of the diffusion rate constant, D' ($= D/a^2$), since the determination of absolute diffusion coefficients, D, from the results of many of the tests awaits the establishment of the value of a for the particular material tested. The published[52] relationship between UO_2 density and a (the radius of the hypothetical sphere from BET surface area measurements) is presumed to be valid only for the fuel material for which the relationship was derived. The inability to determine absolute diffusion coefficients has not proven particularly detrimental, because the use of D' for a particular material is sufficient for evaluation of that material; it does not, however, permit generalization of the results to include all materials. In instances in which the diffusion coefficient has been calculated from a presumed value of a, the results may be regarded as suspect.

In addition to the reported values of D', the results of many experiments on fission-product release have been given in terms of percentage release of the gas generated. The experimental data are usually compared with calculated values determined on the basis of some value of D' that was either calculated or measured in another experiment.

5.1. Percentage Release and Diffusion Coefficients

Diffusion coefficients have been calculated from rates of release of fission products from UO_2 as measured by several techniques. Markowitz, Koch, and Roll[67] used a method which involved the continuous monitoring of the fission products escaping from UO_2 samples undergoing irradiation.

Measurements have also been reported by Booth and Rymer,[2] Eichenberg et al.,[52] Auskern,[70] and Lindner and Matzke[4] of the rates of release of fission products from UO_2 at elevated temperatures out-of-pile following low-temperature irradiation. Bostrom[71] has studied the solubilities and rates of diffusion of inert gases from UO_2. Clayton[72] is currently studying the rate of thoron emanation from UO_2. A compilation of the diffusion coefficients which have been reported by these investigators is shown in Fig. 5.1.

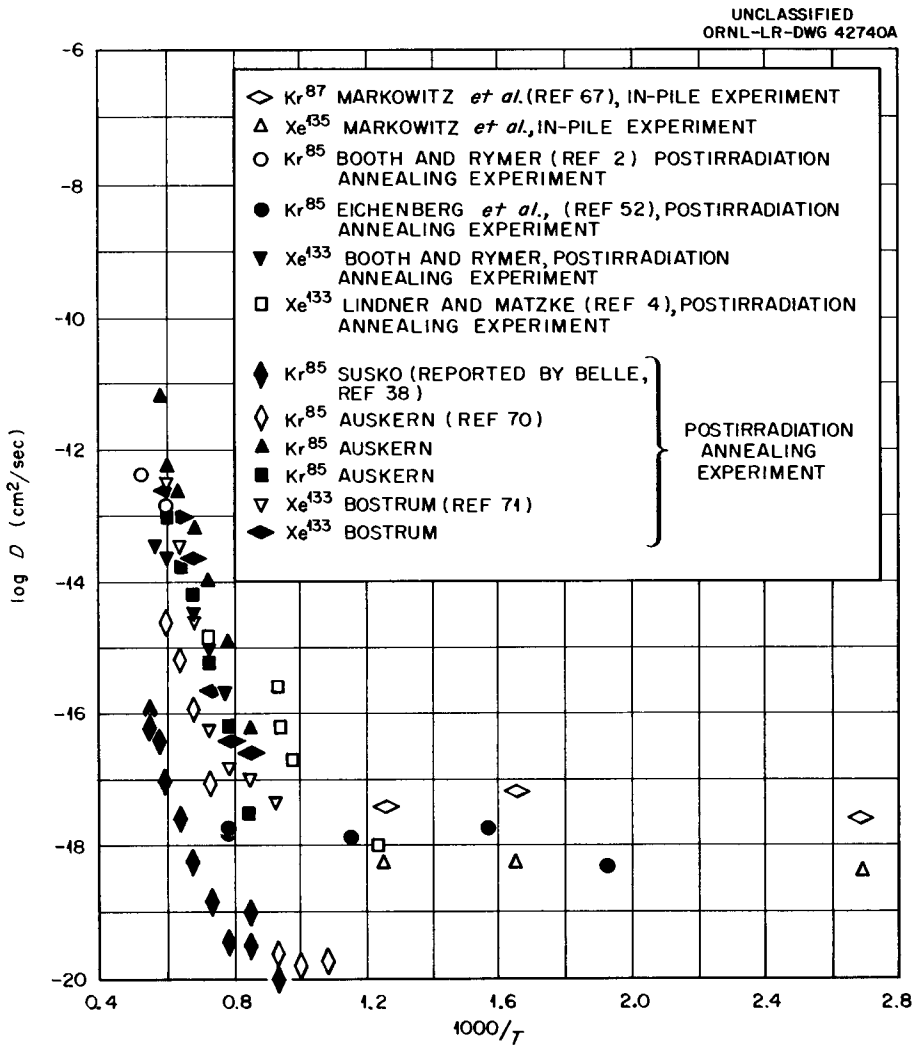

Fig. 5.1. Fission-Gas Diffusion Coefficients in UO_2.

It is most significant that, with the exception of the data from Markowitz et al., all the reported values of diffusion coefficients and activation energies were obtained from postirradiation annealing experiments. Markowitz's data were obtained from continuous in-pile measurements. Thus, although the capsule puncture tests constitute one of the most widely used techniques for investigating the irradiation behavior of UO_2, the available diffusion information on gas release is obviously regarded as inferior to the annealing data. This is undoubtedly due to the large uncertainty that is always associated with the in-pile experiments because of the inherent difficulty in determining the temperature profile of the irradiated specimen. This is indeed unfortunate, inasmuch as accurate techniques of determining diffusion coefficients from both in-pile and out-of-pile diffusion experiments are needed in order to determine whether there is a significant difference in gas release under the two conditions.

Some of the published data on gas release from capsule puncture tests are presented in Tables 5.1 and 5.2, and analyses of ORNL capsule puncture tests are presented in Section 7. The information presented in Table 5.1 includes the observed gas release from a number of WAPD capsules, together with both the Chalk River and WAPD estimates of central temperatures and calculated values of expected percentage gas release. Although the table reveals a definite correlation between the observed and the calculated values of both Chalk River and WAPD, it is not possible to conclude from these data that the correlation is better in one case than in the other. The Chalk River[10] calculated central temperatures were based on $\int k d\theta$ and the surface temperatures, whereas the WAPD[52] central temperatures were estimated from thermal conductivity and surface temperature data. Furthermore, the Chalk River[10] estimates of gas release were based on diffusion coefficients calculated from a D_0 of 8×10^{-9} cm^2/sec and an activation energy of 45.5 kcal/mole, whereas the WAPD[52] estimate was based upon a D_0 of 60 and an activation energy of 115 kcal/mole. Both groups used the radius of the hypothetical sphere calculated from the WAPD[52] density versus surface area relationship.

Table 5.1. Release of Fission-Product Gas in WAPD Capsule Puncture Tests

Specimen	Radius of Hypothetical Sphere, a (cm)[a]	Chalk River Calculated Central Temperature[b] (°C)	WAPD[c] Central Temperature (°C)	Observed Release (% of that generated)[d]		Calculated Release (%)	
				Kr^{85}	Xe^{133}	Chalk River[e]	WAPD[f]
X-1-C-6H	5.2×10^{-3}	1500	1500	0.58		1.5	1.04
X-1-G-3	4.2×10^{-3}	2300	2250	23	19	22	32.3
X-1-G-5	4.2×10^{-3}	1450–1700	2060	16.1	18	6	8.5
X-1-H-r	4.2×10^{-3}	2610–2700		27	42	31	
X-1-H-5	4.2×10^{-3}	1700–1980		8.4	11	10	
WAPD-25-L-2	4.2×10^{-3}	1600[g]	1600[h]	1.62		3	4.7
X-1-D-79S	4.2×10^{-3}	1350	1500	0.11		4	4.1
WAPD-29-1-1	2.6×10^{-3}	1000	1000[i]	0.3		0.5	0.14
WAPD-29-2-2	1.5×10^{-2}	1200	1000[i]	0.3		0.2	0.026

[a]Calculated from UO_2 density, as outlined in ref. 52.

[b]Calculated from $\int k d\theta$ and surface temperature, as outlined in ref. 10.

[c]WAPD data, as reported in ref. 52.

[d]WAPD data, as reported in ref. 10.

[e]Calculated as described in ref. 10.

[f]Calculated as described in ref. 52.

[g]WAPD value taken in absence of necessary data for calculation.

[h]Assumed because no grain growth was noted.

[i]Assumed to be consistent with value for specimen WAPD-25-L-2.

A consideration of the data and techniques employed by both groups in their estimates of gas release indicates that the Chalk River estimate should be the more accurate.

The data presented in Table 5.2 include a comparison of the measured and calculated gas-release values. The temperature data for these calculations were obtained from $\int k d\theta$ and the surface temperature, as before; however, rather than to calculate the gas release from estimated values of D_0, Q, and a, the D' value of the fuel material was determined in a separate experiment. Since the D' value could be extrapolated to cover the temperature range of the puncture experiment by using a nominal value for Q, the resulting agreement between measured and calculated release was expected to be reasonable.

Table 5.2. Release of Fission Products in Chalk River Capsule Puncture Tests[a]

Test	Specimen	Xenon Released		Calculated Central Temperature (°C)	Density (g/cm^3)	Oxygen-to-Uranium Ratio
		Calculated (%)	Observed (%)			
CR-IV-X-2f	3	7–23	5.8	925–1120	9.7 ± 0.4	2.0
	6	6–19	5.6	905–1090	9.7 ± 0.4	2.0
	7	0.3–1.0	0.4	850–1010	9.6 ± 0.2	2.0
	11	0.4–1.5	0.4	860–1020	9.6 ± 0.2	2.0
CR-V-b	UO_2-2	2.3	<0.2	1600	10.5	2.0
	UO_2-3	2.3	<0.2	1600	10.5	2.0

[a]Data taken from Tables 2 and 3 of ref. 10.

It may be noted, however, that in the evaluation of all the capsule data on gas release, the estimated release is singularly dependent on the calculated temperature profile of the fuel. The uncertainty of 100 to 200°C in the central UO_2 temperatures in the capsule tests reported in Table 5.2 is responsible for a range in the calculated release values of a factor of between 3 and 4.

The data in Table 5.1 distinguish between fraction of xenon released and fraction of krypton released. It may be seen from examination of these data that no predominant trend favoring the diffusion of one isotope over the other exists, and in fact it is generally assumed that the two isotopes diffuse at the same rate, even though there are theoretical reasons for expecting a difference. Little or no information exists on the diffusion of volatile elements, e.g., iodine and cesium.

5.2. Activation Energy

The activation energy for diffusion of fission gases through UO_2 has been obtained by a number of experimenters. Inasmuch as the activation energy is the slope of an Arrhenius plot of log D versus the reciprocal temperature, the activation energy is independent, or less dependent than the diffusion constant, on a number of parameters which

would affect the gas released at a particular temperature. Activation energies which have been reported in the literature are listed in Table 5.3. The average of the values listed is approximately 65 kcal/mole. This value is suggested for use in making estimates of fission-gas release until more definitive results are available.

The reported values of activation energy have been either for xenon or krypton, and the existing data are not adequate to make a distinction between the two. As noted above in the discussion of capsule puncture tests, xenon and krypton are assumed to have comparable diffusion characteristics in UO_2. Much additional information is needed on the diffusion of other fission products in UO_2, and the experimental techniques will have to be considerably refined in order to distinguish any difference, assuming such exists, between xenon and krypton.

Table 5.3. Activation Energy for the Diffusion of Xenon and Krypton in UO_2

Investigators	Reference	Type of UO_2	Species Counted	Activation Energy (kcal/mole)
Booth and Rymer	2	Fused powder	Xe^{133}	45
Susko (reported by Belle)	38	97.4% dense pellets	Kr^{85}	58.5
Auskern	70	NUR powder	Kr^{85}	73.8
Auskern	70	Crushed PWR pellets	Kr^{85}	65.5
Lindner and Matzke	4	Reactor-grade UO_2 powder	Xe^{133}	34
Auskern	70	93.7% dense pellets	Kr^{85}	81
Bostrom	71	97% dense plates	Xe^{133}	80

5.3. Discussion of Experimental Results

The wide variations in the data presented in Fig. 5.1 result, in part, from the experimental problems encountered in the various studies.

Markowitz et al.,[67] used unclad UO_2 samples in their in-pile loop, and the total release included recoil as well as diffusion contributions. Only a few recoils were stopped by the helium purge gas, and almost all were embedded in the stainless steel components of the furnace used to maintain the temperature. The volatile fission products subsequently are believed to have diffused out of the stainless steel and contributed to the over-all amount released. Since moderate temperatures (1000°C) were used, the recoil loss from the UO_2 was a major part of the total release. The rate of release from the metal components was apparently sufficiently high that essentially all the recoils which entered the stainless steel were released. Since the number of recoils escaping from UO_2 is independent of temperature, the computed diffusion coefficients were also independent of temperature. The effects of recoils could be eliminated by irradiating the UO_2 at much higher temperatures or by surrounding the sample under study with depleted UO_2.

The data of Booth and Rymer[2] are possibly in error as a result of the high impurity content of the fused UO_2 used in their tests and the fact that the equivalent radius of the particles was determined by sieve measurements. Chemical analyses of fused UO_2, which indicate high carbon, nitrogen, and oxygen contents, have been obtained by several investigators. These analyses have been verified by metallographic evidence. The effects of carbon and nitrogen on the diffusion of fission products in UO_2 are unknown, but a high oxygen content has been shown[4] to result in an accelerated rate of release of Xe^{133}.

Booth and Rymer[2] assumed that the equivalent radius of their UO_2 powder was the mean sieve size. Auskern[70] has compared the equivalent radius obtained by the use of the mean sieve size with that obtained by a BET surface area measurement and has found that the latter radius is consistently a factor of 5 smaller than the former for crushed, fused UO_2 powder. This result has been verified by Thurber[73] at ORNL. Since the BET method is generally regarded as the best method for determining the equivalent radius, Booth and Rymer's value is questionable. If their value is five times too high, the true values of the diffusion coefficients would be lower by a factor of 25 than their reported values.

The diffusion coefficients of Susko which are shown in Fig. 5.1 may be in error as a result of the method by which the total surface area was determined. Instead of making surface area measurements on the particular samples used in the release rate tests, Susko assumed that the total surface area per unit volume of his samples could be determined from the surface area density relationship reported by Eichenberg et al.,[52] for samples of the same density (97.4% of theoretical) and fabricated by the same method. These data indicated that the total surface area of pellets of this density was ten times the geometric surface area. More recent data on total surface area obtained at WAPD[71] indicate that the true surface area of a 97.4% dense UO_2 pellet is close to that of the geometric surface area. Since the equivalent sphere radius is inversely proportional to the surface area, the value for the radius used by Susko could have been an order of magnitude too small. This error would make Susko's values for the diffusion coefficient two orders of magnitude too low.

The diffusion coefficients obtained by making the suggested corrections to the reported values are shown in Fig. 5.2, together with the values of Booth and Rymer[2] and those of Susko that were reported by Belle.[38] The corrections bring the data of these investigators into much better agreement, although the activation energies are different. There are still several orders of magnitude of scatter between the corrected values and some of the more recent data of Auskern[70] shown in Fig. 5.1. Additional work must be done to resolve the discrepancies.

With the exception of the data of Markowitz et al., all the values shown in Fig. 5.1 for the diffusion coefficients of fission products in UO_2 were obtained after irradiation. It is possible that diffusion coefficients for fission products are lower out-of-pile than in-pile at the same temperature. As a result of the neutron flux and of fissioning within the UO_2 lattice, an excess of interstitials and vacancies of both the oxygen and uranium ions would be expected to be present during irradiation. This excess might enhance the rate of diffusion of fission to a degree which depends on the diffusion mechanism.

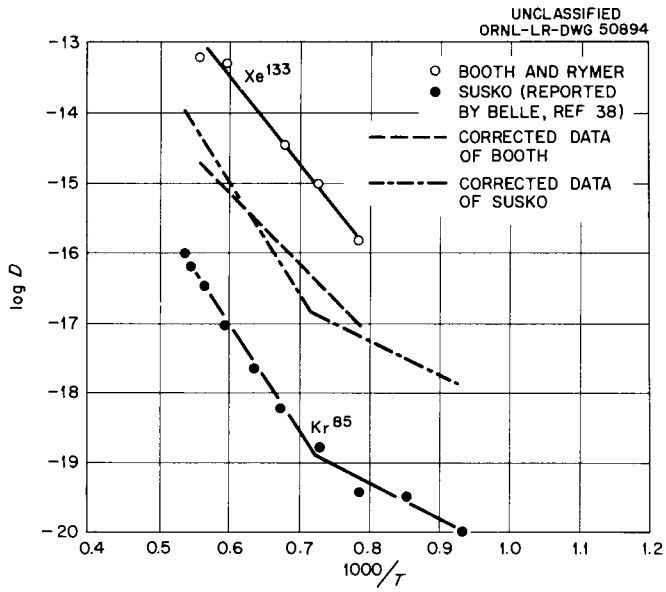

Fig. 5.2. Corrected Values of Fission-Gas Diffusion Coefficients in UO_2.

In the analysis of pressure buildup in high-temperature UO_2 fuel elements, diffusion coefficients are needed for all the volatile fission products in UO_2. Unfortunately these data have been reported only for Xe^{133} and Kr^{85}. Although it is reasonable to assume that these diffusion coefficients apply to all isotopes of xenon and krypton, it cannot be assumed that they also apply to other fission products as well. Factors which would be expected to affect diffusion coefficients are solvent and solute ionic radii (both cations and anions), the valences of the diffusing species, and the solubilities of the fission products in UO_2.

If the effects of fission products other than xenon and krypton are neglected, the pressure buildup in a given fuel element may be estimated from the data in Fig. 5.1, the BET surface area of the fuel, and the model discussed in Section 2. At the present time this approach is fraught with uncertainties as a result of the scatter in the data concerning diffusion coefficients. The scatter in the data relating BET surface area and density (Fig. 3.6) for pellets fabricated under supposedly identical conditions makes the applicability of Eq. (1) of Section 2 doubtful. Because of the uncertainties in the true values of D and a , Robertson[10] has suggested that the most suitable method of

estimating release rates is to measure directly the D' ($= D/a^2$) values for production-run pellets being used in a given reactor. Such measurements are generally made by low-temperature irradiation, out-of-pile annealing experiments.

Since D' is a function of the surface area of a given oxide, a greater spread would be expected in D' values than in values of the diffusion coefficient, D, for various UO_2 materials. Even for pellets of very high density, widely different values of D' at 1400°C have been reported, as shown in Table 5.4. These results show that D' values for 97% dense UO_2 at 1400°C vary between 5×10^{-10} and 8.8×10^{-13} sec^{-1}. Except for the ADU oxide, there is insufficient information on these materials to indicate why the variations occur. The different ADU oxides were fabricated under identical conditions, so the observed differences in D' values are probably due to the postfabrication environments.

The highest values of D' for Chalk River-ADU oxide were found in samples which had been exposed to air for several days. These results can be accounted for by assuming that the surface layers of the oxide were slowly oxidized to UO_{2+x}. The subsequent release rates of xenon and krypton would be expected to be high from the oxidation layers.

Table 5.4. D' Values for 97% Dense UO_2 at 1400°C

Oxide Manufacturer	D' at 1400°C (sec^{-1})	Remarks	Reference
Mallinckrodt	1.3×10^{-10}	PWR material used	2
Canadian Bureau of Mines	2×10^{-10}	Long sintering time used in fabrication	2
Canadian Bureau of Mines	5×10^{-10}	Standard method of fabrication used	2
Chalk River, ADU	5.2×10^{-12}	Specimen exposed to air for 15 min	34
Chalk River, ADU	1×10^{-10}	Specimen exposed to air 10 days	34
Chalk River, ADU	4.4×10^{-11}	Specimen exposed to air 16 days	34
Chalk River, ADU	8.8×10^{-13}	Specimen exposed to CO_2	34
Mallinckrodt	5.2×10^{-11}	97.5% dense UO_2 used	38

Lindner and Matzke[3] have shown that marked increases in release rates are observed when UO_2 is oxidized. It should not be concluded from these results that UO_2 pellets need to be handled in an inert atmosphere, because the volume of UO_2 which is oxidized is small. The apparent increase in release rate is, however, much greater in a short time test than one would expect from a long time test.

6. RELEASE OF FISSION PRODUCTS FROM EGCR FUEL ELEMENTS

In previous sections of this report, the many factors which influence fission-product release from UO_2 have been described, and the models used in estimating fission-product release have been given for various conditions. In this section and in greater detail in the Appendix, the factors that influence the amount of fission-product release are evaluated by computing the fractional release of the fission gases and the resulting pressure buildup inside the fuel elements from the gas release.

In order to make a study of the pressure buildup in a particular fuel rod, it is necessary to know the conditions which the fuel rod will see during its lifetime. The service conditions will vary in different reactors depending on the choice of coolant, cladding material, size of reactor, moderator, etc. The conditions chosen for the discussions which follow are based on the preliminary design of the Experimental Gas-Cooled Reactor (EGCR),[74] but the methods used are, in general, applicable to any reactor that uses UO_2 fuel. The EGCR design conditions were chosen to evaluate the performance of UO_2 at conditions typical of gas-cooled reactors, since it was considered that these conditions were more severe than those encountered in water-cooled reactors.

In addition to calculating pressure buildup in the fuel rod, an estimate is made of the activity release from a defective or ruptured rod using the diffusion models previously described. These estimates are then compared to activity release computed by escape-rate data.

6.1. Basis for Calculations

When fuel is irradiated in a reactor, the temperature of the fuel will vary appreciably in both the radial and the axial directions. Therefore, in order to calculate the fission-gas release from the fuel, the model for the nonisothermal case is used. The two cases of general interest mentioned in Section 2.2 were for (1) the temperature distribution remaining constant with time and (2) the temperature distribution varying with time. Although the first of these cases is somewhat

hypothetical, since frequent changes in reactor power will result in changes in the temperature distribution in the fuel, it is the easier of the two cases to compute. Studies of this type are illustrated in the Appendix. When the temperature distribution in the fuel changes with time, the solution to the problem is more laborious and is best done by machine calculations. The temperature distribution in the fuel will vary as a function of time in the reactor because of several factors: (1) the power in the reactor will vary with time; (2) the neutron flux will shift as the fuel is irradiated and shim rod action is initiated to maintain criticality; (3) the introduction of experimental assemblies may cause flux perturbations; (4) fuel will be shifted in the reactor in order to achieve a uniform burnup of 10 000 Mwd/MT; and (5) if a gap exists between the UO_2 fuel and its stainless steel jacket, the accumulation of xenon and krypton will cause an increase in fuel temperatures as exposure time increases. The pressure buildup in fuel elements has been calculated for some of these situations to indicate the relative importance of the more questionable conditions.

The fuel for the EGCR consists of cored pellets of UO_2 (0.705 in. o.d. and 0.323 in. i.d.) contained in 20-mil-thick type 304 stainless steel tubes with welded end caps. In a coolant channel of the EGCR there are six fuel elements, each containing seven fuel rods. The length of each rod is 26.6 in. Fuel is loaded into 216 channels of the core.[74]

An average burnup in the fuel of 10 000 Mwd/MT has been assumed for these studies. In order to attain this burnup during reactor operation, a new element is irradiated in one of the three top positions (1–3) in a channel for a specified time and is subsequently moved in corresponding order to positions 4-6 which are in the lower portion of the core in the same channel. The exposure time in a particular channel will depend upon the neutron flux in that particular channel. Since the greatest pressure buildup in the fuel will occur in those fuel elements which have the highest heat generation and UO_2 temperatures, studies of fuel element performance have been limited to the fuel in the hottest channel. The ratio of the core peak-to-average flux in the radial direction is assumed

to be 1.37. Therefore, although the method of calculation discussed in this section will apply to all the fuel rods in the reactor, the particular calculations of fuel performance will apply to only a small fraction of the 9072 rods in the EGCR.

The conditions which are assumed in the following calculations for estimating the fission-gas release from the fuel in the EGCR are shown in Fig. 6.1 and are tabulated in the Appendix. These conditions are based on data given in the EGCR hazards report[74] and are representative of conditions which are expected during EGCR operation.

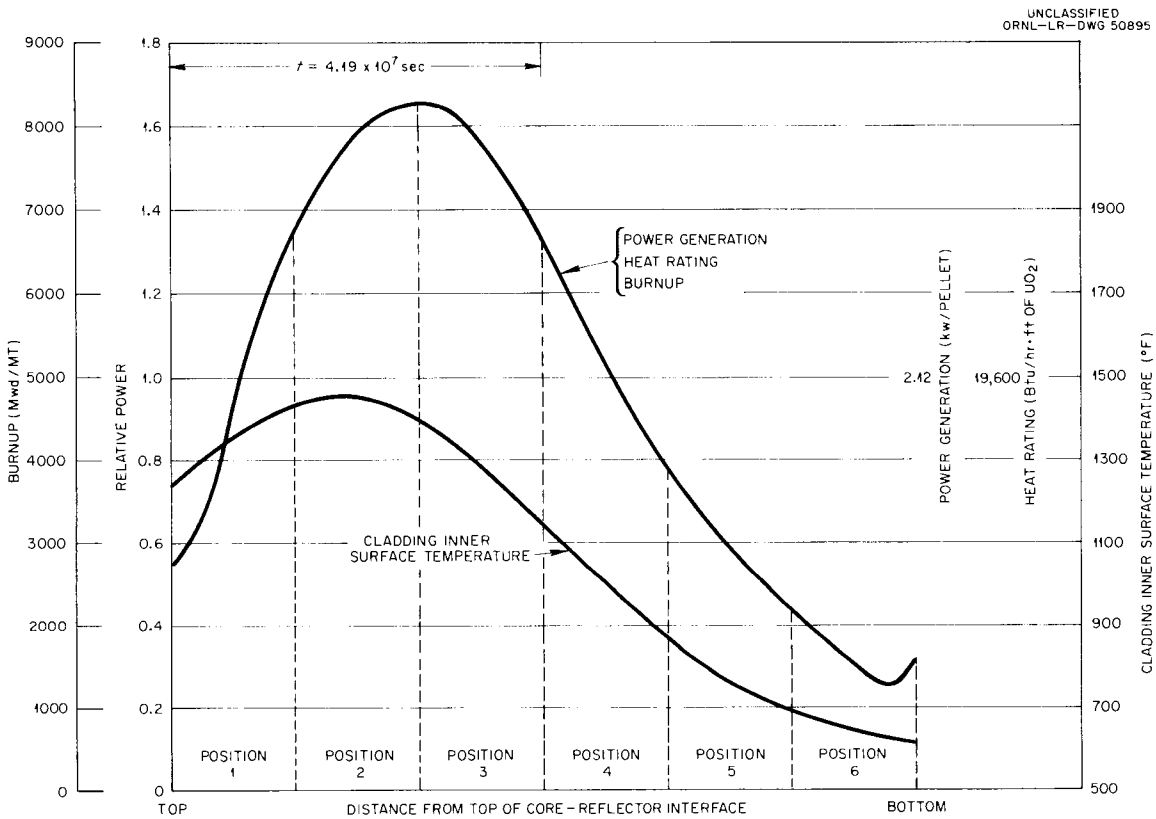

Fig. 6.1. Axial Power and Temperature Distribution in EGCR Central Channels.

6.2. Effect of Fuel Location on Fission-Gas Release

The fission-gas release and pressure buildup in the fuel rods in various positions along the hot channel were investigated to determine which position resulted in the greatest pressure buildup. For these calculations it was assumed that no gap existed between the UO_2 and the cladding and that the power generation and inner cladding temperatures were as shown in Fig. 6.1. The results of this study, presented in Figs. 6.2 and 6.3, indicate that the fuel in position 2 will always have the

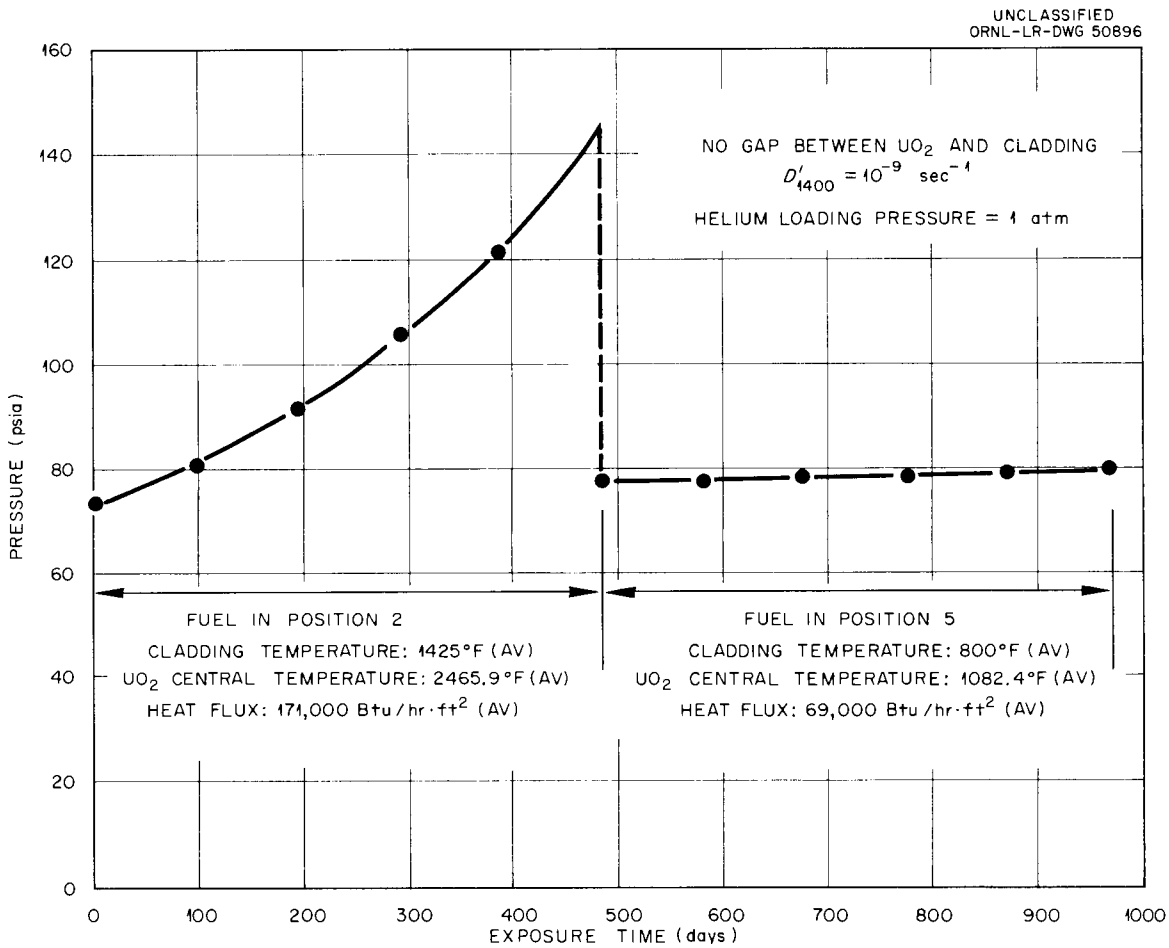

Fig. 6.2. Pressure Buildup in EGCR Fuel Elements in Positions 2 and 5.

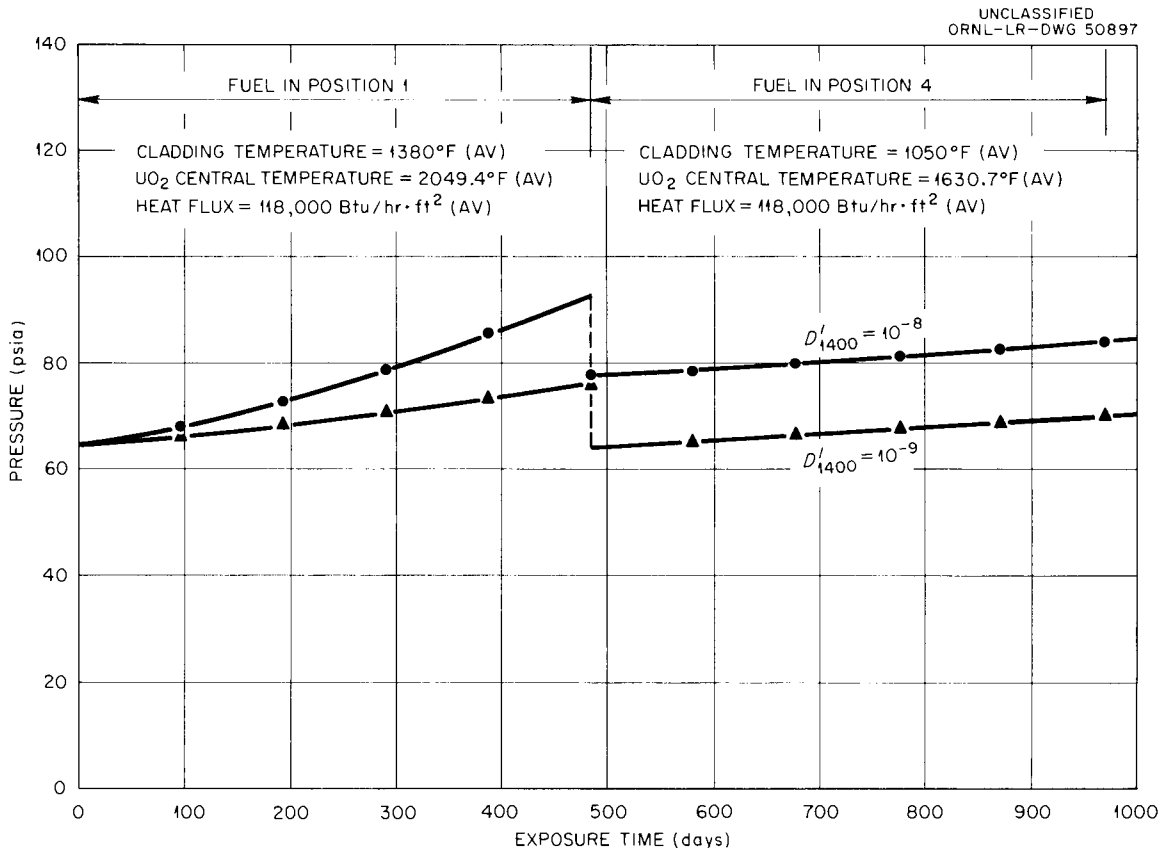

Fig. 6.3. Pressure Buildup in EGCR Fuel Elements in Positions 1 and 4.

largest pressure buildup and that, when the fuel is moved from position 2 to position 5, the pressure inside the fuel rod is not only greatly reduced but thereafter remains almost constant. The large decrease in pressure is due primarily to the reduced UO_2 central temperature which results from the lower heat flux and lower UO_2 surface temperature. For the case of the fuel in positions 1 and 4, the pressure buildup is not excessive in either position. In subsequent investigations therefore the performance of the fuel elements is evaluated by studying the effects of various parameters on pressure buildup in the fuel in position 2 only.

6.3. Effect of Gap Between UO_2 and Cladding

In Section 3.5 it was pointed out that if a gap existed between the UO_2 and the stainless steel jacket during reactor operation, the temperatures in the fuel rod would increase with extended burnup because of the accumulation of the fission gases xenon and krypton. Increases in fuel temperature will depend upon the size of the gap, the amount of helium initially introduced into the fuel rod, and the ability of the UO_2 to retain the fission gases. The time to achieve the higher temperatures will, of course, be very much greater as the gap decreases or as D' decreases. The decrease in the thermal conductivity of the gas mixture is shown in Fig. 6.4 for the case of $D'_{1400} = 10^{-9}$ sec^{-1}. As would be expected, the thermal conductivity decreases very rapidly if there is a small amount of helium present in the fuel rod initially.

Because of the uncertainty as to what the actual gap thickness will be during the lifetime of a fuel rod, the pressure buildup in a fuel rod has been studied for various assumed gap thicknesses and D'_{1400} values. In making these studies, the amount of helium introduced into the fuel rod at the time of fabrication has been varied.

If a given gap thickness exists during irradiation, in order to reduce the fission-gas release from the fuel, it is desirable to have a good heat transfer medium in the gap. Since the thermal conductivities of both the xenon and the krypton that diffuse from the fuel are low, the thermal conductivity of the gas mixture in the gap may be improved by initially filling the gap with a gas such as helium, whose thermal conductivity is large relative to the thermal conductivities of xenon or krypton. Although the helium will improve the heat transfer rate, it will contribute directly to the pressure buildup in the fuel, since most of the helium will be in the center of the fuel rods at high temperatures. The initial loading of helium that will result in the lowest pressure buildup in the fuel rod will depend upon two factors: (1) the diffusion rate of fission gases from the UO_2 and (2) the gap thickness during irradiation. Calculations of pressure buildup in the fuel rod for various

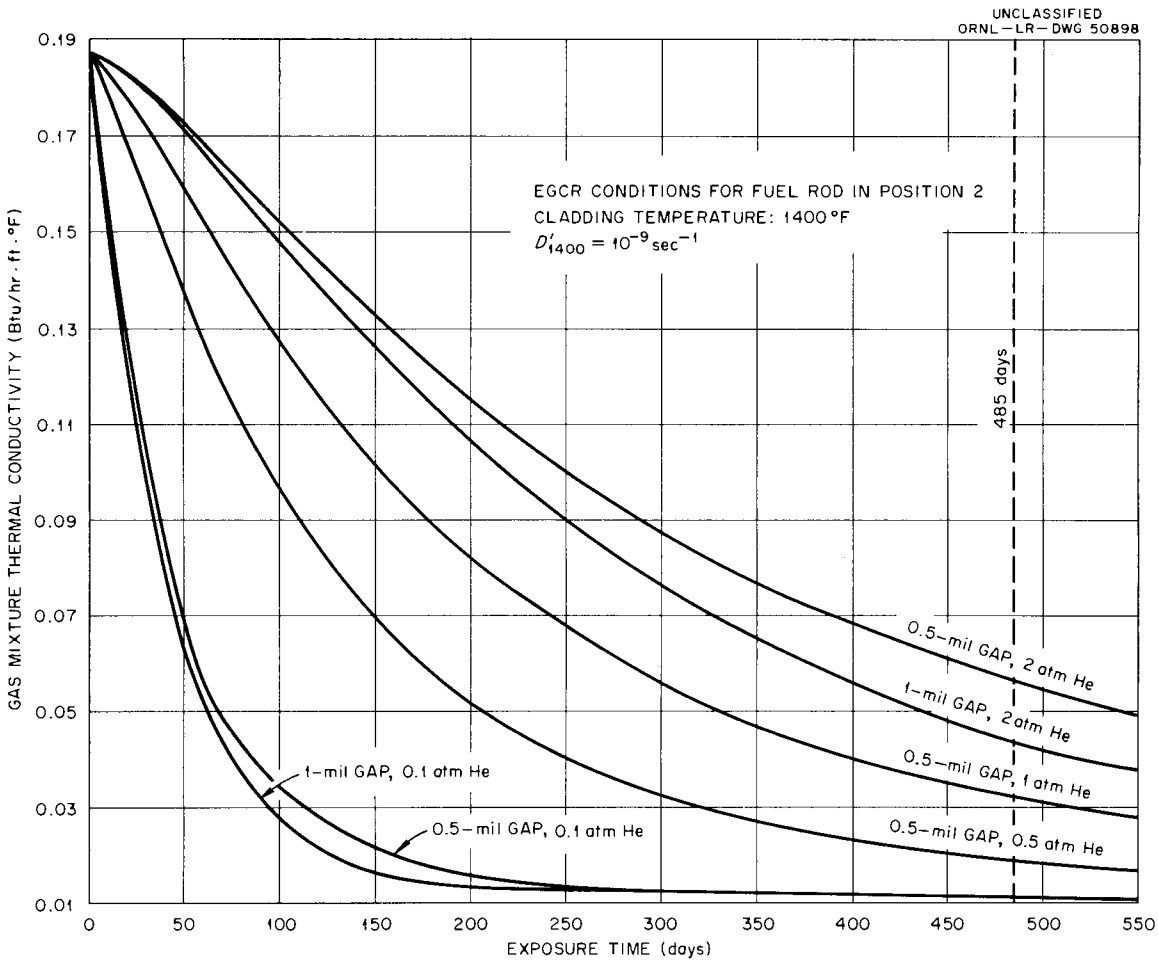

Fig. 6.4. Thermal Conductivity of Gas Mixture in Gap Between Fuel and Cladding.

helium loadings and assumed gap thicknesses are shown in Figs. 6.5 and 6.6 for an assumed D'_{1400} of 10^{-9} sec^{-1}.

From these curves it may be seen that introducing large amounts of helium results in large initial pressures, but, when the gap is large, the pressure at the end of fuel rod lifetime may be appreciably smaller than for the rods with less helium initially. The pressure in the fuel rod at 485 days for various gap thicknesses and for D'_{1400} values of 10^{-8}, 10^{-9}, and 10^{-10} sec^{-1} are shown in Figs. 6.7, 6.8, and 6.9. Figure 6.7 indicates that, if the release rate is relatively great, there is no

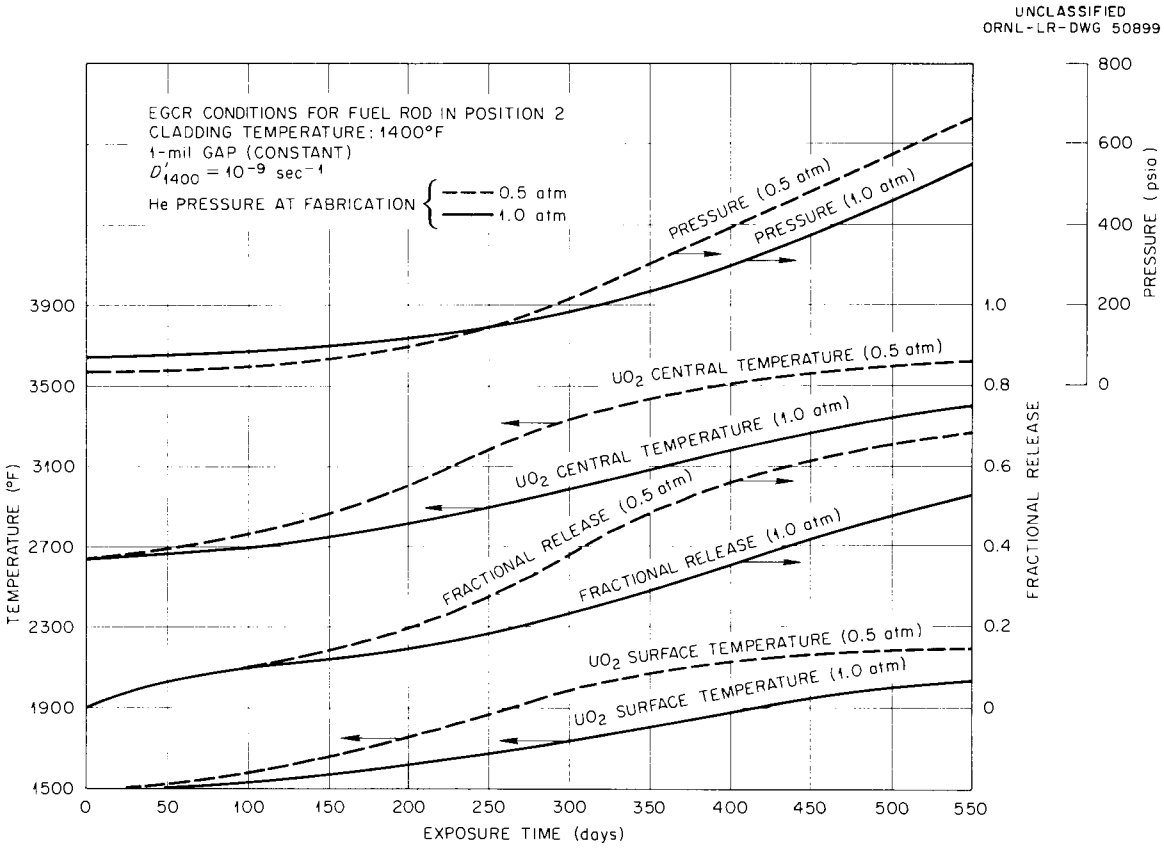

Fig. 6.5. Typical Performance Data for EGCR Fuel Elements.

appreciable difference in the pressure buildup at 485 days for various initial helium loadings. Furthermore, with such a high release rate, unless no gap exists, pressure buildup will be excessive. Figure 6.9, on the other hand, indicates that when the release rate is quite small there is an appreciable difference in the pressure buildup for various initial helium loadings. If, however, D'_{1400} is of the order of 10^{-10}, the pressure buildup in the fuel is not excessive even if the gap size is as large as 1 mil, and therefore there is little incentive to alter the amount of helium introduced into the fuel rod in order to reduce pressure buildup. The case of greatest interest occurs for the conditions illustrated in Fig. 6.8, where D'_{1400} is 10^{-9}. In this case it may be seen that, with a large gap (~1 mil), the pressure buildup is greatly

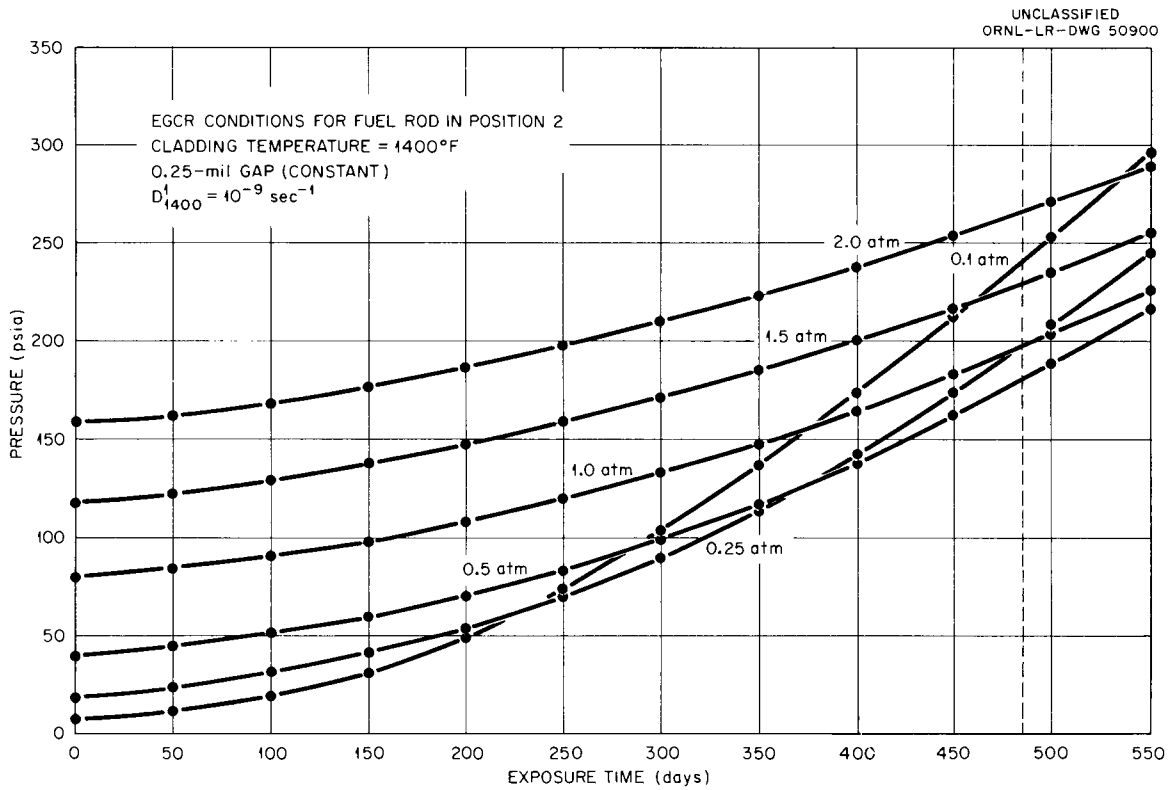

Fig. 6.6. Effect of Helium Loading Pressure on Pressure Buildup in Fuel Rod.

decreased by increasing the amount of helium above 1 atm. The pressure buildup will still exceed 300 psia, however, even for the optimum helium loading pressure. For smaller gaps (0.5 mil or less) it may be seen that the optimum helium loading pressure will be ≤1 atm, depending on the gap thickness assumed. From Fig. 6.8 it could be concluded that 1 atm of helium would be the most desirable amount to introduce into the fuel capsule, since it would not create a problem if the gap were small and would reduce the pressure if the gap were of the order of 0.5 mil. In arriving at the amount of helium to introduce into the fuel capsules at the time of fabrication, however, the problems of fabrication would also have to be considered.

The importance of the gap thickness for a given initial helium loading pressure is also illustrated in Figs. 6.7, 6.8, and 6.9. The

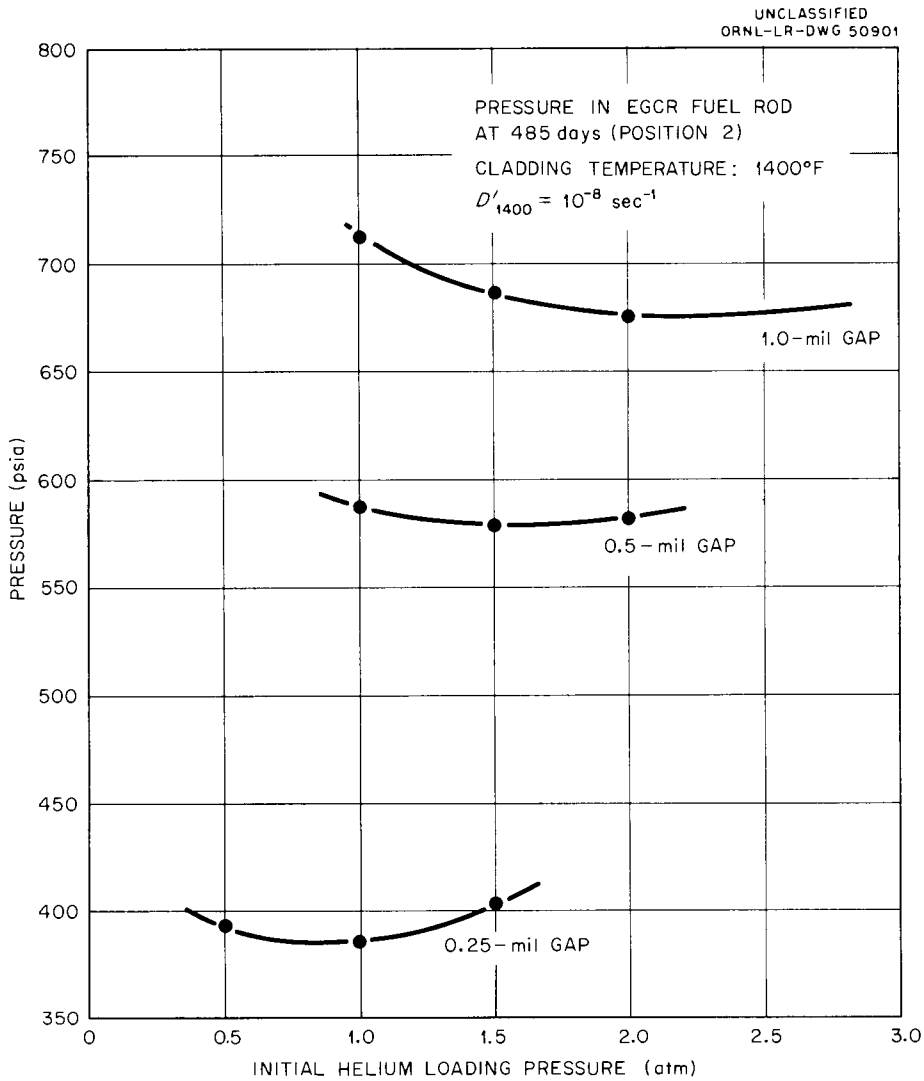

Fig. 6.7. Pressure Buildup in EGCR Fuel Rod for $D'_{1400} = 10^{-8}$ sec^{-1}.

much larger gas release with the larger gaps is due to the large increase in the temperatures in the UO_2 which result from the increase in the UO_2 surface temperature. As the thermal conductivity of the gas mixture decreases, both the increased gas release and the higher gas temperature (or UO_2 central temperature) cause a large increase in pressure buildup.

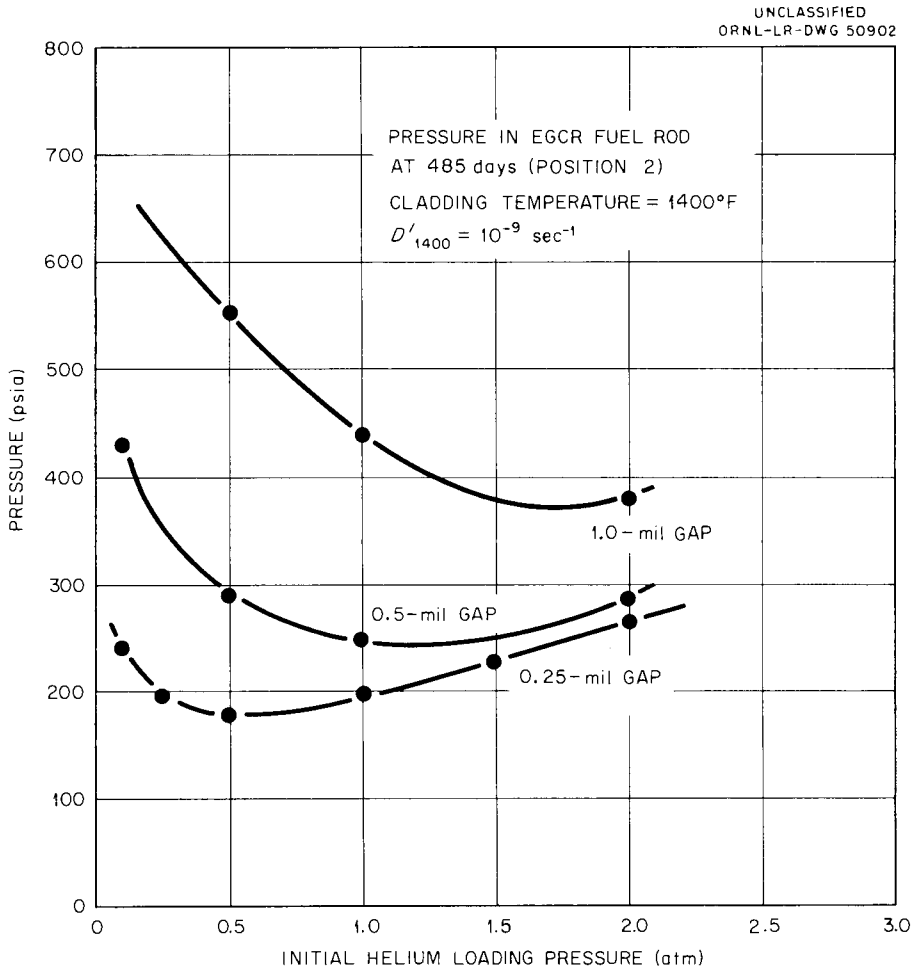

Fig. 6.8. Pressure Buildup in EGCR Fuel Rod for $D'_{1400} = 10^{-9}$ sec^{-1}.

6.4. Effect of Cladding Temperature

An increase in the cladding temperature of a fuel element will cause a corresponding increase in the UO_2 surface temperature. Since the thermal conductivity of UO_2 decreases with temperature, the increase in central temperature in the UO_2 will be somewhat higher than the corresponding increase in cladding temperature. Fission-gas release in the fuel element in position 2 is shown in Fig. 6.10 for cladding temperatures of 1425 and 1725°F. The increase in pressure will depend upon the D'_{1400} assumed. For no gap, Fig. 6.10 indicates that the pressure buildup will not be excessive with a cladding temperature of 1425°F unless D'_{1400} is

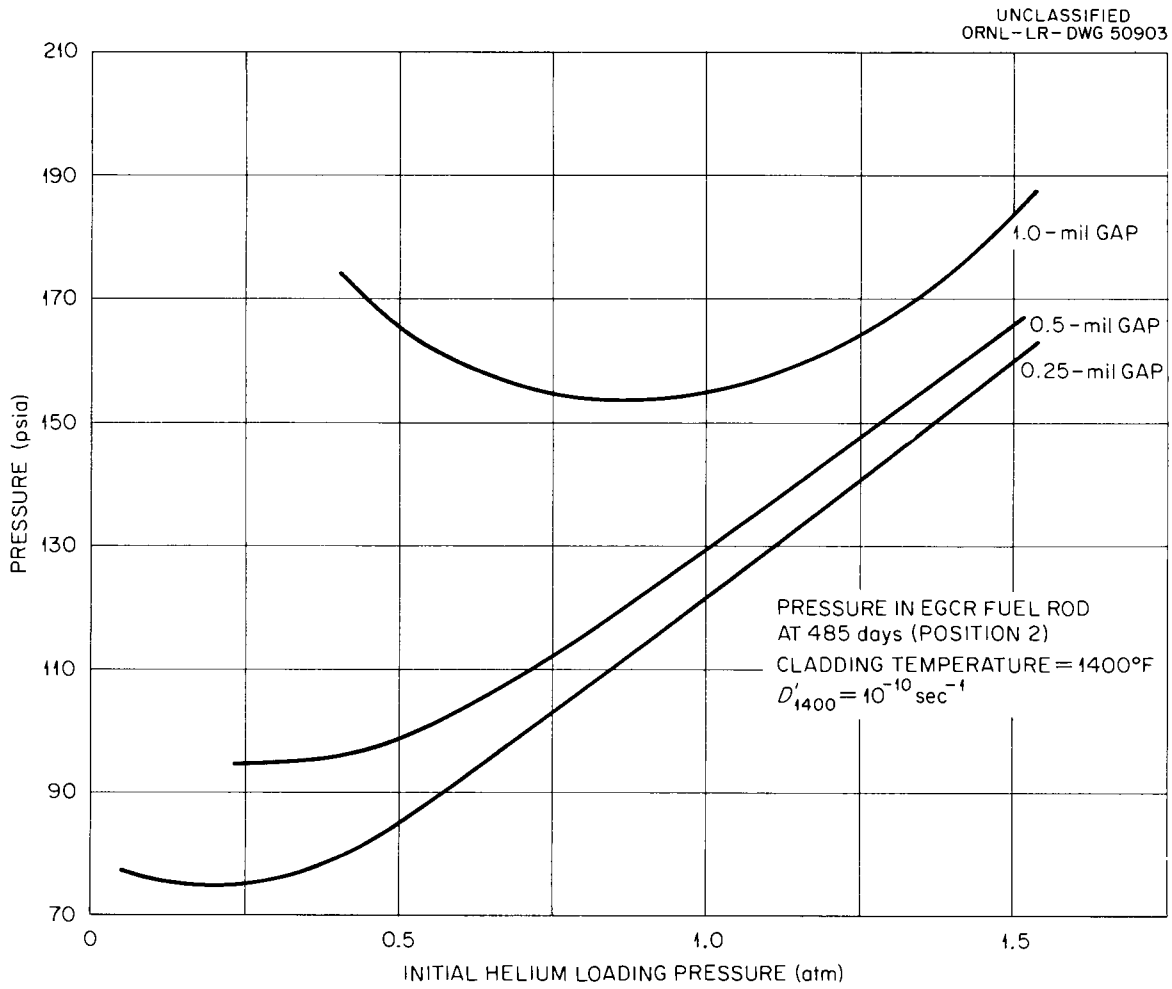

Fig. 6.9. Pressure Buildup in EGCR Fuel Rod for $D'_{1400} = 10^{-10}$ sec^{-1}.

greater than 10^{-8}. For a cladding temperature of 1725°F, however, the pressure buildup will be excessive if D'_{1400} is greater than $\sim 10^{-9}$.

6.5. Requirements of EGCR Fuel

The various studies which have been discussed indicate that the fuel in position 2 of the hot channel will have the greatest pressure buildup. The allowable release to limit pressure buildup to 300 psia will depend on the maximum cladding temperature in position 2, as well as on the probable gap thickness during fuel irradiation.

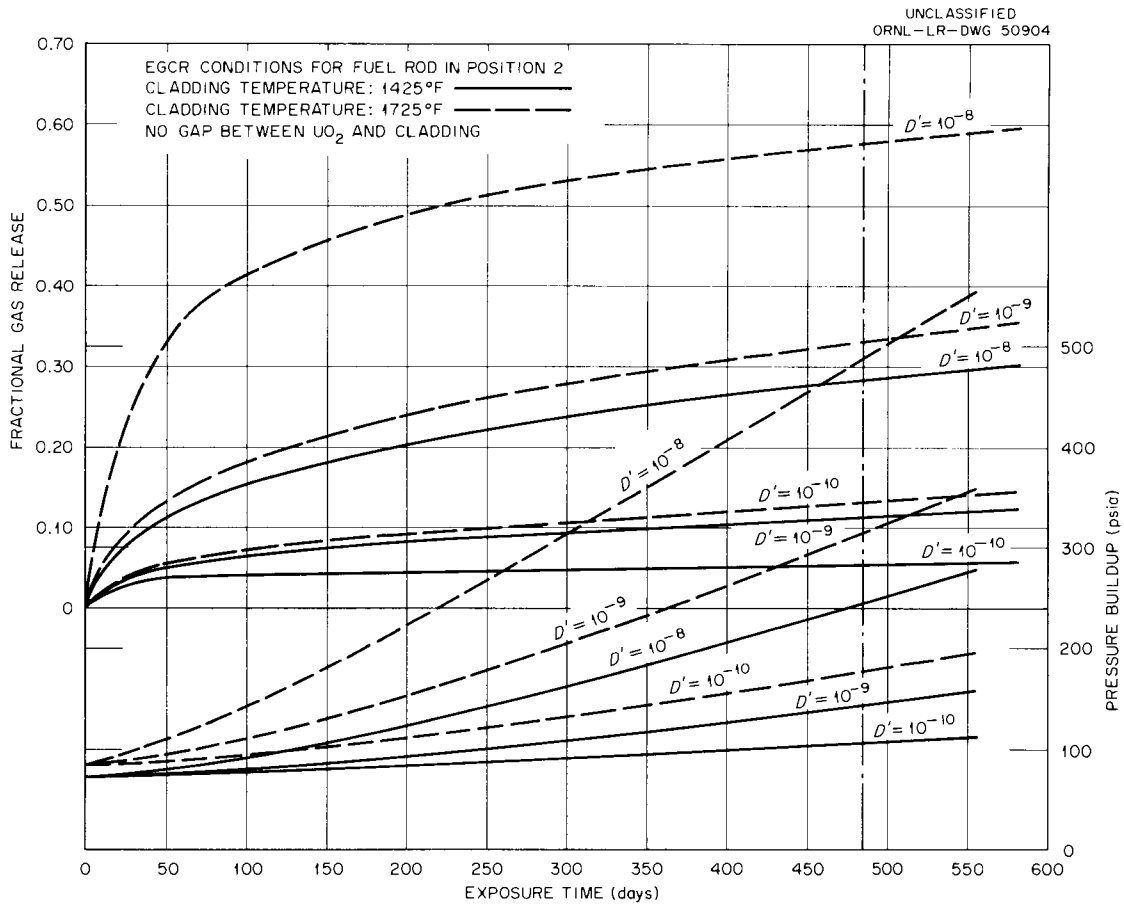

Fig. 6.10. Effect of Cladding Temperature and D'_{1400} on Fractional Gas Release and Pressure Buildup in EGCR Fuel Elements.

Present studies indicate that the cladding temperature will not be appreciably higher than 1400 to 1450°F,[75] and therefore, if the fuel material has a D'_{1400} of 10^{-9}, the pressure buildup will not be excessive unless the gap thickness exceeds 0.5 mil. With this D′ value and a helium loading pressure of 1 atm, the pressure buildup at 485 days will be 245 psia with a 0.5 mil gap and 144 psia with no gap. The fractional release for the 0.5 mil gap is ~24%, and with no gap the fractional release is 11.5% at the end of 485 days.

If experiments indicate that there are no conditions during fuel irradiation which can cause a gap to exist, then fuel with a D'_{1400} of 10^{-8} would be allowable, since the pressure buildup at 485 days would be only 244 psia. The fractional release for this case would be 28%.

6.6. Activity Release from EGCR Fuel

The activity which is released by diffusion from the UO_2 fuel material may be studied in a manner similar to that employed to estimate the capsule pressure. There is, however, a significant difference in the calculation of activity in that the important activities released may not be confined to the noble gases or volatile fission products, as was the case in the pressure calculations, but may originate from the diffusion of other elements out of the UO_2. Consequently, a thorough evaluation of the activity that is released from UO_2 must include not only that which decays from noble gas precursors, but also that which diffuses out of the UO_2 as other than a noble gas. In order to do this, however, diffusion coefficients for all fission-product elements in UO_2 would need to be known, whereas diffusion coefficients for only xenon and krypton have been measured.

The calculation of the escape of fission products from UO_2 from existing data is thus extremely tenuous, and, in lieu of adequate experimental data, the considerable work done at both Chalk River and Bettis on measurements of the release of activity from intentionally defective capsules operated in pressurized-water loops[52] provides the basis for estimating the release of nongaseous activity in gas-cooled systems. Data obtained in this fashion are generally employed to define an escape rate, ν, i.e., the probability per second that a given isotope will escape from the fuel element. Such data have a wide range of uncertainty, however; so the additional assumptions involved in their extrapolation to a gas-cooled reactor system yield results which must be regarded as indicative rather than conclusive. One of the most significant differences between a pressurized-water system and an inert-gas-cooled system is that the former provides an oxidizing ambient which may react with the UO_2 fuel in the event of a defect. As previously indicated (sec. 3.4), the release of fission products from nonstoichiometric uranium oxide is greatly enhanced and would lead to an overestimate of the released activity if these data were applied to a helium-cooled system. Thus, although a definite relationship may be shown to exist between the escape rate, ν, and the diffusion coefficient, D, the resulting values

of D would be extremely uncertain. On the other hand, it would be entirely feasible to determine the escape rate, ν, once the diffusion properties of the fuel were known and it was assumed that the chemical reactions would not occur.

The relationship between ν and D may be illustrated rather simply for the first isotope in a radioactive decay chain. The differential equation representing the amount of an isotope which exists external to the fuel element is

$$\frac{dN^G}{dt} = \nu N^F - \lambda N^G \quad , \tag{1}$$

where N^G is the number of atoms in the primary coolant, N^F is the number of atoms in the fuel element, ν is the escape rate from the fuel element, λ is the decay constant, and t is the time. The number of atoms in the fuel element is given by

$$\frac{dN^F}{dt} = B - \lambda N^F - \nu N^F \quad , \tag{2}$$

where B is the generation rate. Also, the release of fission products from the fuel by diffusion, as previously defined (see sec. 2.3), is given by

$$\frac{\partial C}{\partial t} = D\nu^2 C + B - \lambda C \quad . \tag{3}$$

These equations may be solved for the condition of interest, and an expression for ν can be obtained in terms of D. As may be seen from Section 2.3, the time-dependent solution of Eq. (3) is rather complex. At equilibrium, however, and when $\lambda > 100\ D'$, the ratio of the number of atoms external to the fuel element to the number which would exist in the fuel element if there were no diffusions is

$$F = 3\left(\frac{D'}{\lambda}\right)^{1/2} \quad , \tag{4}$$

where $D' = D/a^2$, and a is the radius of the hypothetical fuel particle, as previously defined.

The fraction, F, of an iostope external to the fuel element may also be found by solving Eqs. (1) and (2) for the ratio N^G to N^F, assuming equilibrium conditions. At equilibrium this ratio becomes

$$F = \frac{\nu}{\lambda} \quad , \tag{5}$$

and, when F is eliminated from Eqs. (4) and (5),

$$\nu = 3(D'\lambda)^{1/2} \quad . \tag{6}$$

It may be noted that from an examination of the definition of terms that the ν defines activity external to the fuel element, whereas D permits the calculation of activity external to the fuel material, i.e., the UO_2 itself. If the time for activity external to the UO_2 to diffuse out of the defect in the cladding is small compared with the time for diffusion out of the UO_2, the activities calculated from ν and D for the same conditions should be comparable.

The determination of fission-product activities becomes increasingly more difficult when other isotopes in the decay chain are considered and when an attempt is made to provide for the dependence of D' on temperature. An analysis that includes these considerations has been undertaken[76] with the diffusion coefficient as a parameter. The results will be published in a separate ORNL report.

In lieu of better information, it was assumed in the EGCR hazards report,[74] in estimating the amount of activity which would be released from the EGCR fuel elements, that the escape rate determined experimentally for UO_2 fuel operated in a pressurized-water loop would be applicable to the EGCR. It was also assumed that all isotopes of a given element had the same escape rate, despite the fact that Eq. (6) indicates otherwise. Furthermore, since escape-rate data were not available for all elements, the escape rates of those for which data did not exist were interpolated by analogy to others for which data were available.

A list of the escape rates used for the various fission products was included in the EGCR hazards report[74] and is presented here in Table 6.1.

Also shown in Table 6.1 is the activity which would exist external to the fuel material, as calculated from an estimated or assumed diffusion coefficient. For a number of iostopes there is no justification for assuming even an approximate diffusion coefficient, and no estimate of the activity released by diffusion has been made. For most other isotopes, namely Rb, Br, Xe, Kr, I, and Cs, an effective D' of 5×10^{-11} sec^{-1} was assumed. This D' would correspond to a D'_{1400} of 10^{-9} and an effective average fuel temperature of 2150°F. The amount of the remaining isotopes listed in Table 6.1 has been assumed to exist because of the radioactive decay of precursors which had escaped by diffusion without postulating an additional contribution by the diffusion of the daughter isotopes out of the UO_2. This is not to say that such diffusion does not occur, but, rather, that within the accuracy of the model, which is not good, the observed phenomena may be explained in terms of the diffusion of only the gaseous and volatile fission products. The last column in Table 6.1 lists the isotope (or isotopes) whose diffusion was assumed to contribute to the total amount of the isotope in question external to the fuel.

The significance of the activities estimated from experimental values of ν and an estimated D' value lies not in the absolute value but, rather, in the degree of correlation which exists between the two. That the absolute values are comparable could indicate that the integrated temperature structure and diffusion properties of the UO_2 material in the pressurized-water test were comparable to the integrated value of temperature and diffusion coefficient assumed here for the gas-cooled reactor fuel element. On the other hand, were the values of ν from the pressurized-water tests found to be due to the oxidation of the surface UO_2, the comparison between the two methods of estimating activity could not have any real significance. Furthermore, if isotopes such as Mo, Zr, and Te are observed to exist outside the fuel element, they must be accounted for by some process other than that used for the diffusion

Table 6.1. Calculated Fission-Gas Release from a Defective EGCR Fuel Rod

Isotopes	Decay Constant λ (sec^{-1})	Escape Rate,[a] ν	Activity Calculated from Escape Rate,[a] (curies)	Activity Calculated from Diffusion,[b] (curies)	Principal Diffusing Isotopes
Kr^{85m}	4.4×10^{-5}	1×10^{-7} (est.)	0.2	0.9	Rb^{85}, Kr^{85m}
Kr^{85}	2.1×10^{-9}	1×10^{-7} (est.)	5.0	2.1	20% Kr^{85m}, Kr^{85}
Kr^{87}	1.5×10^{-4}	1×10^{-7} (est.)	0.1	0.8	Kr^{87}
Kr^{88}	7.0×10^{-5}	1×10^{-7} (exp.)	0.4	1.6	Kr^{88}
Sr^{89}	1.5×10^{-7}	7×10^{-10} (exp.)	1.5	0.9	Kr^{89}, Rb^{89}
Sr^{90}	7.9×10^{-10}	7×10^{-10} (exp.)	2.8	0.3 (if in equi.)	Rb^{90}
Te^{99}	1.04×10^{-13}	1×10^{-7} (est.)	0.1	c	
Ru^{103}	2.0×10^{-7}	4×10^{-8} (est.)	57.6	c	
Ru^{105}	4.3×10^{-5}	4×10^{-8} (est.)	0.1	c	
Ru^{106}	2.2×10^{-8}	4×10^{-8} (est.)	22.3	c	
Rh^{105}	5.3×10^{-6}	4×10^{-8} (est.)	0.5	c	
Sb^{125}	8.1×10^{-9}	4×10^{-8} (est.)	4.3	c	
Sb^{127}	2.1×10^{-6}	4×10^{-8} (est.)	0.1	c	
Te^{129}	1.6×10^{-4}	3×10^{-9} (est.)	0.2	c	
Te^{132}	2.5×10^{-6}	3×10^{-9} (exp.)	0.4	c	
I^{131}	4.7×10^{-4}	4×10^{-8} (exp.)	9.4	10.3	I^{131}
I^{133}	5.8×10^{-3}	4×10^{-8} (exp.)	2.2	7.5	I^{133}
I^{135}	5.9×10^{-3}	4×10^{-8} (est.)	0.6	3.9	I^{135}
Xe^{131m}	6.7×10^{-7}	7×10^{-8} (est.)	0.2	1.4	1% I^{131}, Xe^{131m}
Xe^{133}	1.5×10^{-6}	7×10^{-8} (exp.)	23.5	24.3	I^{133} + Xe^{133}
Xe^{135}	2.1×10^{-5}	7×10^{-8} (exp.)	1.6	8.7	~I^{135} + Xe^{135}
Cs^{137}	6.7×10^{-10}	1×10^{-7} (exp.)	33.5	27.4 (100% release)	Cs^{137}
Cs^{138}	3.6×10^{-4}	1×10^{-7} (exp.)	1.4	1.9	Xe^{138}, Cs^{138}
Cs^{139}	1.2×10^{-3}	1×10^{-7} (exp.)	0.4	0.7	Xe^{139}, Cs^{139}
Ba^{140}	6.3×10^{-7}	6×10^{-10} (exp.)	0.25	0.2	Cs^{140}
La^{140}	4.8×10^{-6}	6×10^{-10} (est.)	0.25	0.2	Cs^{140}

[a]As in ref. 75.

[b]Calculated from an assumed D' of 5×10^{-11}.

[c]Not calculated; no diffusion information available.

calculations above. Direct measurements of the diffusion of such fission products in UO_2 have not been made, but it may be inferred from the escape-rate data that their diffusion coefficients are orders of magnitude smaller than those for the volatile fission products.

The amount of activity which will exist because of diffusion external to an EGCR element at equilibrium was calculated (Table 6.1) with the use of Eq. (4), as follows:

$$A = \frac{20\ 000 \times Y \times 3.1 \times 10^{10}}{3.7 \times 10^{10}} \times 3\left(\frac{D'}{\lambda}\right)^{1/2} ,$$

where A is activity in curies and Y is the fractional yield for power production in a fuel rod of 20 000 watts; thus

$$A = 0.353 \frac{Y}{\lambda^{1/2}} .$$

The calculation may be carried out for any D' which might be considered to be representative of the fuel in question. Were the D' of the fuel to be increased by a factor of 10 (i.e., a D'_{1400} value of 10^{-8} used with the same temperature distribution, or a fuel with a D'_{1400} of 10^{-9} used with an effective average temperature ~300° greater), the activity release would be increased by a factor of 3.2 (i.e., $10^{1/2}$). In all these calculations, an activation energy of 65 kcal/mole has been assumed on the basis of the experimental data included in Section 5.2.

7. THE ORNL EXPERIMENTAL FUEL-IRRADIATION PROGRAM

The objectives of the EGCR fuel-irradiation program,[63-65,77] as initially planned, were to provide adequate in-pile proof testing for the proposed fuel pellet geometry and the proposed fuel container at conditions comparable to EGCR operating conditions. As a backup program, several minor design variations were also planned for testing in the event that potential problem areas of the proposed design proved to be real. Information was to be obtained on the following items: (1) the dimensional stability of the cored pellets, (2) the dimensional changes of the pellets and container, (3) fusion, cracking, and chipping of the pellets, (4) the effect of irradiation on UO_2 density, (5) the effects of cracks or faults in the UO_2 on the cladding, (6) axial or radial migration of fuel, and (7) fission-product release from the fuel.

Evaluation of the experimental results obtained in a fuel-irradiation program is a complex problem. Uncertainties in (1) the fuel temperature profile, (2) the effect of the gap between cladding and fuel, (3) the effect of fuel breakup on the temperature profile, and (4) the time-temperature history of the irradiation, as well as variations in the oxide fuel, all contribute to the complexity. BET surface area measurements have indicated that an order of magnitude variation exists in the initial surface area of fuel of nominal 95% density. This, in turn, will contribute to variations in the measured D' values for the material.

The present EGCR fuel-irradiation program will permit only the detection of gross defects in the container and pellet design. Excessive pressure buildup sufficient to vary or distort the container can be observed. Poor fuel pellet stability due either to excess fuel migration or spalling of the fuel pellet surface can be determined in postirradiation analyses. Effects of thermal cycling on pellet stability will be studied.

7.1. Description of Fuel-Irradiation Program

Fuel irradiations are being carried out at three reactor installations: the LITR, the ORR, and the ETR. Some tests have been conducted

at the GETR, but these tests have been discontinued because of technical difficulties. The principal data on fission-product release are to be obtained from the LITR in-pile tests, although some data are expected from tests in the ORR and ETR. A brief description follows of the tests, the measurements taken, and the particular problems as they relate to fission-gas measurements.

7.1.1. LITR Irradiations

The capsules for LITR tests are designed with two individual compartments, each compartment containing approximately four miniature cored pellets. The pellet dimensions are 0.156 in. o.d., 0.078 in. i.d., and 0.4 in. long. Thermocouples are located in the pellet hole to measure, essentially, the maximum UO_2 temperatures. Metal cladding temperatures are also measured. Exposures in the tests are 7000 and 13 000 Mwd/MT. Initial plans called for tests up to internal UO_2 temperatures of 3500°F, but difficulties were encountered early in measuring temperatures in excess of approximately 2500°F. Recent improvements in thermocouples have, however, permitted the measurement of temperatures up to 3400°F. The external cladding temperature for these tests was established at 1300°F. The capsules are designed to have diametral clearances of 0.001 to 0.003 in. between the UO_2 pellet and the cladding. The capsule cladding is Inconel. Oxide densities of 75, 85, and 95% of theoretical were initially included in the schedule of tests, but recent revisions of the plans have emphasized the testing of 95% dense material.

Upon completion of a scheduled irradiation, the irradiated capsules are removed to hot cells, where they are punctured and the fission gas is collected. Some capsules irradiated at lower temperatures are inserted in a furnace and D′ measurements are made at elevated temperatures.

Analyses of the experimental data obtained from the tests are complicated by the following factors:

1. The effect of the initial gap is uncertain. This is particularly important in that the EGCR pellet cladding is not mocked up in the LITR capsules, and the collapse of the cladding against the UO_2 expected in

the EGCR does not occur in the heavy-walled Inconel LITR capsules. The temperature profiles may thus be quite different from those in the EGCR, even for identical cladding and central temperatures.

2. The geometry of the LITR capsules and the temperature gradient during irradiation are such that it is quite probable that the pellet fracture will not duplicate the fracture that will occur in the EGCR. This will affect both the contact with the Inconel wall and the effective thermal conductivity of the cracked oxide in LITR tests and will complicate extrapolation of the results to predict reactor fuel element conditions.

3. The majority of the temperature measurements to date have shown a drift of the internal temperatures, which is believed to be a result of the deterioration of the thermocouple. If this interpretation is correct, internal temperatures have not been measured over the irradiation cycle, and therefore initial measurements have been used as the correct temperature throughout the test. Recent improvements in thermocouples may help alleviate this problem.[65]

4. The contribution to pressure buildup of stable cesium, cesium compounds, and other condensibles will not be measured by the normal counting techniques. Thus the determination of their contribution to the total pressure buildup can best be obtained from pressure measurements on the irradiated capsule. For the small amount of gas generated in an LITR capsule, such measurements are difficult to make.

5. The cycling of the reactor during the history of the irradiation complicates the analysis because of the temperature variation and consequent variation in diffusion coefficients. If the time at reduced power is relatively small or the UO_2 temperature at reduced power is low, the effect will not be significant.

6. Until confirmatory burnup analyses are available, the use of cobalt monitors for determining the total integrated exposure is subject to significant error. This is particularly true in the earlier designs in which the cobalt monitor was placed at the end of the capsule beyond the fueled region. In the modified capsules the monitors are adjacent to the fuel pellets.

7. The fuel materials used in the irradiation tests thus far have not been characterized by a diffusion parameter. Thus the diffusion coefficient used for any analytical check on experimental results will be an assumed value, probably based on data from Westinghouse and Chalk River. Equipment is currently being set up to make D' measurements by annealing experiments at temperatures in excess of 1400°C.

7.1.2. ORR and ETR Irradiations

The capsules designed for operation in the ORR and ETR contain full-diameter prototype pellets of both solid and cored design. The pellets are clad with type 304 stainless steel and thus duplicate the EGCR design. The container can is bathed in NaK maintained at approximately 300 psia so that the effects of the 300-psia helium coolant pressure can be studied. The sheath temperatures used in the tests are 1300 and 1600°F. Capsules are designed with a cold radial gap of 0.0025 in. A number of the capsules in the ORR are to be thermally cycled in order to determine the effects of such cycles on both the can and the fuel material.

The fuel tests in the ORR and ETR have been termed proof tests of the EGCR fuel rod design. Data concerning fission-product release will be obtained, although this is not the primary purpose for the tests. Cored pellets with and without a central bushing are being tested. The purpose of the central bushing is to support the UO_2 pellets in the event fragmentation and spalling off into the central hole occur.

It is planned to make postirradiation pressure measurements at elevated temperatures of the fission-product pressure buildup within the ORR capsules. The complex time-temperature history of those capsules that undergo thermal cycling will impose further difficulties on the analysis of the data on fission-gas release. The initial information on the integrated flux will depend on monitoring of the cobalt-stainless steel bands holding the thermocouples in contact with the stainless steel cladding. Because of the background activity from other constituents in the stainless steel and the small amount of cobalt present, this method

is less accurate than the use of cobalt wire monitors. There are no internal thermocouples for measuring temperatures inside the fuel container.

The effect of thermal cycling on fission-gas release will be difficult to evaluate from the ORR tests because of the large number of cycles on the control samples. Further, the NaK bath will have the effect of giving a more homogeneous cladding temperature than may exist in EGCR operation.

7.2. Puncture Tests of LITR-Irradiated Capsules

Of the various experiments in the fuel-irradiation program, the capsule irradiations in the LITR are expected to provide the most pertinent data on the release of fission products from UO_2. Unfortunately analyses of the irradiation results have thus far produced values of the material diffusion rate constant, D', that vary widely, not only from experiment to experiment, but also when based on data for different isotopes in the same experiment. Nonetheless, the data do suggest that the release rate may be sufficiently low, i.e., $D' \ll 10^{-9}$, so that the fission-gas buildup within the EGCR fuel elements will not cause cladding failure, as discussed in Section 6 of this report.

The LITR fuel irradiations were described in the preceding section (sec. 7.1), and the results obtained thus far are presented in Table 7.1, which includes preirradiation and operational data, as well as the results of postirradiation puncture tests in terms of the percentages of the various gaseous fission-product isotopes evolved during irradiation. The method used for determining D' from the data is described below, but it should be emphasized that there are a number of significant uncertainties in the evaluation of D' from these data, including (1) the accuracy of the temperature measurement, (2) the assumed temperature distribution, (3) the recoil contribution, and (4) the accuracy of fission-gas measurements.

7.2.1. Calculational Procedure

In order to be able to compare readily the calculated diffusion rate constant, D', from one experiment with that from another, the rate

Table 7.1. Fission-Product Release from LITR Capsules[a]

Experimental Assembly Designation	Capsule Status	UO_2 Surface Area (m^2/g)	Oxygen-to-Uranium Ratio	Pellet Theoretical Density (%)	Irradiation Time (hr)	Pellet Enrichment (% U^{235})	Irradiation Flux (neutrons/ $cm^2 \cdot sec$)	Burnup (Mwd/MT)	Average Internal Temperature (°F)	Temperature Difference Between Cladding and Pellet Center (°F)	Fission Products Released (%)			
											Kr^{85m}	Kr^{88}	Xe^{133}	Xe^{135}
UO_2-1-1	Removed			96		15	1×10^{13}	4 000	1760	100	0.026		9.1×10^{-3}	2.4×10^{-3}
UO_2-1-2a	Removed			96		15	3.1×10^{13}	16 000	1770	280		0.01	0.033	0.012
UO_2-1-2b	Removed			97		15	3.1×10^{13}	16 000	2000			0.02	0.033	0.012
L-1a	Removed 2-25-59[b]	$<1.7 \times 10^3$	2.02	92.7	2479	10	2.8×10^{13}	7 000	1850	300				
L-1b		$<1.7 \times 10^3$	2.02	93.9	2479	10	2.8×10^{13}	7 000	2100[c]					
L-2a	Ruptured 4-7-59		2.13	84.9	726	20	2.5×10^{13}	5 000	2480	500	d	d	d	d
L-2b	Removed		2.13	84.4	726	20	2.5×10^{13}	5 000	2540[c]				9.0	
L-3a	Removed 8-10-59		2.12	75.0	1820	10		5 000	e				0.42	
L-3b			2.12	74.9	1820	10		5 000	e				19.3	
L-4a	Removed 4-28-59	$<1.7 \times 10^3$	2.02	92.1	4194	10	1.5×10^{13}	13 000	2350	200	0.011	0.021	0.028	8.5×10^{-3}
L-4b		$<1.7 \times 10^3$	2.02	93.3	4194	10	1.5×10^{13}	13 000	2500[c]		0.012	0.020	0.04	7.5×10^{-3}
L-6a	Removed 5-18-59			73.6	4208	10		13 000	2250					
L-6b				74.2	4208	10		13 000	2500[c]					
L-7a	Removed 6-8-59		2.04	95.5	1761	20		7 000	2160					
L-7b			2.04	95.2	1761	20		7 000	2600[c]					
L-8a	Removed 6-29-59		2.13	84.6	1324	20		8 000	2600					
L-8b			2.13	85.0	1324	20		8 000	2800[c]					
L-10a	Ruptured 9-22-59[f]		2.04	95.3		20			2450					
L-10b	Removed[f]		2.04	95.2		20			3000					
L-11a	Being irradiated		2.14	~95		20			1950					
L-11b			2.14	~95		20			2400					

Table 7.1. (Continued)

Experimental Assembly Designation	Capsule Status	UO_2 Surface Area (m^2/g)	Oxygen-to-Uranium Ratio	Pellet Theoretical Density (%)	Irradiation Time (hr)	Pellet Enrichment (% U^{235})	Irradiation Flux (neutrons/ $cm^2 \cdot sec$)	Burnup (Mwd/MT)	Average Internal Temperature (°F)	Temperature Difference Between Cladding and Pellet Center (°F)	Fission Products Released (%)			
											Kr^{85m}	Kr^{88}	Xe^{133}	Xe^{135}
L-13a	Removed 6-8-59	$<1.7 \times 10^3$	2.02	93.7	4290	10			2230					
L-13b		$<1.7 \times 10^3$	2.02	92.1	4290	10			2560[c]					
L-14a	Removed 3-17-59		2.03	94.1	1565	20	1.6×10^{13}	7 000	2080	300	0.029	0.011	0.014	0.006
L-14b			2.03	95.4	1565	20	1.6×10^{13}	7 000	2260[c]		0.057	0.019	0.029	0.017
L-15a	Removed 4-2-59		2.03	91.6	2155	20	1.4×10^{13}	7 000	1620	200	0.019	0.004	0.010	0.004
L-15b			2.03	89.7	2155	20	1.4×10^{13}	7 000	2055[c]		d	d	d	d
L-16a	Removed 9-21-59		2.04	94.4		30			1810					
L-16b			2.04	94.4		30			2040					
L-17a	Removed 8-10-59		2.04	93.7	2695	30		4 000	2410		0.04	0.04	0.02[g]	0.05[g]
L-17b			2.04	93.8	2695	30		4 000	2600[c]		0.13	0.24	0.13[g]	0.32[g]
L-18a	Removed 6-29-59		2.08	84.1	1324	30			h					
L-18b			2.08	85.2	1324	30			h					
L-18xa	Removed 10-13-59		2.08	84.7		30		13 000	2860					
L-18xb			2.08	84.6		30		13 000	3180					
L-20xa	Ruptured 6-18-59		2.19	75.4	1	15			i					
L-20xb	Removed		2.19	75.4	1	15			i					
L-21a	Ruptured[f] 10-6-59			96.0		10			1500					
L-21b	Removed[f]			96.2		10			1650					
L-22a	Being irradiated			~95		10			1400					
L-22b				~95		10			1800					

Table 7.1. (Continued)

Experimental Assembly Designation	Capsule Status	UO_2 Surface Area (m^2/g)	Oxygen-to-Uranium Ratio	Pellet Theoretical Density (%)	Irradiation Time (hr)	Pellet Enrichment (% U^{235})	Irradiation Flux (neutrons/ $cm^2 \cdot sec$)	Burnup (Mwd/MT)	Average Internal Temperature (°F)	Temperature Difference Between Cladding and Pellet Center (°F)	Fission Products Released (%)			
											Kr^{85m}	Kr^{88}	Xe^{133}	Xe^{135}
L-23a	Being irradiated			~95		15			2550					
L-23b				~95		15			3200					
L-24a	Being irradiated			~95		20			2600					
L-24b				~95		20			3100					
L-7-xa	Being irradiated		2.04	~95		20			j					
L-7-xb			2.04	~95		20			2300					
L-16xa	Removed 11-2-59		2.04	~95		30		7 000	2860					
L-16xb			2.04	~95		30		7 000	3400					
L-17xa	Removed 10-13-59		2.04	~95		30		7 000	3100					
L-17xb			2.04	~95		30		7 000	3300					

[a]Data taken from refs. 64, 65, and 77. Where reports list conflicting data the information in the latest report is assumed to be correct.

[b]Capsule L-1 was used only for a postirradiation heatup experiment.

[c]Estimated from capsule wall and "a" capsule central temperature measurement.

[d]Capsule has lost its gas.

[e]Calculated temperature 3000°F; tungsten-rhenium thermocouple failed during heatup.

[f]Cladding failed.

[g]Subsequent measurement of Xe^{133} and Xe^{135} release in this experiment gave values of 56.0 and 12.5%, respectively; these discrepancies are currently unresolved.

[h]Calculated temperature 2760°F; tungsten-rhenium thermocouple failed during heatup.

[i]Capsule ruptured during startup and was therefore removed; temperature not established.

[j]Thermocouple failed during initial heatup.

constant associated with each measurement is expressed in terms of its extrapolated value at 1400°C. This extrapolation is made by calculating the value of the diffusion rate constant at the temperature in question and then determining the value at 1400°C based on the diffusion process having an activation energy of 65 kcal/mole. This value of the activation energy for the diffusion of xenon and krypton in UO_2 is rather descriptive of values obtained in a number of recent experiments, as discussed in Section 4.2. The use of the diffusion rate constant, D', rather than the diffusion coefficient implies that the material used in the EGCR will be the same as that tested.

The procedure that is employed here in the calculation of the diffusion rate constant assumes that the entire UO_2 pellet is at the maximum temperature. This assumption is justified because the temperature measurements are not precise and also because the temperature drop across the capsule is relatively low — varying from 100 to 500°F for the capsules tested to date. It should be noted that the actual value of the diffusion coefficient will be somewhat larger than that calculated by this procedure, and, should the data warrant it, the calculation may be refined by dividing the capsule volume into as many temperature regions as desired. An error in the UO_2 temperature of 200°F above or below a 2500°F reference temperature will change the calculated 1400°C diffusion coefficient by a factor of 4.

Although fission-product release data have now been obtained for approximately 20 individual capsules irradiated in the LITR, many of the irradiations were at temperatures so low that the measured gas release was much less than 1%. Since the loss of any single fission product by the recoil process may be as high as 0.7%, the determination of diffusion coefficients from measured releases in this range is questionable. While few of the experiments had gas releases greater than 1%, a correction for the recoil contribution may be made which should not introduce a significant additional error in the results. Since in most LITR irradiations, two identical UO_2 specimens are separately enclosed in the same assembly but seldom are irradiated at the same temperature, the fractional releases

are usually significantly different. The fractional release, as determined from the lower temperature UO_2 pellet, will provide an overestimate of the recoil releases which may be subtracted from the fractional release of the higher temperature pellet. The diffusion constants calculated from this difference tend to be somewhat smaller than they actually are. In analyses of this type, however, the fractional releases differ by more than a factor of 2, so the error introduced in the calculated diffusion constants is no more than a factor of 2.

7.2.2. Calculated Diffusion Constants

The diffusion constant associated here with the average internal temperature of the pellet was calculated from Eq. (18) of Section 2, since the condition of the experiment describes the model from which this equation was derived. Furthermore, since the value of $(\lambda/D')^{1/2}$ is always greater than 10 for the isotopes measured, the simplified expression may be employed, e.g.,

$$f = 3\left(\frac{D'}{\lambda}\right)^{1/2} \tag{1}$$

or

$$D' = \frac{f^2\lambda}{9} \quad , \tag{2}$$

where f is the fractional release, λ is the decay constant (sec^{-1}), and D' is the diffusion rate constant for the irradiated fuel material, (sec^{-1}).

The values of D' thus calculated are extrapolated to the value at 1400°C by assuming an activation energy of 65 kcal/mole and the following relationship:

$$D'_{1400} = D'_T \, e^{(65 \times 10^3)/1.986 \left(\frac{1}{T + 273} - \frac{1}{1673}\right)} \quad , \tag{3}$$

where D'_T is the calculated value of D' at any given temperature T in °C.

The D'_{1400} values thus calculated are listed in Table 7.2. It may be seen that most values of D'_{1400} fall between 10^{-11} and 10^{-14} except for two of the four values calculated from Xe^{133} releases. There is no

Table 7.2. D'_{1400} Values Calculated from Experimental Data Obtained from LITR-Irradiated Capsules

Experimental Assembly	Oxygen-to-Uranium Ratio	UO_2 Density (%)	Calculated D'_{1400} (sec^{-1})			
			Kr^{85m}	Kr^{88}	Xe^{133}	Xe^{135}
L-14[a]	2.03	94.2	5.3×10^{-13}	6.9×10^{-14}	5.3×10^{-13}	3.9×10^{-14}
L-2b[b]	2.13	84.4			1.92×10^{-9}	
L-18b[b]	2.08	85.2			2.2×10^{-10}	
L-17[a]	2.04	93.7	3.0×10^{-12}	2.4×10^{-11}	1.5×10^{-13}	1.3×10^{-11}
L-3a[b]	2.12	75.0			2.1×10^{-16}	
L-3b[b]	2.12	74.9			4.3×10^{-13}	

[a]Recoil correction made by taking the difference in the values of fractional release from the two capsules.

[b]Fractional releases were so large that recoil correction was unnecessary.

apparent reason for this spread; indeed, if the large differences (greater than a factor of 10) were entirely between measurements on different fuel materials, there would be a temptation to attribute them to the material properties, e.g., oxygen-to-uranium ratio, density, surface area, etc. The LITR data are not adequate to estimate an activation energy; in fact, the variation in the D'_{1400} values, as shown in Table 7.2, does not permit any correlation with material properties, although such dependence is known to exist.

7.3. Annealing Tests of LITR-Irradiated Capsules

Two of the LITR-irradiated capsules were subjected to thermal annealing at a higher temperature than was attained during the irradiation after the fission-products had been measured. The fission gas, as well as other fission-product activity evolved during the annealing, was measured. One of the two annealing experiments was performed on fuel capsule L-1a, the other on both capsules of assembly L-14. Capsule L-1a was heated to an annealing temperature of 2100°F and capsules L-14a and b were heated to 2500°F. The capsules were placed in tubes and heated in a tube furnace. In each case, 3 hr was required to attain the annealing temperature, and the annealing temperature was held for 1 hr. The activity evolved during this period, whether in the gas, on the filter, or deposited on the system walls, was collected and measured. Additional information on these experiments and analytical techniques may be found in the progress report on this work.[64] The release data are given in Table 7.3.

Table 7.3. Fission Products Released in Annealing Experiments

Capsule	Fission-Product Release (%)						
	Nb^{95}	Zr^{95}	I^{131}	Cs^{137}	Sr^{89}	Ru^{103}	Xe^{133}
L-1a	0.16	0.05	12.4	11.4	0.02	0.007	
L-14a,b	0.005	0.007	7.4	5.5	0.01	0.001	5.6

Although these capsules had lost some fission-product activity during the puncture test following irradiation, the annealing temperatures were sufficiently higher than the irradiation temperatures that the loss during the irradiation may be ignored in calculating the diffusion from the annealing experiment. In experimental assembly L-14, for example, the Xe^{133} lost during irradiation was only 0.02% compared with 5.6% during annealing, despite the fact that the capsules were maintained at the 2200°F irradiation temperature for 1565 hr and were only held at the 2500°F annealing temperature for 1 hr. Furthermore, in calculating the D' value for diffusion during annealing, the heatup time preceding the time at the annealing temperature has also been ignored, since the lower temperature apparently contributes relatively little to the total release.

The diffusion during annealing may be calculated from the following formula, whose derivation was discussed in Section 2.1:

$$f = 6\left(\frac{D't}{\pi}\right)^{1/2}$$

The value of D' for 5.6% release of Xe^{133}, as listed in Table 7.3, is 7.6×10^{-8}. Extrapolating this value from the 2500°F temperature of the experiment to 1400°C, based on an activation energy of 65 kcal/mole, gives a D' value of 1.06×10^{-7} sec^{-1}. This value of D' is significantly lower than any of the values of Table 7.2, which were obtained from the puncture-test data. While postirradiation annealing should inherently provide a more accurate measure of the diffusion rate constant than does a puncture test, examination of the experimental procedure from which the data in Table 7.3 were obtained reveals that the UO_2 had the opportunity to become surface oxidized. If oxidation did occur, diffusion rate constants significantly larger than those determined from the puncture tests would be expected.

The annealing also caused the evolution of measurable quantities of Sr^{89}, Nb^{95}, Zr^{95}, I^{131}, Cs^{137}, and Ru^{103}, as indicated in Table 7.3. Values of D'_T have been calculated for I^{131} and Cs^{137}, but the measured releases for the other isotopes were so low that the recoil contribution

(during the irradiation) would mask the diffusion during annealing. Even the results for iodine and cesium are not consistent in that the capsule heated to 2100°F for 1 hr evolved approximately twice as large a fraction of I^{131} and Cs^{137} as did the capsule heated to 2500°F for the same time. The D_T' values for I^{131} and Cs^{137} from the two experiments are tabulated in Table 7.4.

No attempt was made to determine the D_{1400}' value for these diffusion processes because their activation energies are not known. Although the effect of the oxygen-to-uranium ratio on the diffusion of iodine and cesium is not known, it may be supposed that it would increase the diffusion of these isotopes even as it affected that of xenon and krypton.

Table 7.4. D_T' Values for I^{131} and Cs^{137} from Annealing Experiments

Experimental Assembly	Annealing Temperature (°F)	D_T' (sec^{-1})	
		I^{131}	Cs^{137}
L-1a	2100	3.73×10^{-7}	3.14×10^{-7}
L-14a,b	2500	1.33×10^{-7}	0.73×10^{-7}

8. CURRENT AND PROPOSED RESEARCH PROGRAMS

The accurate prediction of fission-product release from UO_2 will require a more thorough understanding of the effects of temperature and irradiation on the rates of release. Diffusion-rate constants, D', must be obtained that are characteristic of each of the volatile fission products and are representative of the diffusion parameter throughout the fuel element life. Until such data are available, calculations of the pressure buildup in fuel capsules will be fraught with uncertainties. Since a reactor fuel element based on UO_2 clad with stainless steel cannot be optimized without accurate calculations of this type, the strongest effort should be directed toward finding the relationships between temperature, burnup, and rates of release of fission products.

Implicit to the understanding of the relationships between temperature, burnup, and rates of release is the connection between UO_2 structure and D' values. Further, it is necessary for the application of these relationships to be able to determine accurately the operating temperature structure in UO_2 fuel elements. At elevated temperatures, sintering may occur, as well as changes in grain size, surface area, and ratios of open to closed porosity. Burnup or burnup rate may accelerate some of these processes. Thus detailed data are needed concerning the relationships between D' values and density, grain size, distribution of open and closed porosity, surface area, type of UO_2 powder, and method of fabrication of the fuel body. Information which relates time and temperature to these structural variables is also needed. Additional information is needed concerning the effect of temperature on release rates in samples where no structural changes occur, as well as continued efforts to verify experimentally the operating temperature structure in fuel elements. Values of the activation energy for the diffusion of volatile fission products are essential to the calculation of over-all release rates in fuel elements in which temperature gradients exist during operation. For these calculations, the activation energy should be determined as a function of burnup and burnup rate because the compositional changes and fission fragment damage may change the activation energy markedly.

At temperatures above 2000°C release may be enhanced by vaporization of the UO_2. If vaporization occurs, the rate should be measured as a function of temperature.

The effects of burnup and burnup rate on release rate are difficult to evaluate because of the handling difficulties associated with samples with high burnups; nevertheless an understanding of the magnitude of such effects is necessary. If irradiation effects, such as composition changes and fission-fragment damage, enhance sinterability or increase the diffusion coefficients, the D′ values measured out-of-pile on low-burnup material may not apply to UO_2 fuel bodies, and calculations based on these values may lead to a false sense of security. In Section 3.1, evidence was cited which indicated that irradiation changes the thermal conductivity of UO_2. Thus the temperature distribution and hence the over-all rate of release will change as a result of changes in thermal conductivity.

There is ample evidence that no dimensional changes occur in UO_2 irradiated to burnups on the order of 1 to 2% of the total uranium atoms present,[52] but whether or not such changes occur at burnups of the order of 10% is questionable. Information obtained at KAPL[78] on UO_2 in dispersion-type elements indicates that UO_2 may swell at high burnups. If bulk UO_2 is to be used in a fuel element with high burnups, more should be known about the swelling phenomenon.

Extensive evaluations of bulk UO_2 and various fuel elements containing UO_2 are being conducted at ORNL, the Westinghouse Bettis Plant, Chalk River, and HAPO. A more limited effort is being made to develop knowledge on bulk UO_2 at a number of other sites. Some of the techniques being used and current results have been discussed in Sections 3 to 6 and will not be repeated here; however, a number of new programs which have been initiated are discussed in the following paragraphs.

8.1. Determination of D′

A program has been initiated at ORNL[66] to determine D′ values of various types of UO_2 at elevated temperatures by the low-temperature-irradiation, out-of-pile-annealing technique. The types of UO_2 being

studied include a random sampling of batches of UO_2 fabricated for the EGCR, as well as special batches with controlled densities, grain size, surface area, or composition. The temperature range being studied is 1000 to 2000°C. Only the rates of release of xenon and krypton are being measured quantitatively, but qualitative information is also being obtained on the release of other volatile isotopes. The program will involve the determination of the effects of density, surface area, powder history, fabrication procedure, initial grain size, and porosity distribution on D′ values of very low burnup materials.

Since the effects of burnup will not be evaluated in these studies, a second ORNL program[79] involves the remeasurement of D′ values of EGCR fuel bodies at elevated temperatures after burnups of up to 13 000 Mwd/T have been achieved. Associated with these measurements will be the determination of changes in density, surface area, grain size, etc., during irradiation. In this way the causes of changes in D′ values during irradiation may be determined.

Out-of-pile tests do not provide the information needed for evaluating the effects of burnup rates. Such effects may be determined by continuous monitoring, during irradiation, of the rates of release from unclad UO_2 samples. Tests of this type are being run by Sisman and Carroll in the ORR.[80] Rates of release of a number of short-lived fission products are being determined in these tests. The results will be correlated with out-of-pile D′ values.

The study of rates of release of fission products from single crystals of UO_2 of known geometry should result in true diffusion coefficients. These values can be compared with approximate values obtained on UO_2 fuel bodies fabricated by normal techniques. A series of such tests is being planned at Battelle Memorial Institute, and personnel at ORNL have similar plans.

8.2. The Study of Grain Growth

The effects of grain growth on the release of fission products from UO_2 have been discussed at length, and it is clear that there is, as yet,

insufficient understanding as to the magnitude of the effect and the mechanisms governing the effect on gas release. A program of study to determine grain growth characteristics out-of-pile for sintered UO_2 compacts has been initiated at ORNL.[81] For the material being studied the threshold temperature for grain growth will be established, as well as the temperature-time relation for grain growth in the material.

The substantial increase in fission-gas release from areas where grain growth has occurred has been demonstrated. It is not clear, however, from the literature, whether the increase in gas release occurs only during the period of grain growth or whether areas where grain growth has occurred subsequently produce high gas release. The problem is of obvious importance because of the effect of temperature transients in fuel elements and the effect of such transients on the grain size. This problem can be studied by establishing conditions for grain growth through short-term high-temperature irradiations and then subsequent long-term irradiation at well below grain growth temperatures. Fission-gas release may be compared with that from identical control specimens which were not cycled to the grain-growth temperatures. The effect of the temperature cycle on surface area and density may be determined by postirradiation measurement.

Further information on grain-size effects may be obtained by irradiating different samples of UO_2 which are identical except for the initial grain size and measuring differences in release rates under the same conditions of irradiation. A measure of the effect of grain growth on release rates might be determined also by continuously monitoring the release from samples irradiated at temperatures at which grain growth is rapid.

Examinations to date of capsules from the ORNL fuel-irradiation program have shown no areas of grain growth. These results include, however, only evidence from capsules irradiated at low temperatures. More recent tests have been made at irradiation temperatures (3400°F) sufficiently high for evidence of grain growth to be present. If a correlation between grain growth and UO_2 temperature can be established,

it will permit an added cross check on the temperature profile through the UO_2 pellet by postirradiation determination of grain-size distribution within the pellet.

8.3. Studies of the UO_2-Capsule Interface

For a fuel element of the EGCR type, one of the largest uncertainities is the effect of the gap at the UO_2-cladding interface on the temperature profile through the UO_2. Studies referred to in the discussion on gap effect (sec. 3.5) have shown somewhat conflicting interpretations of results.

The extent to which the medium filling an interfacial gap is effective in influencing the temperature in the UO_2 can be studied by testing capsules with controlled atmospheres to determine the effect of the atmosphere. Thus capsules operating initially with helium gas may be flushed with xenon and the central UO_2 temperature effects determined. This can be accomplished at temperatures within the range of accurate measurements. The effect of external pressure on the gap may be determined by testing capsules under variable external pressures obtained by controlling, for example, the pressure of a NaK bath surrounding the capsule.

With cored pellets it is particularly important to determine the effect of pellet fracture on interface conditions. Deliberately thermally cycling a previously uncycled specimen operating at reduced temperatures may show the effect of pellet fracture as a difference in UO_2 surface and central temperatures.

8.4. Effects of Porosity

In the discussion of the effect of porosity on fission-gas release it was pointed out that the role of closed porosity as a holdup volume for fission gas is not clear. The Chalk River grinding experiments indicate that closed pores do retain some of the fission products. However, many of these tests give conflicting results that make difficult

the interpretation of the experiments. If grinding experiments were conducted on large, single crystals of UO_2, a comparison of results with data on pressed and sintered pellets might lead to an understanding of the role of closed porosity.

8.5. Temperature Structure During Irradiation

The thermal conductivity of unirradiated UO_2 has been studied by many investigators. In addition, effects of irradiation on the conductivity values and effects of oxygen-to-uranium ratio and impurities have been studied. However, additional work is required to evaluate the effective conductivity, which is dependent on items such as interface resistance, material cracking, and long-term burnup effects.

It is necessary that accurate calorimetric measurements be made and that these values be checked from burnup analysis and by results from flux monitors. Only with such cross checks can confidence be placed in the results. Progress is being made on in-pile temperature measurements, and, with the above heat-loading measurements, effective conductivity values can be determined.

If the grain-growth studies are able to show correlations with temperature, and if studies of the UO_2-to-cladding interface effects yield information on the effective resistance at the interface, then meaningful comparisons can be made between measured and calculated effective-conductivity values.

8.6. Pressure Measurements on Irradiated Capsules

The problem of determining the contribution to pressure buildup within the fuel capsule of components which may be volatile at operating fuel element temperatures is currently being studied at ORNL in a series of pressure measurements on irradiated fuel capsules.[82] The capsules will be placed in a furnace and held at fixed temperatures, and the pressure will be measured through a metal pressure-balance diaphragm employing electrical contact points and a controlled external pressure

on the diaphragm. A similar in-pile device is being considered that would give information not only on the pressure contribution of condensible fission products, but, if operated at reduced temperatures, would give added valuable information on release of fission xenon and krypton from the oxide material.

Concurrent with studies of pressure buildup in irradiated capsules, information should be obtained on vapor pressure, stability, and the chemical equilibria which may exist in the UO_2 environment. Such information is required to permit interpretation of the pressure measurements.

8.7. Additional Considerations

The information obtained to date has strongly indicated that, as the oxygen-to-uranium ratio in UO_2 increases, the fission-gas-retention capability decreases. Therefore studies of the effects of high oxygen-to-uranium ratios on fission-gas release can probably be deferred until many of the questions on stoichiometric material have been answered. Certain advantages of higher oxygen-to-uranium ratio material, particularly in sintering behavior, have been recognized, but at the present time in-pile effects seem to rule out their use.

The existence of a mechanism whereby fission products re-enter the oxide lattice has been demonstrated at Chalk River. Work in this area may yield fruitful results in determining a limiting maximum possible pressure for clad UO_2 fuel elements.

9. SUMMARY AND CONCLUSIONS

The buildup of pressure within the cladding of a fuel element because of the release of volatile fission products from the fuel is one of the most important factors governing the design of a fuel element of high-density UO_2 clad with stainless steel for use in gas-cooled power reactors. As a result of the high cladding temperatures and low external pressures in such systems, the rates of release of fission products must be predicted with considerable accuracy if the over-all power costs are to be minimized. The purpose of this study was to determine the most suitable model for predicting fission-product release, to evaluate the applicability of existing data on UO_2 to the problem, and to determine what research and development work will be required to obtain an accurate method of predicting rates of release of fission products from UO_2.

From a study of existing literature relative to the release of fission products from UO_2 and discussions with people at Battelle Memorial Institute, the Westinghouse Bettis Plant, and the Chalk River Laboratory, it was concluded that the fission products may be released by recoil and a two-step diffusion process. It is apparent that the diffusion of fission products out of the UO_2 crystal lattice is the controlling escape process. However, it has also been shown that, at moderate temperatures, recoil escape may be controlling and that, under conditions which create a change in the crystal structure of the UO_2 (i.e., grain growth, sublimation, melting), a significant increase in the rate of release of fission products is experienced. At the present time it may be concluded with certainty only that the aforementioned diffusion process is both applicable and controlling in the relatively narrow temperature regime above that of significant recoil escape and below that of grain growth. The general diffusion formulae have, however, been employed with moderate success in interpreting results of experiments in which significant grain growth has occurred. This may either be indicative of the more general applicability of the diffusion relationship than conceded above, or it may merely point up the fact that the existing data are not sufficiently accurate to determine the applicability of the model in this region.

The diffusion model has been described mathematically for a number of conditions which are of interest in interpreting the results of release experiments or in extrapolating these data to reactor operating conditions. These conditions include those in which fission-product generation and diffusion occur either simultaneously or independently, in which the fuel is either isothermal or nonisothermal, and in which radioactive decay is either considered or neglected. In all instances the model may have significant limitations, such as the assumed particle shape, effect of closed porosity, effect of re-entry mechanisms, etc. In addition to inherent limitations in the model, there exists considerable uncertainty in the determination of the diffusion coefficient even in regions where the model is presumed to be applicable.

In order to determine values for the diffusion coefficient, two experimental techniques have been employed, annealing experiments and puncture tests. The results obtained with these tests are subject to question. In annealing experiments, although temperatures of the fuel are closely controlled, the effect of irradiation on the diffusion process is not duplicated, and therefore the extrapolation of these results to reactor conditions may not be justified. In evaluating results of puncture tests, great uncertainty normally exists as to the temperature structure and history of the fuel during irradiation. In this case, it is difficult to correlate the condition of the fuel with the occurrence of diffusion. It is significant in this connection that all published values of activation energy and diffusion coefficients have been obtained from annealing experiments.

The available experimental data and techniques combine to permit the conclusion that a reasonably consistent picture of fission-gas release may be made despite the fact that much detail is missing and many gaps remain. The data which have been developed from these various experiments are reported here, together with an interpretation of the results. The activation energy undoubtedly lies between 34 and 81 kcal/mole and is probably reasonably close to 65 kcal/mole — the average of all measurements and the value which has been employed in calculations on the performance of the EGCR fuel elements.

The determination of an absolute value of the diffusion coefficient for general use in the diffusion equation is extremely difficult, not only because of the many parameters involved in such an evaluation, but also because of significant differences from one fuel material to another. At the present state of understanding of these phenomena, any particular fuel material must be characterized by a measurement of the diffusion-rate constant, D', and preferably under conditions as closely approximating those of the anticipated service as possible. Such measurements of D' for material of the same density but manufactured by different processes are known to differ by several orders of magnitude. While the reasons for such discrepancies are under investigation at numerous installations, much additional work will have to be done to understand thoroughly and control the various contributing factors.

The wide scatter in release rate data which has been reported precludes the optimization of the design of a reactor with stainless-steel-clad UO_2 fuel elements at this time. The scatter is a result of a lack of understanding of effects of many of the important parameters affecting release, such as thermal conductivity, density, distribution of open and closed porosity, grain growth, oxygen-to-uranium ratio, material discontinuities, and temperature structure. Nevertheless, the accumulated experience permits a number of conclusions to be drawn with regard to the effect of these parameters on gas release.

Measurements of the thermal conductivity of unirradiated UO_2 have been made by a number of investigators and reasonably consistent values have been obtained. In addition the effect of irradiation on thermal conductivity has been studied, and irradiation is known to cause a decrease in conductivity of approximately 25% for a wide range of the integrated neutron exposure. Annealing of the irradiated samples permits a recovery of the thermal conductivity that is dependent on the annealing temperature and the integrated neutron exposure.

The presence of excess oxygen in UO_2 causes a sharp decrease in thermal conductivity of the material, but the reasons for this effect are not understood. The available evidence suggests that the net effect

of in-pile operation on the thermal conductivity of UO_2 will not be serious. Estimated values for in-pile thermal conductivity from measured specimen temperatures and integrated heat loadings indicate no serious deterioration of the thermal conductivity, at least for short burnups, but longer burnup tests are required.

In addition to the observed decrease in thermal conductivity with an increase in the oxygen content of UO_2, the oxygen-to-uranium ratio is known to have a significant and presumably independent effect on both grain growth and fission-gas release. The temperature for grain growth is lowered and fission-gas release is increased. Thus the known effects all point to the desirability of using stoichiometric fuel material.

The presence of gaps either within the fuel material or between cladding and fuel material imposes temperature discontinuities on the fuel element temperature structure. In the case of gas-cooled reactors operating at high gas temperatures with high gas-film temperature drops, the cladding operates within the creep range of the material, and collapse of the cladding material onto the UO_2 occurs. This contrasts with pressurized-water reactors in which the fuel element cladding temperature remains close to the primary coolant temperature, and collapse of the cladding material does not occur. The existence of a gap between the cladding and the fuel material markedly increases the temperature within the fuel region. This occurs as a result of dilution of the initial gas composition within the fuel gap with fission-product xenon and krypton gases, which have the lowest of thermal conductivities. A large initial clearance may also result in nonuniform collapse of the cladding material onto the fuel and consequent wrinkling of the cladding material. The UO_2 fuel material will thermally crack early in its operating life, and therefore the effect of an initial gap cannot be accurately predicted for conditions in which collapse of the cladding is not expected.

The calculation of a temperature profile within the fuel material requires knowledge of the effect of the variables discussed above and requires an accurate reference temperature measurement. The determination and verification of the correct temperature structure of the fuel material

while under irradiation is an important and difficult task remaining in the accurate determination of fission-gas release from fuel material.

An increase of fuel temperature promotes grain growth within the fuel material, and, in regions where grain growth occurs, fission-gas release is very high. Although the time-temperature relationship for in-pile grain growth of UO_2 has not been established, grain growth has been observed in some types of UO_2 at temperatures thought to be approximately 1500°C. The diffusion model is not believed to be applicable in regions where grain growth occurs, and the controlling mechanism for gas release in these regions is not understood. Present practice, however, is to use the diffusion model in areas where grain growth has occurred.

Increases in the bulk density of UO_2 material have been observed upon irradiation, and UO_2 is known to exhibit plastic deformation at temperatures in the order of 1000°C. The effects of property changes during irradiation, together with the uncertainties in temperature and grain structure within the material, are reflected in the results of fission-product release experiments.

Density, porosity, and surface area are related and all have important, though not necessarily independent, effects on fission-gas release. In general, an increase in the density results in lower porosity and surface area and lower fission-product release. For a specific UO_2 material, definite relationships have been established between density and surface area and between density and open and closed porosity. The relationship between density and surface area has been employed to determine the radius of the hypothetical fuel particle. However, this relationship, as well as that between density and porosity, is believed to be valid only for the fuel material for which the measurement was made, and use of these relationships for other materials is questionable. The effect of closed porosity has not been considered in the models describing the release process, although it may be shown analytically to reduce the calculated gas release, particularly for fuel materials in which the total surface area, including open porosity, approaches that of the geometric surface area.

Since the rates of release of fission products cannot be determined accurately, calculations were made to determine what value of the release-rate parameter, D', at 1400°C would be acceptable in the EGCR. For these calculations it was assumed that xenon and krypton diffuse at the same rate with an activation energy of 65 kcal/mole and that other fission products may be neglected. In lieu of more definitive information, the calculations have been carried out as a function of a number of parameters, most significant of which are fuel-capsule gap, initial helium pressure in capsule, and D'. Analytical studies have indicated that excessive pressures will not be generated within any EGCR capsule if the D'_{1400} value for the EGCR fuel material is equal to or less than 10^{-9}, the initial capsule internal pressure is 1 atm, the operating gap is equal to or less than 0.5 mil, and the cladding temperature is no greater than 1450°F. Recent experiments have indicated that the capsule wall will collapse onto the surface of the UO_2 under EGCR operating conditions. Obviously smaller gaps and a lower D' will further improve an acceptable situation. On the basis of the measured diffusion rate constants, there is no doubt that a fuel which has an acceptable D' value may be specified, and current investigations are being directed toward the economics of various fuel fabrication processes.

ORNL has embarked on a rather extensive fuel-irradiation program which is only now beginning to develop significant experimental results. While the principal objective of this fuel-irradiation program was to proof-test the particular configuration proposed for the EGCR, the program has many objectives, one of which is the study of the release of fission products from the fuel material. While the preliminary results indicate that D'_{1400} may be considerably smaller than 10^{-9} for EGCR fuel elements, the results are not yet conclusive.

As a result of these and other studies since the initiation of this fuel-irradiation program, the desirability of a basic experimental program in conjunction with the proof tests has become appreciated. The areas in which research should be performed and, in some instances, the specific experiments are indicated in Section 8 of this report. The

studies which are outlined should permit a meaningful interpretation of the data being obtained in the present EGCR fuel-irradiation program. An understanding of the effects of pellet fracture, densification, gap resistance, grain growth, and other parameters is necessary to help explain variations in the measured gas release from the fuel capsules and permit designs to be placed on a much firmer basis than is presently the case.

Furthermore, it is recognized that UO_2 does not represent the ultimate fuel material. The limitations of container-type elements are also recognized. As a result of these recognized limitations, there is considerable interest in fuels such as uranium carbide and in unclad fuel elements containing uranium carbide or oxide in a matrix of graphite or BeO. Basic information is required to determine the mechanism and magnitude of fission-product release from these materials. The rate of diffusion of fission products through graphite, BeO, or other suitable ceramic material may well determine the practicality of unclad systems. Much of the experience, effort, and equipment utilized in the study of fission-product diffusion from UO_2 will be useful in the study of diffusion of fission products from other fuel materials.

Appendix

CALCULATION OF FISSION-PRODUCT RELEASE FROM EGCR FUEL ELEMENTS

The fractional release of fission gas, as well as the pressure buildup in a fuel rod, is estimated below by using the model described in Section 2.2 and by assuming that the temperature distribution in the fuel rod does not change with time. The calculations have been based on the preliminary EGCR conditions described in Section 6.1 and listed in Table A.1. A plot of f from Eq. (6), Section 2.1, for values of $D't$, as well as for values of D', for a time of 485 days, is shown in Fig. A.1.

In order to obtain the fractional release from the fuel, it is necessary to know the diffusion parameter D', which varies throughout the fuel as a function of the temperature. For these calculations, the activation energy, Q, was assumed to be 65 kcal/mole (see Section 5.2); therefore

$$D' = D'_0 \, e^{-65\,000/RT} \quad . \tag{1}$$

In order to obtain the proper D' value for the fuel, it is necessary to investigate the temperature in the fuel both in the radial and longitudinal directions.

A.1. Temperature Distribution in the Fuel

The uncertainty which exists in the fuel temperature distribution in the UO_2 is due mainly to two factors: (1) the uncertainty in the value of the thermal conductivity of UO_2 and (2) the uncertainty as to temperature discontinuities in the UO_2 because of a gap between the UO_2 and the metal cladding or the breaking up of the UO_2. It is assumed for this analysis that no gap exists between the UO_2 and the metal container, that is, that the inner surface of the cladding and the UO_2 surface are at the same temperature. This does not imply that during operation of the reactor no gap will exist. The effect of a temperature

Table A.1. EGCR Operating Conditions Used for Fission-Gas Release and Pressure Buildup Calculations

Fuel Element Position	Fuel Sub-division	Relative Power	Average Burnup (Mwd/MT)	Cumulative Burnup (Mwd/MT)	Average Power Generation (kw/fuel subdivision)	Average Heat Rating (Btu/hr·ft)	Average Cladding Temperature at Inner Surface (°F)
1	1	0.575	2875		1.22	11 270	1230
	2	0.655	3275		1.39	12 838	1300
	3	0.82	4100		1.74	16 072	1335
	4	1.02	5100		2.16	19 992	1370
	5	1.185	5925		2.51	23 226	1395
	6	1.31	6550		2.78	25 676	1420
2	1	1.41	7050		2.99	27 636	1440
	2	1.49	7450		3.16	29 204	1450
	3	1.56	7800		3.31	30 576	1450
	4	1.61	8050		3.42	31 556	1445
	5	1.64	8200		3.48	32 144	1435
	6	1.65	8250		3.50	32 340	1415
3	1	1.65	8250		3.50	32 340	1385
	2	1.625	8125		3.45	31 850	1345
	3	1.575	7875		3.34	30 870	1305
	4	1.525	7625		3.23	29 890	1265
	5	1.455	7275		3.09	28 518	1220
	6	1.375	6875		2.92	26 950	1175
4	1	1.275	6375	9 250	2.70	24 990	1125
	2	1.165	5825	9 100	2.47	22 834	1075
	3	1.065	5325	9 425	2.26	20 874	1025
	4	0.975	4875	9 975	2.07	19 110	975
	5	0.895	4475	10 400	1.90	17 542	930
	6	0.815	4075	10 625	1.73	15 974	885
5	1	0.74	3700	10 750	1.57	14 504	850
	2	0.675	3375	10 825	1.43	13 230	815
	3	0.615	3075	10 875	1.30	12 054	780
	4	0.56	2800	10 850	1.19	10 976	755
	5	0.505	2525	10 725	1.07	9 898	725
	6	0.46	2300	10 550	0.98	9 016	700
6	1	0.415	2075	10 325	0.88	8 134	680
	2	0.37	1850	9 975	0.78	7 252	665
	3	0.325	1625	9 500	0.69	6 370	650
	4	0.28	1400	9 025	0.59	5 488	635
	5	0.26	1300	8 575	0.55	5 096	625
	6	0.285	1425	8 300	0.60	5 586	620

drop which may exist in this gap is, however, evaluated by investigating the influence of a higher UO_2 surface temperature. Temperature discontinuities in the UO_2 have not been investigated, and it is assumed that they do not exist. The influence of a higher cladding temperature as a result of flow uncertainties has been investigated.

The temperature distribution in a cored pellet is given by the expression:

$$\int_{T_r}^{T_b} k dT = \frac{Q}{2\pi l}\left[\frac{r^2 - b^2}{2(b^2 - a^2)} + \frac{a^2}{b^2 - a^2} \ln\left(\frac{b}{r}\right)\right], \qquad (2)$$

where

T_c = temperature of cladding, °F,

Q = heat generation, Btu/hr,

l = length of fuel pellet, ft,

k = thermal conductivity, Btu/hr·ft·°F,

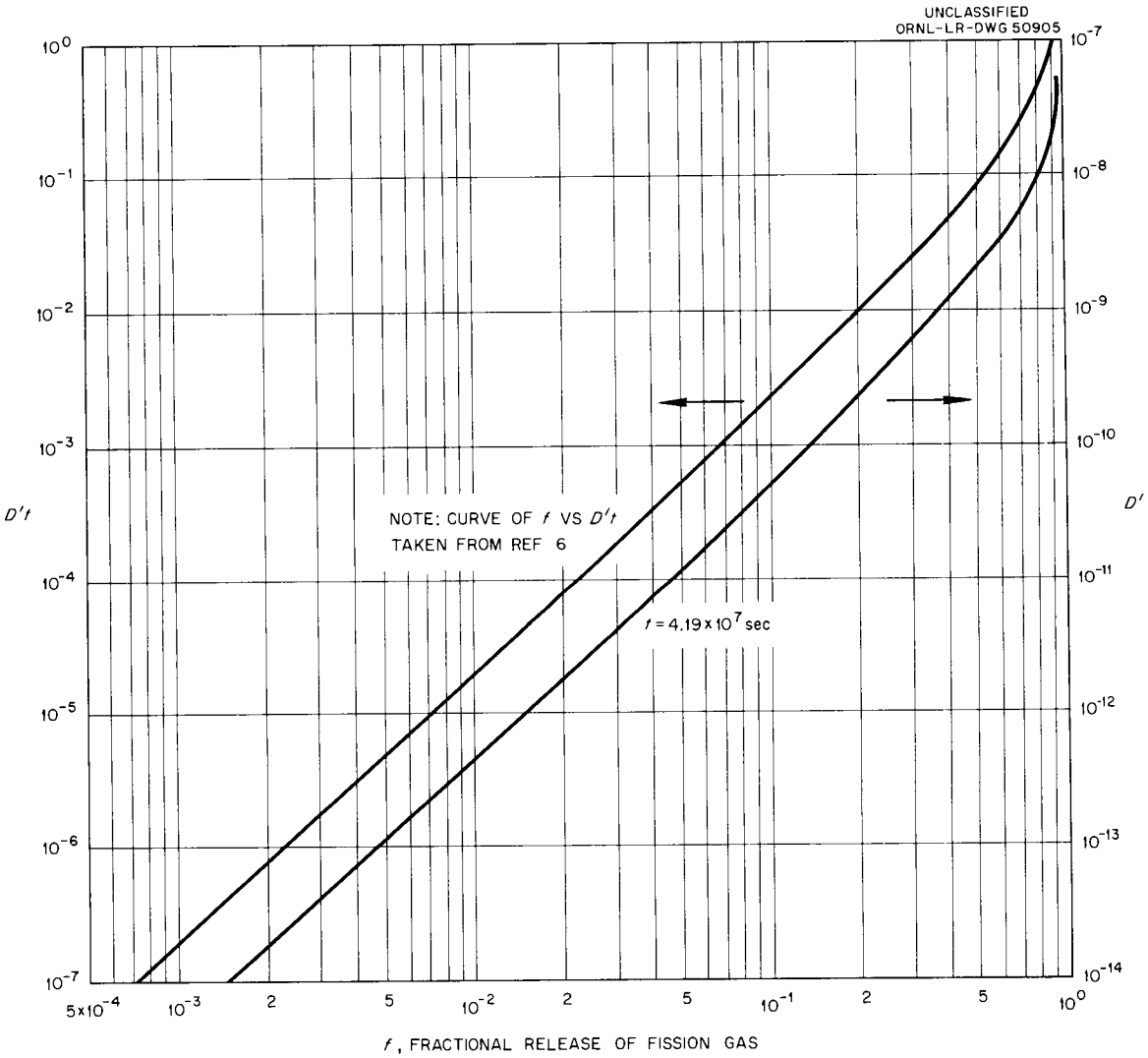

Fig. A.1. Fractional Release of Fission Gas from UO_2 as a Function of D′t and D′.

b = outside radius of pellet, ft,

a = inside radius, ft,

r = distance from center of pellet, ft,

T(r) = temperature at r, °F.

Since

$$H = \frac{Q}{l} \quad ,$$

and, for the case under consideration, a = 0.1615 in. and b = 0.3525 in.,

$$\int_{T_r}^{T_b} k dT = 0.159\ H \left[\frac{r^2 - 0.124}{0.198} + 0.253 \ln \frac{0.3525}{r} \right] \quad . \qquad (3)$$

The uncertainty in the thermal conductivity of UO_2 is discussed in Section 3.1, and Fig. 3.1 shows the various values of k reported in the literature. For this analysis the thermal conductivity is assumed to follow the following relationship:

$$k = 84\ T^{-0.535} \quad , \qquad (4)$$

where T is in °F. Therefore, substituting Eq. (4) in Eq. (3),

$$T_r^{0.465} = T_b^{0.465} - 4.45 \times 10^{-3}\ H \left[(r^2 - 0.124) + 0.05 \ln \left(\frac{0.3525}{r} \right) \right] \quad . \qquad (5)$$

Four cases are studied in this analysis. For case I, the inner cladding temperature is as shown in Fig. 6.1 (i.e., 1400 to 1450°F). For cases II, III, and IV, the UO_2 surface temperatures in position 2 are arbitrarily assumed to be 300, 600, and 900°F higher, respectively, than for case I. The higher temperatures for cases II, III, and IV could be due either to a gap between the UO_2 and the cladding or to a

higher outer cladding surface temperature. The temperature distribution in the fuel in position 2 for these various conditions is shown in Figs. A.2 through A.5.

In order to compute the fission-gas release in a rod in position 2, the rod is divided into six equal subdivisions along its length, which have been identified as subdivisions 1–6. Each subdivision is then subdivided into shells in order to obtain an effective temperature of the shell in the subdivision. The subdivisions were arbitrarily divided into ten shells of equal volume. The shell boundaries are indicated in Figs. A.2 through A.5. It was also assumed that the effective temperature for calculating D′ values for the shell is given by the expression

$$T_{eff} \approx \frac{2T_{max} + T_{min}}{3} \quad . \tag{6}$$

A.2. Fission-Gas Release

Fission-gas release from a given shell in a particular fuel rod subdivision is obtained with the following steps:

1. Compute the effective temperature from Eq. (6) using the data of Figs. A.2 through A.5.

2. Determine D′ from Eq. (1), using the temperature found in step 1.

3. Obtain f from Fig. A.1, using the value of D′ found in step 2.

Values of the fractional release from the subdivisions are given in Tables A.2 through A.5 for the case of $D'_{1400} = 2.4 \times 10^{-9}$ and for the four cases of assumed UO_2 surface temperatures. Similar calculations for other values of D′ are not included, but the results of these calculations are shown in Figs. A.6 and A.7. The results indicate that the fractional release is extremely sensitive to the UO_2 surface temperature and to D′. From Fig. A.7 it may be seen that for a value of $D' = 10^{-9}$, the amount of fission gas released will increase by about 8% for each additional 100°F increase in the UO_2 temperature.

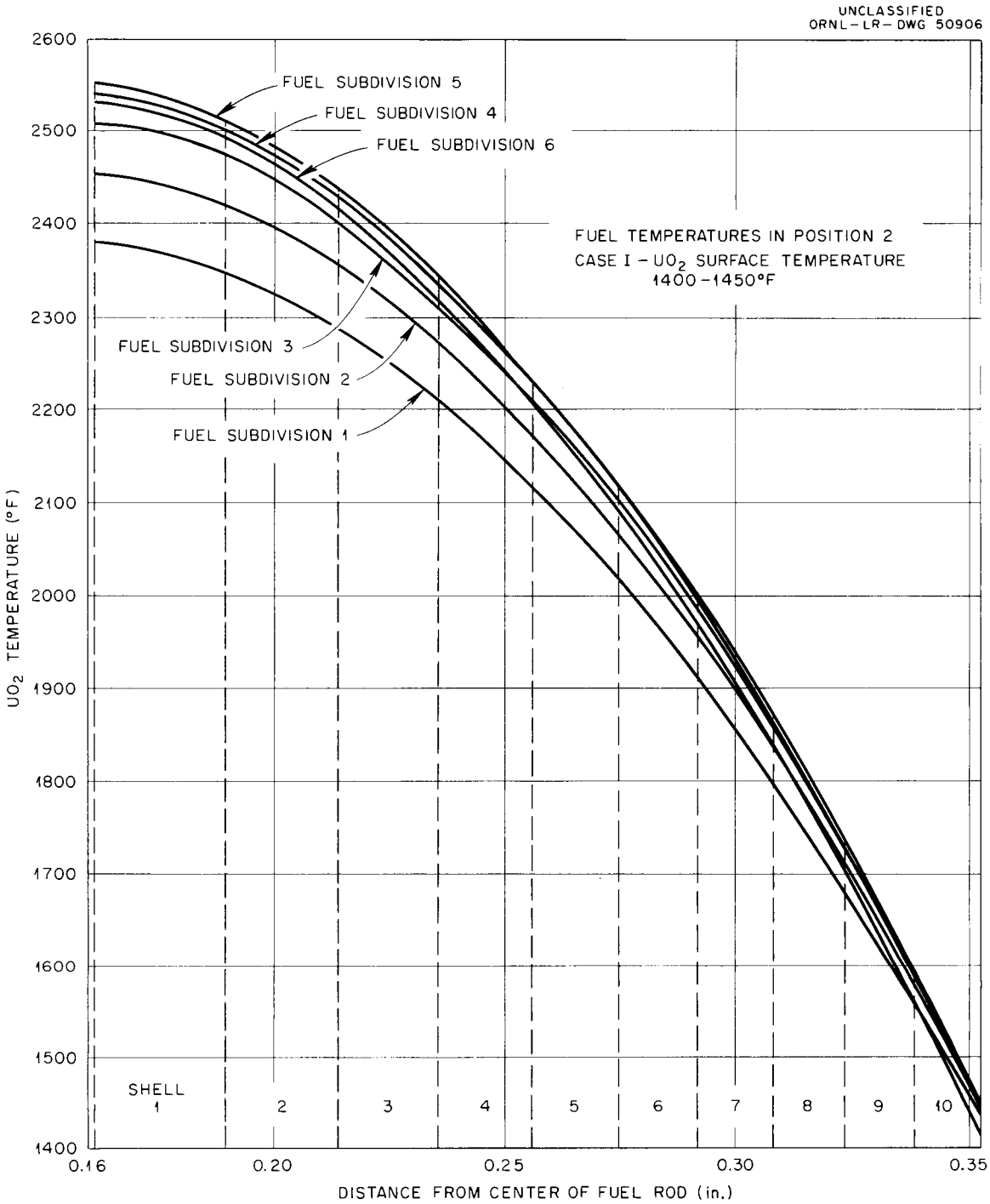

Fig. A.2. Fuel Temperature Distribution — Case I.

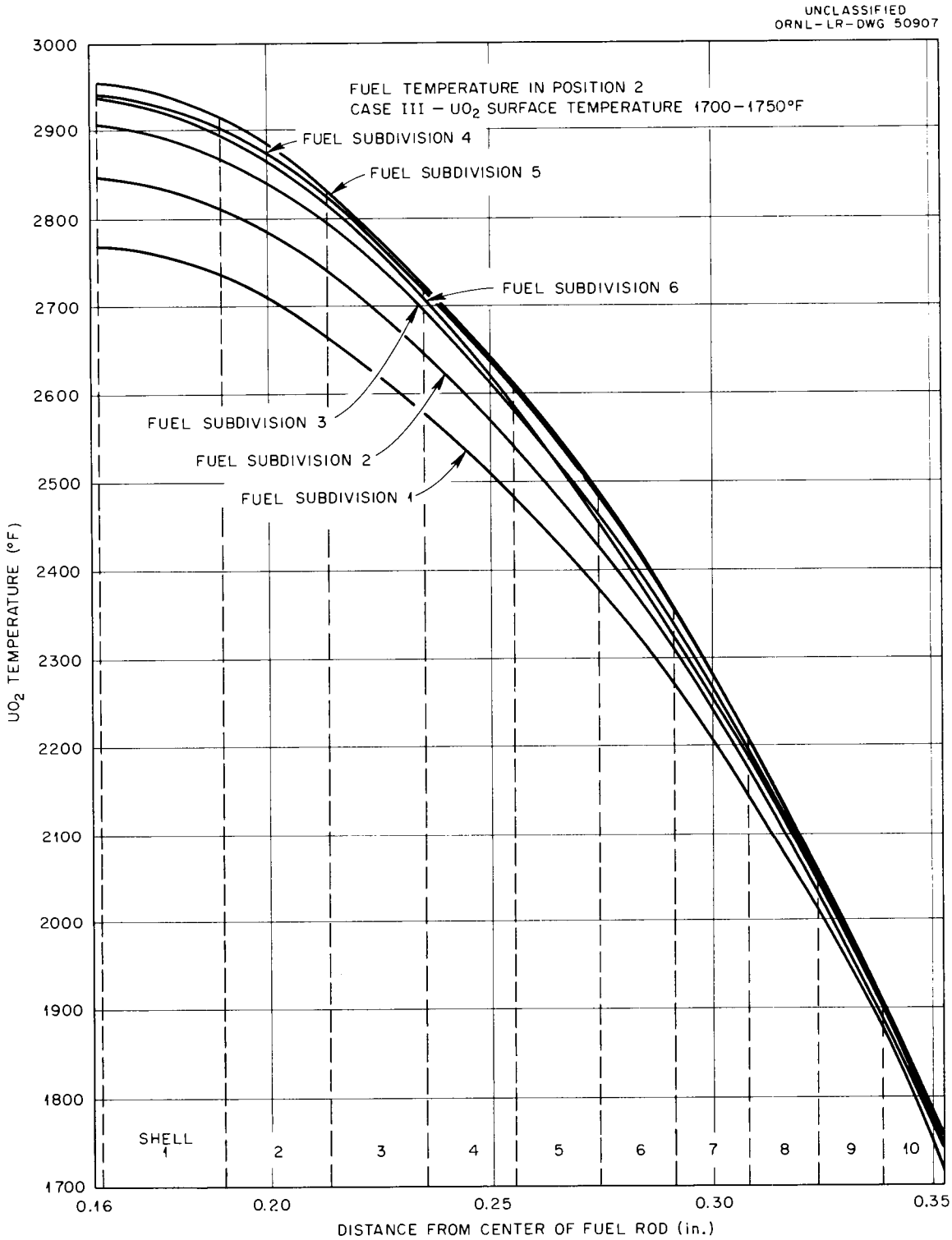

Fig. A.3. Fuel Temperature Distribution – Case II.

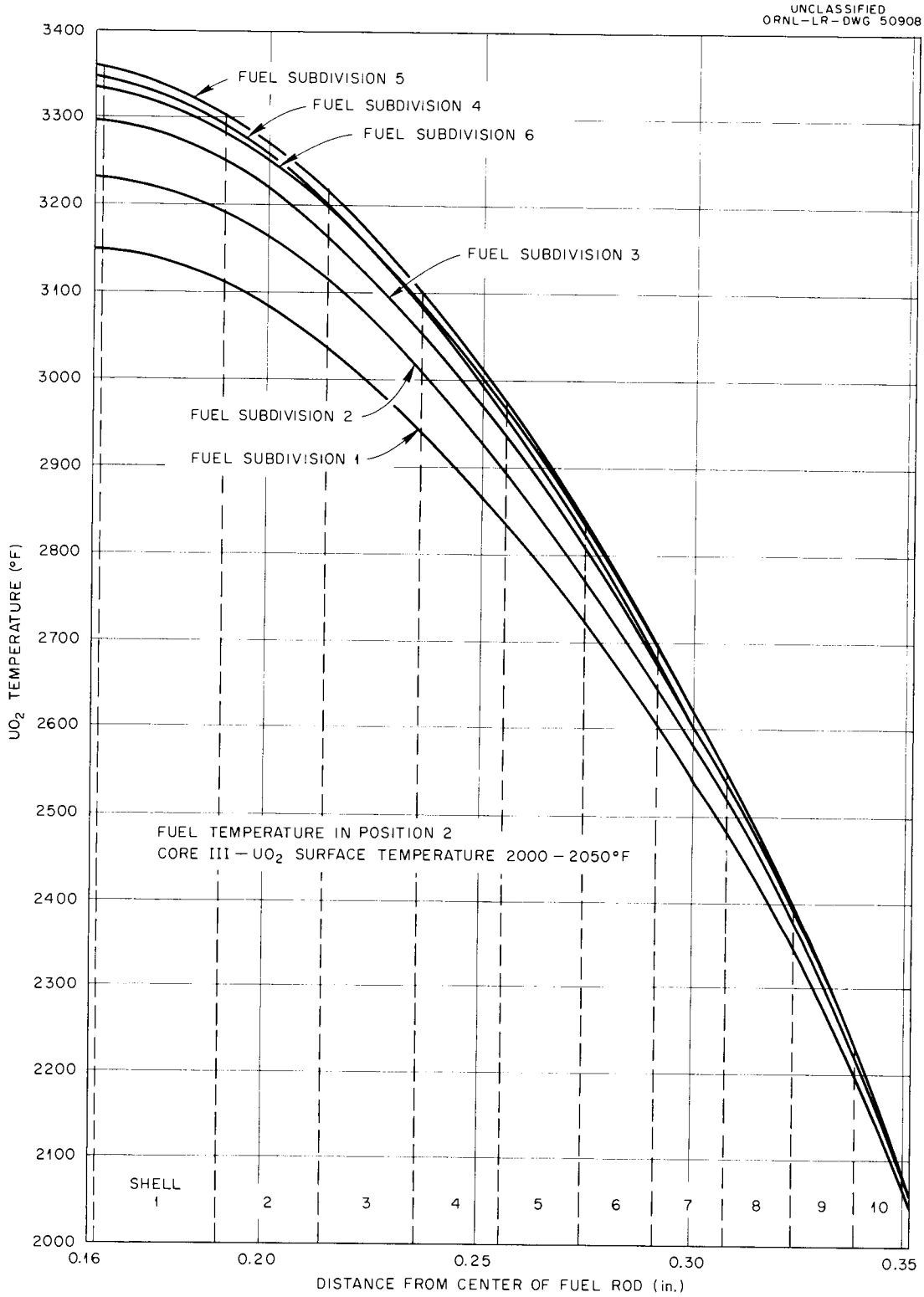

Fig. A.4. Fuel Temperature Distribution – Case III.

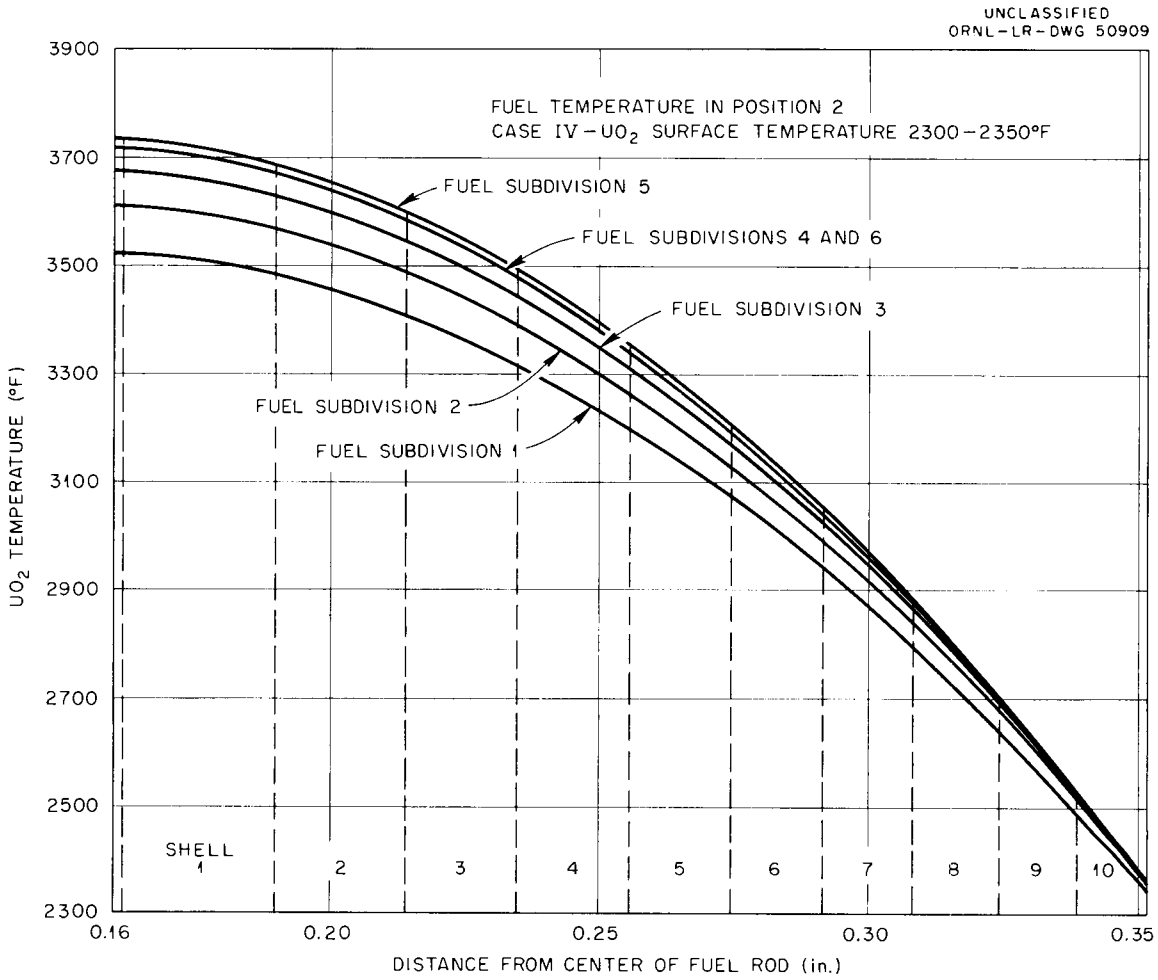

Fig. A.5. Fuel Temperature Distribution — Case IV.

Table A.2. Release of Fission Products – Case I

Shell	Fission Products Released (%)					
	Fuel Rod Subdivision					
	1	2	3	4	5	6
1	32.0	42.0	50	53.5	56.0	51.0
2	28.0	37.0	43	46.0	47.0	45.0
3	23.0	29.0	34	36.0	39.0	35.0
4	16.5	21.5	24.5	26.0	27.0	25.0
5	11.5	14.5	17	18.0	18.5	16.5
6	7.2	9.2	10.5	11.5	11.7	10.0
7	4.6	5.2	6.0	6.4	6.5	5.6
8	2.15	2.55	3.0	3.0	3.2	2.85
9	1.05	1.25	1.35	1.35	1.35	1.17
10	0.45	0.52	0.52	0.52	0.52	0.45
Average for fuel rod subdivision	12.65	16.27	18.99	20.23	21.08	19.26

Table A.3. Release of Fission Products – Case II

Shell	Fission Products Released (%)					
	Fuel Rod Subdivision					
	1	2	3	4	5	6
1	81.0	88.0	90.0	92.0	92.5	92.0
2	76.0	84.0	88.0	90.0	90.0	89.0
3	66.0	76.0	81.0	83.0	83.0	83.0
4	54.0	63.0	67.0	72.0	72.0	72.0
5	44.0	49.0	54.0	58.0	58.0	55.0
6	30.0	34.5	39.5	41.0	41.0	37.5
7	20.0	22.5	25.0	26.0	26.0	24.0
8	12.5	13.8	15.5	15.5	15.5	15.5
9	7.0	8.6	8.6	8.6	8.6	8.6
10	3.35	3.35	3.35	3.35	3.35	3.35
Average for fuel rod subdivision	39.39	44.28	47.20	48.95	49.00	48.00

Table A.4. Release of Fission Products — Case III

Shell	Fission Products Released (%)					
	Fuel Rod Subdivision					
	1	2	3	4	5	6
1	97.0	98.0	99.0	100.0	100.0	100.0
2	96.0	97.0	98.0	99.0	99.0	99.0
3	94.0	96.0	97.0	97.0	98.0	97.0
4	90.0	93.0	96.0	96.0	97.0	96.0
5	82.0	87.0	90.0	91.0	91.0	92.0
6	72.0	78.0	80.0	80.0	83.0	83.0
7	58.0	65.0	66.0	67.0	67.0	67.0
8	41.0	46.5	46.5	46.5	46.5	46.5
9	29.5	29.5	29.5	29.5	29.5	29.5
10	16.5	16.5	16.5	16.5	16.5	16.5
Average for fuel rod subdivision	67.60	70.65	71.85	72.25	72.75	72.65

Table A.5. Release of Fission Products — Case IV

Shell	Fission Products Released (%)					
	Fuel Rod Subdivision					
	1	2	3	4	5	6
1	100.0	100.0	100.0	100.0	100.0	100.0
2	100.0	100.0	100.0	100.0	100.0	100.0
3	100.0	100.0	100.0	100.0	100.0	100.0
4	99.0	100.0	100.0	100.0	100.0	100.0
5	97.0	99.0	99.0	100.0	100.0	100.0
6	96.0	97.0	97.0	97.0	98.0	97.0
7	91.0	92.0	94.0	95.0	95.0	95.0
8	78.0	80.0	82.0	82.0	82.0	82.0
9	62.0	68.0	68.0	68.0	68.0	68.0
10	42.0	42.0	42.0	42.0	42.0	42.0
Average for fuel rod subdivision	86.5	87.8	88.2	88.4	88.5	88.4

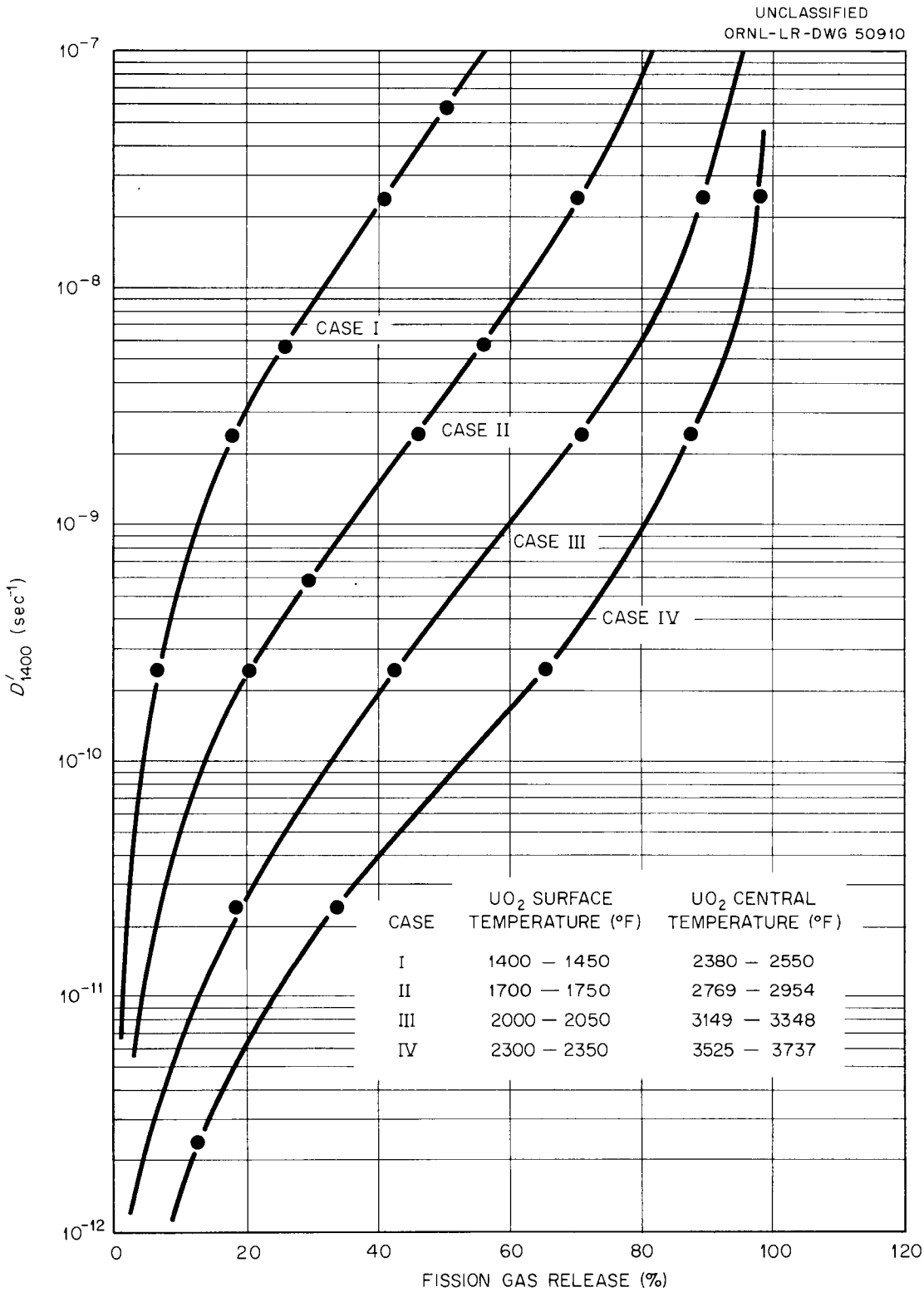

Fig. A.6. Fission-Gas Release as a Function of D′.

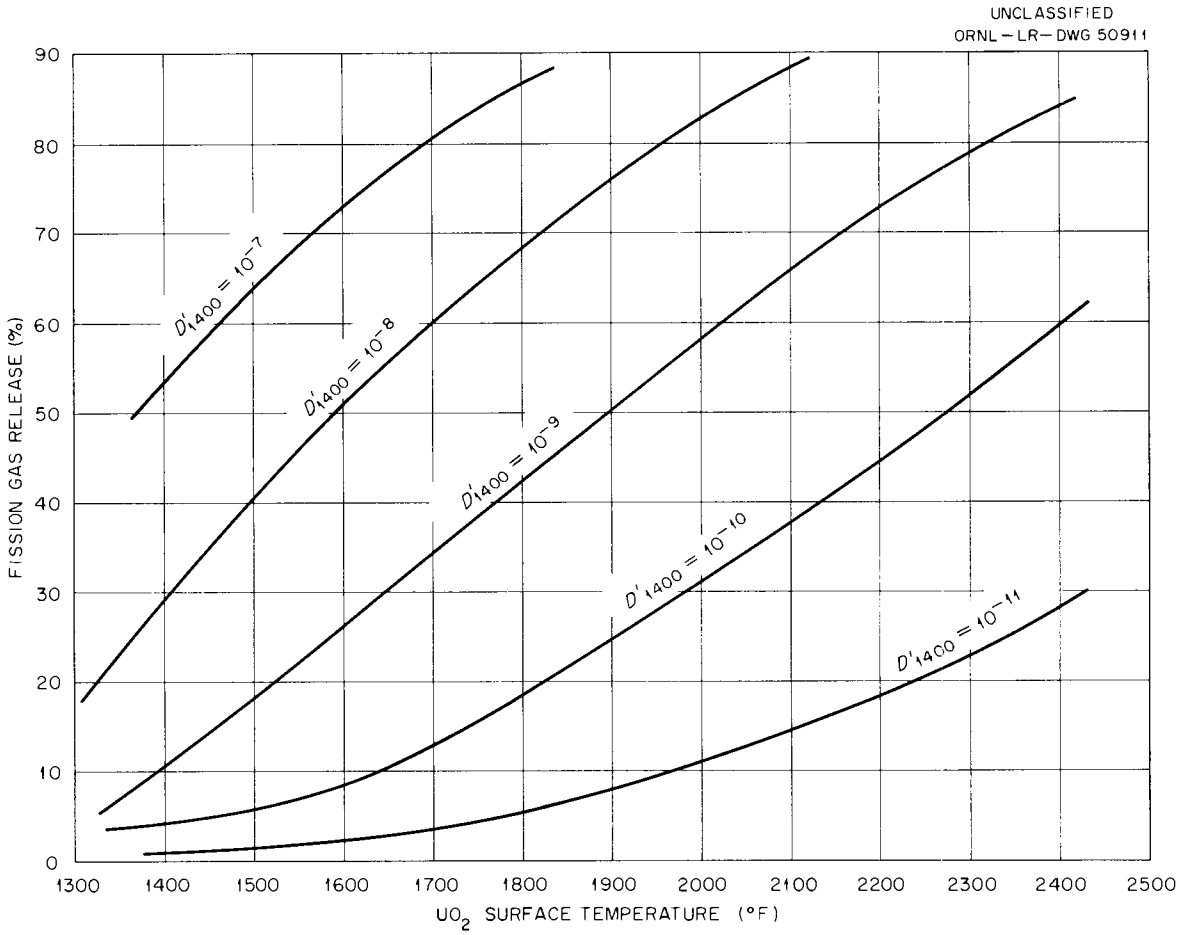

Fig. A.7. Fission-Gas Release as a Function of Surface Temperature.

A.3. Pressure Buildup in Fuel Elements

The atoms of xenon produced in a fuel rod subdivision are given by the expression:

$$N_p = 3 \times 10^{10} \gamma_{Xe} Pt \quad ,$$

where P is power in watts, t is time in seconds, and γ_{Xe} is the total fission yield of stable atoms of xenon. Neglecting radioactive species,

$$\gamma_{Xe} = 22.2 \quad .$$

Including the capture in Xe^{135} to produce Xe^{136} (stable),

$$\gamma_{Xe} = 22.2 + 6.2 \frac{\sigma\phi}{\sigma\phi + \lambda} \quad .$$

Since the flux varies in each fuel subdivision, the average flux in the reactor is multiplied by the factors indicated in Fig. 6.1.

The exposure time from Fig. 6.1 is 4.19×10^7 sec. Relative values of P are given in Table A.1 and Fig. 6.1. Upon substituting values,

$$N_p = (3 \times 10^{10})(4.19 \times 10^7)\ P \left[22.2 + 6.2 \frac{\sigma\phi}{\sigma\phi + \lambda}\right] 10^{-2}$$

$$= 1.26 \times 10^{16}\ P\gamma_{Xe} \quad .$$

The total number of atoms released from the fuel is given in Table A.6.

The atoms of nuclides other than xenon released from the fuel will be equal to the values given in Table A.6 multiplied by the ratio of γ_i/γ_{Xe}. Therefore, using a total yield for krypton of 4.0 and 18.6 for cesium, the atoms of cesium and krypton released are as indicated in Table A.7, compared with the xenon atoms released.

The volumes of the gases at standard conditions (0°C and 14.7 psia) are given by

$$V_{Xe} = \frac{\text{atoms of Xe}}{6.02 \times 10^{23}} (22\ 414) = 3.72 \times 10^{-20}\ (\text{atoms of Xe})\ \text{cm}^3$$

and

$$V_{Kr} = \frac{\text{atoms of Kr}}{6.02 \times 10^{23}} (22\ 414) = 3.72 \times 10^{-20}\ (\text{atoms of Kr})\ \text{cm}^3 \quad .$$

The volume for storing gases inside the fuel element is ~42 cm^3; therefore for xenon and krypton, the partial pressure is

Table A.6. Atoms of Xenon Released from EGCR Fuel

Fuel Rod Subdivision	Power Generation (watts)	γ_{Xe}	Atoms of Xenon Produced	D'_{1400} (sec^{-1})	Fractional Release of Xenon				Atoms of Xenon Released			
					Case I	Case II	Case III	Case IV	Case I	Case II	Case III	Case IV
			$\times 10^{21}$						$\times 10^{20}$	$\times 10^{20}$	$\times 10^{20}$	$\times 10^{20}$
1	2990	26.4	0.995	2.4×10^{-8}	0.3299	0.6658	0.893	0.981	3.28	6.62	8.89	9.76
2	3160	26.5	1.06		0.3930	0.6943	0.899	0.9815	4.17	7.36	9.53	10.40
3	3310	26.5	1.11		0.4264	0.7103	0.901	0.9825	4.73	7.88	10.00	10.91
4	3420	26.6	1.15		0.4411	0.7193	0.901	0.9825	5.07	8.27	10.36	11.30
5	3480	26.6	1.17		0.4493	0.7193	0.901	0.9825	5.26	8.42	10.54	11.50
6	3500	26.6	1.17		0.4278	0.7113	0.901	0.9825	5.01	8.32	10.54	11.50
Total			6.655						27.52	46.87	59.86	65.37
1	2990	26.4	0.995	2.4×10^{-9}	0.1265	0.3939	0.676	0.865	1.26	3.92	6.73	8.61
2	3160	26.5	1.06		0.1627	0.4428	0.7065	0.878	1.72	4.65	7.49	9.31
3	3310	26.5	1.11		0.1899	0.4720	0.7185	0.882	2.11	5.24	7.98	9.79
4	3420	26.6	1.15		0.2023	0.4895	0.7225	0.884	2.33	5.63	8.31	10.17
5	3480	26.6	1.17		0.2108	0.4900	0.7275	0.885	2.47	5.73	8.51	10.35
6	3500	26.6	1.17		0.1926	0.4800	0.7265	0.884	2.25	5.62	8.50	10.34
Total			6.655						12.14	30.83	47.52	58.57
1	2990	26.4	0.995	2.4×10^{-10}	0.0431	0.1571	0.367	0.6115	0.429	1.56	3.65	6.08
2	3160	26.5	1.06		0.0568	0.1879	0.4052	0.643	0.602	1.99	4.30	6.82
3	3310	26.5	1.11		0.0672	0.2097	0.4307	0.665	0.746	2.33	4.78	7.38
4	3420	26.6	1.15		0.0722	0.2246	0.4492	0.670	0.831	2.58	5.17	7.71
5	3480	26.6	1.17		0.0754	0.2271	0.4592	0.675	0.883	2.66	5.37	7.90
6	3500	26.6	1.17		0.0687	0.2185	0.4547	0.670	0.804	2.56	5.32	7.84
Total			6.655						4.295	13.68	28.59	43.73
1	2990	26.4	0.995	2.4×10^{-11}			0.1376	0.2868			1.37	2.85
2	3160	26.5	1.06				0.1591	0.3225			1.69	3.42
3	3310	26.5	1.11				0.1747	0.3475			1.94	3.86
4	3420	26.6	1.15				0.1849	0.3585			2.13	4.12
5	3480	26.6	1.17				0.1914	0.3635			2.24	4.25
6	3500	26.6	1.17				0.1869	0.3585			2.19	4.19
Total			6.655								11.56	22.69
1	2990	26.4	0.995	2.4×10^{-12}				0.1026				1.02
2	3160	26.5	1.06					0.1173				1.24
3	3310	26.5	1.11					0.1284				1.43
4	3420	26.6	1.15					0.1334				1.53
5	3480	26.6	1.17					0.1357				1.59
6	3500	26.6	1.17					0.1334				1.56
Total			6.655									8.37

Table A.7. Atoms of Fission Gas Released from EGCR Fuel

D'	Atoms of Xenon Released				Atoms of Krypton Released				Atoms of Cesium Released			
	Case I	Case II	Case III	Case IV	Case I	Case II	Case III	Case IV	Case I	Case II	Case III	Case IV
	$\times 10^{20}$	$\times 10^{20}$	$\times 10^{20}$	$\times 10^{20}$	$\times 10^{20}$	$\times 10^{20}$	$\times 10^{20}$	$\times 10^{20}$	$\times 10^{20}$	$\times 10^{20}$	$\times 10^{20}$	$\times 10^{20}$
2.4×10^{-8}	27.52	46.87	59.86	65.37	4.15	7.06	9.02	9.85	19.28	32.84	41.94	45.80
2.4×10^{-9}	12.14	30.83	47.52	58.57	1.88	4.64	7.16	8.82	8.50	21.60	33.29	41.03
2.4×10^{-10}	4.295	13.68	28.59	43.73	0.647	2.06	4.31	6.59	3.01	9.58	20.03	30.64
2.4×10^{-11}			11.56	22.69			1.74	3.42			8.10	15.90
2.4×10^{-12}				8.37				1.26				5.86

$$p_i = \frac{(14.7)(3.72 \times 10^{-20})(\text{atoms of i})(\text{temperature})}{(42)(492)}$$

$$= 2.65 \times 10^{-23}\ N_i T \quad ,$$

where i is xenon or krypton and T is temperature in °R.

The gas temperature inside the fuel element is given in Table A.8 as obtained by averaging the values at the fuel subdivision inner surface given in Figs. A.2 through A.5.

The pressure in the rod at 485 days is indicated in Table A.9 and is plotted in Figs. A.8 and A.9. It may be seen in Fig. A.8 that if $D'_{1400} = 10^{-9}$ for case I, the pressure buildup is 160 psia. This compares with the 144 psia shown in Fig. 5.9 for comparable conditions. The difference in the results is due to the assumptions made for the two cases. In the hand calculation the gases were assumed to be at an average UO_2 central temperature, whereas in the machine calculations allowance was made for some gases being at colder temperatures at the ends of the rods.

Table A.8. UO_2 Temperatures

Fuel Rod Subdivision	UO_2 Inner Surface Temperature (°F)			
	Case I	Case II	Case III	Case IV
1	2380	2768.6	3149	3525
2	2454.7	2847.3	3232.7	3612.9
3	2508.9	2905.8	3294.5	3679.3
4	2540.8	2941.4	3334.2	3720.7
5	2550.1	2953.7	3348.2	3736.8
6	2530.9	2935.5	3330.6	3720.5
Average	2494.2°F 2954.2°R	2892.1°F 3352.1°R	3281.5°F 3741.5°R	3665.9°F 4125.9°R

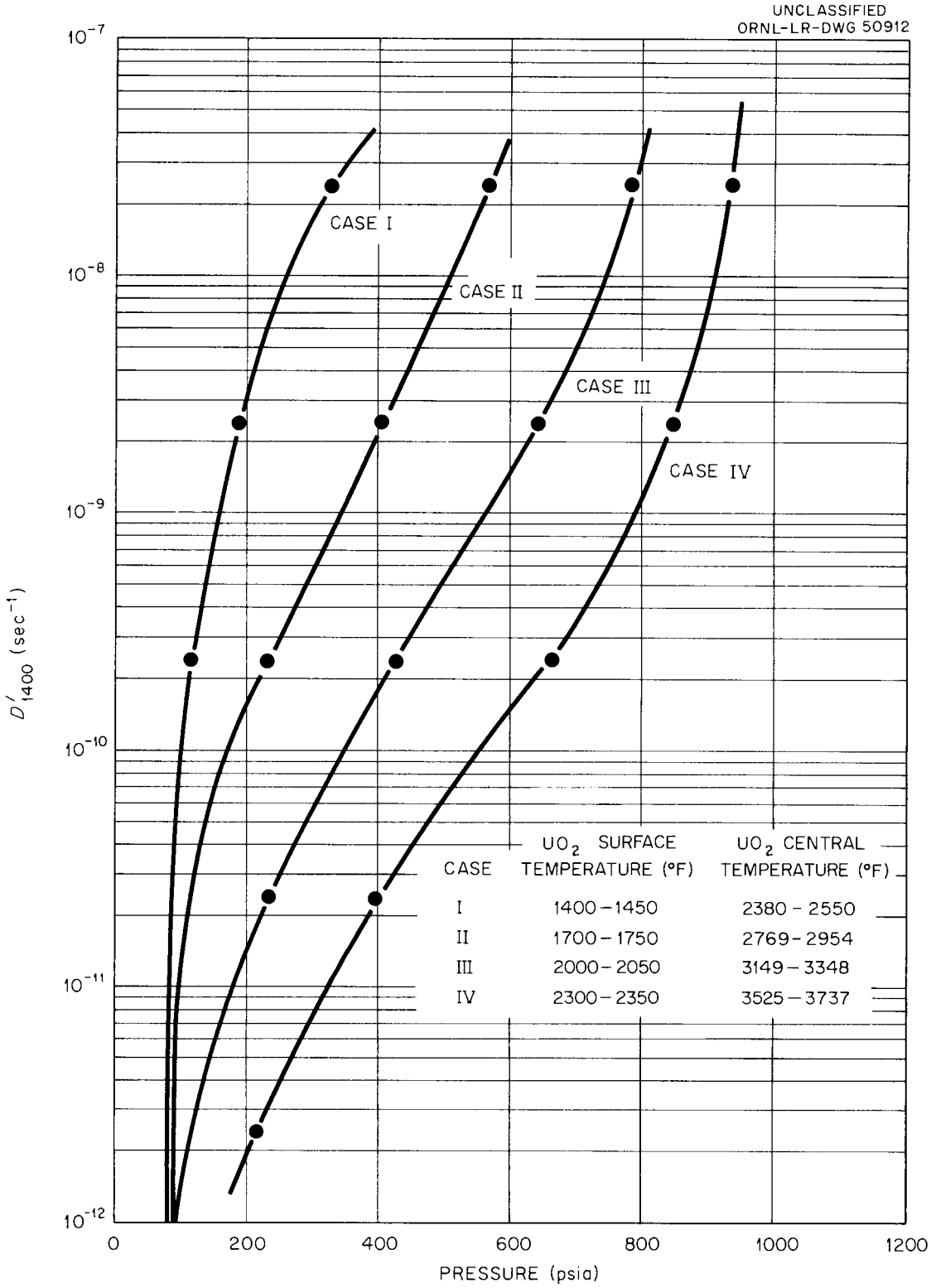

Fig. A.8. Pressure as a Function of D′.

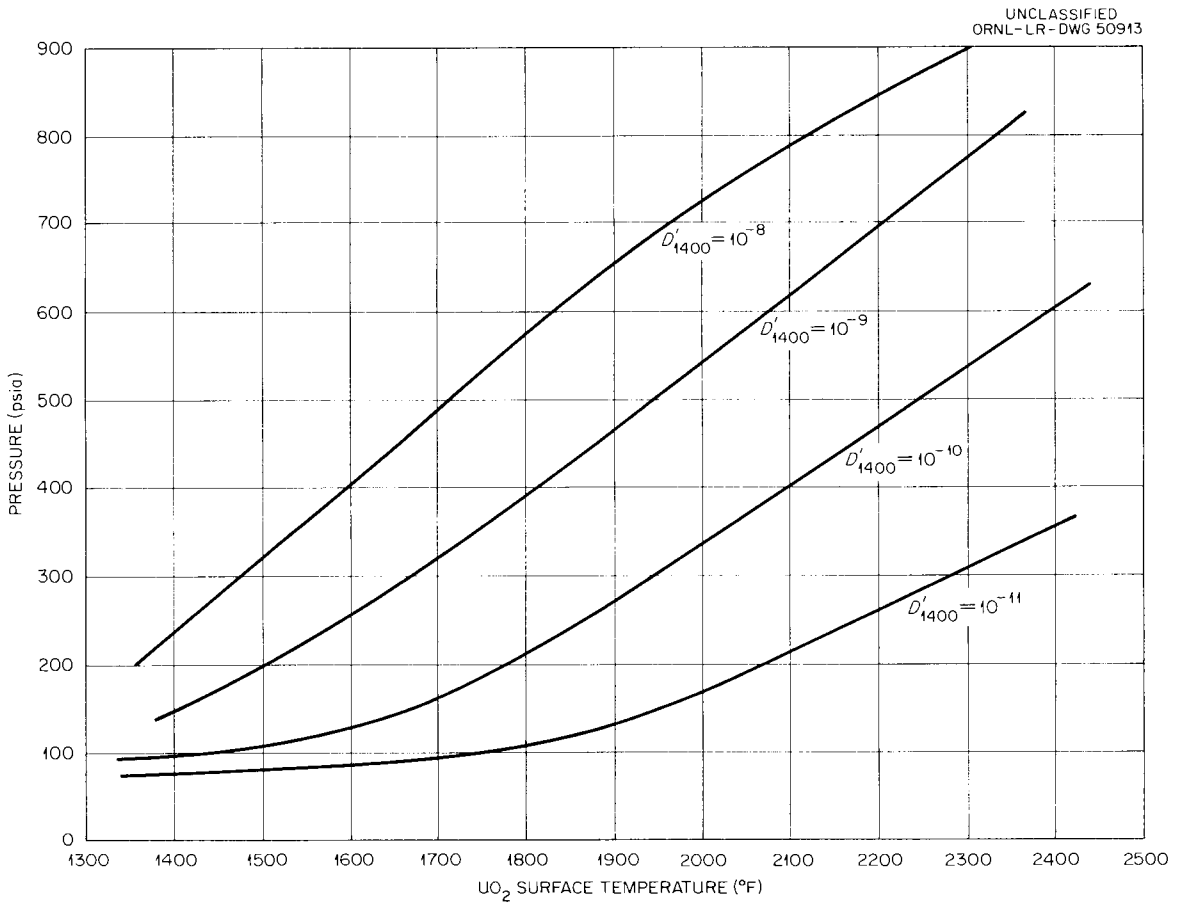

Fig. A.9. Pressure as a Function of Surface Temperature.

Table A.9. Pressure in Fuel Rod

Case	Assumed Value of D'_{1400} (sec^{-1})	Partial Pressures (psia)			Total Pressure (psia)
		Xe	Kr	He	
I	2.4×10^{-8}	215.44	32.49	79.68	327.61
	2.4×10^{-9}	95.04	14.33	79.68	189.05
	2.4×10^{-10}	33.62	5.07	79.68	118.37
II	2.4×10^{-8}	416.35	62.71	90.41	569.47
	2.4×10^{-9}	273.86	41.22	90.41	405.49
	2.4×10^{-10}	121.52	18.30	90.41	230.23
III	2.4×10^{-8}	593.51	89.43	100.92	783.86
	2.4×10^{-9}	471.16	70.99	100.92	643.07
	2.4×10^{-10}	283.47	42.73	100.92	427.12
	2.4×10^{-11}	114.62	17.25	100.92	232.79
IV	2.4×10^{-8}	714.73	107.70	111.28	933.71
	2.4×10^{-9}	640.38	96.43	111.28	848.09
	2.4×10^{-10}	478.13	72.05	111.28	661.46
	2.4×10^{-11}	248.08	37.39	111.28	396.75
	2.4×10^{-12}	91.51	13.78	111.28	216.57

A.4. Partial Pressure Due to Cesium

The pressures shown in Figs. A.8 and A.9 include the partial pressures due to the stable fission gases xenon and krypton. When UO_2 is operated at high temperatures, fission products such as I, Br, Xe, Kr, Rb, and Cs will also tend to diffuse from the oxide. An analysis of the chains of these diffusing nuclei indicates that, in addition to the stable gases xenon and krypton, conditions are favorable in some cases for the buildup of appreciable amounts of cesium. The number of atoms of cesium which escape from the UO_2 are given in Table A.7 for the assumed D' values. The vapor pressure of cesium as a function of temperature is shown in Fig. A.10. If it is assumed that the lowest temperature of the fuel cladding for case I is 1100°F (the low temperature is at the end where there is no heat generation), then the maximum partial pressure due to cesium would be ~6 psia. If it is assumed for

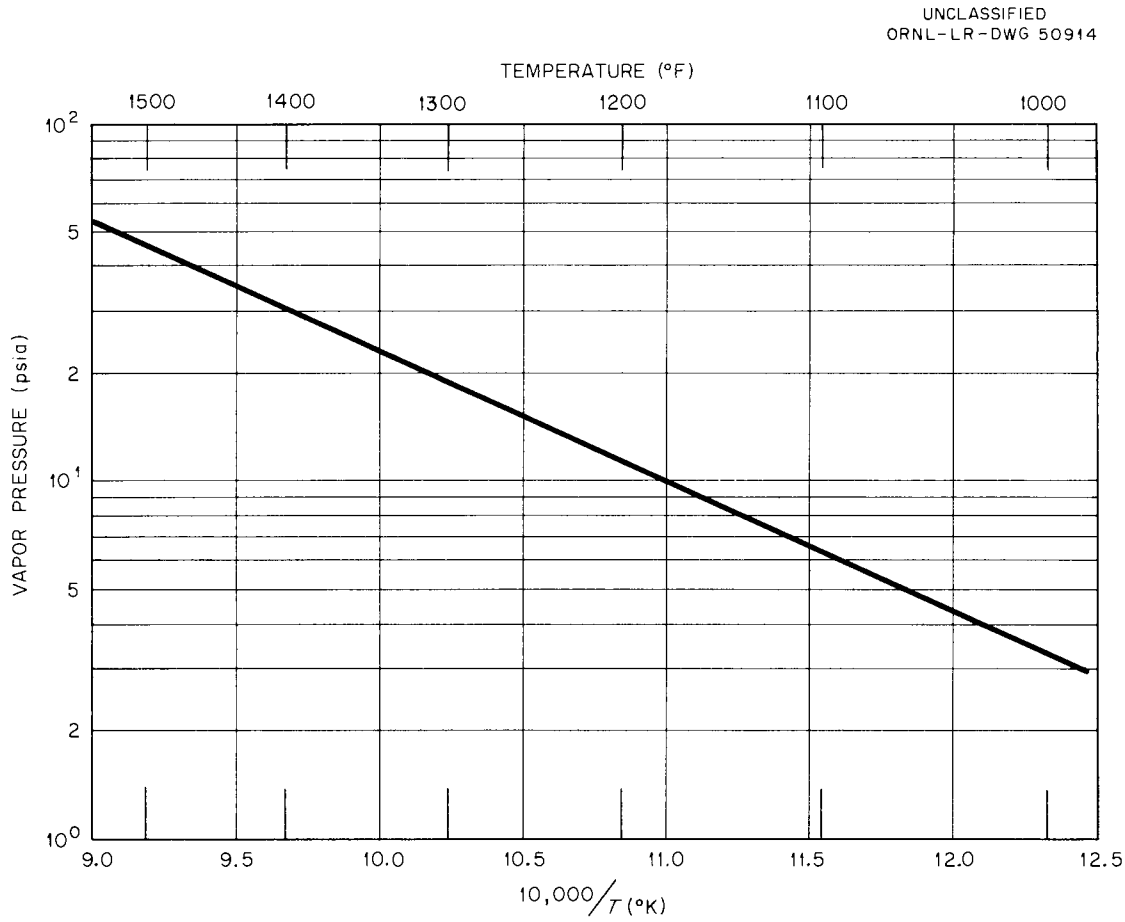

Fig. A.10. Vapor Pressure of Cesium.

cases II, III, and IV that the cladding temperature does not exceed 1300°F, the maximum partial pressure due to cesium is 19 psia. These pressures are small compared with the pressure buildup due to xenon, krypton, and helium and are therefore not included in Figs. A.8 and A.9.

REFERENCES

1. "The ORNL Gas-Cooled Reactor," ORNL-2500 (April 1, 1958).

2. A. H. Booth and G. T. Rymer, "Determination of the Diffusion Constant of Fission Xenon in UO_2 Crystals and Sintered Compacts," CRDC-720 (August 1958).

3. J. D. Eichenberg et al., "Effects of Irradiation on Bulk UO_2," pp. 24–36, WAPD-183 (Oct. 1957).

4. V. R. Lindner and H. J. Matzke, "Some Tests on the Diffusion of Xe-133 from Oxides of Uranium," Z. Naturforsch. 13a, 794 (1958).

5. W. B. Cottrell et al., "The HGCR-1, A Design Study of a Nuclear Power Station Employing a High-Temperature Gas-Cooled Reactor with Graphite-UO_2 Fuel Elements," p. 119, ORNL-2653 (July 1959).

6. A. H. Booth, "A Method of Calculating Fission Gas Diffusion from UO_2 Fuel and its Application to the x-2-f Loop Test," CRDC-721 (Sept. 1957).

7. B. Lustman, "Release of Fission Gases from UO_2," WAPD-173 (March 1957).

8. J. Crank, "The Mathematics of Diffusion," p. 84, Clarendon Press, Oxford, 1956.

9. W. B. Lewis, "The Significance of Developing a High Performance Uranium Oxide Fuel," AECL-DM-44 (April 27, 1957).

10. J. A. L. Robertson et al., "Behavior of Uranium Oxide as a Reactor Fuel," A/Conf.15/P/193 (June 23, 1958).

11. M. W. Rosenthal, "Pandora — A Computer Program for Estimating Fission-Gas Release and Its Effect on the Mechanical Life of Clad Fuel Elements," ORNL CF-60-5-1 (to be published).

12. A. H. Booth, "A Suggested Method for Calculating the Diffusion of Radioactive Rare Gas Fission Products in UO_2," DCI-27 (Sept. 1957).

13. "GCR Semiann. Prog. Rep. Dec. 31, 1958," ORNL-2676, p. 67.

14. M. W. Rosenthal, "The Effect of Closed Porosity on the Accuracy of the Model for Fission-Gas Release from UO_2," ORNL CF-59-11-24 (Nov. 10, 1959).

15. W. B. Lewis, "Uranium Dioxide," AECL-DL-34 (Dec. 1, 1958).

16. J. A. Davies and R. O. Kelly, personal communication, April 30, 1959.

17. J. Belle and B. Lustman, "Properties of Uranium Dioxide," pp. 15–33, WAPD-184 (Sept. 1957).

18. V. J. Tennery, "Review of Thermal Conductivity and Heat Transfer in Uranium Dioxide," ORNL-2656 (April 1959).

19. A. M. Ross, "A Literature Survey of the Measurement of Thermal Conductivity of Several Solids Including Uranium Dioxide," CRFD-762 (March 1958).

20. W. D. Kingery et al., "Thermal Conductivity, Data for Several Pure Oxide Materials Corrected to Zero Porosity," Journal of American Ceramic Society, Part II, p. 107 (Feb. 1954).

21. J. C. Hedge and I. B. Fieldhouse, "Measurement of Thermal Conductivity of Uranium Oxide," AECU-3381 (Sept. 1956).

22. R. Scott, "Thermal Conductivity of UO_2," AERE M/R 2526 (1958).

23. "Progress Relating to Civilian Applications During January 1959," p. 7, BMI-1315 (Feb. 1, 1959).

24. "Quarterly Progress Report Fuels Development Operation," p. 5.14, HW-59235 (Jan. 15, 1959).

25. "Atomic Energy of Canada Limited, Progress Report Chemistry and Metallurgy Division, July 1, 1958 to Sept. 30, 1958," p. 71 ff, PR-CM-15.

26. "Atomic Energy of Canada Limited, Progress Report Chemistry and Metallurgy Division, Oct. 1, 1958 to Dec. 31, 1958," p. 81, PR-CM-16.

27. R. W. Nichols, "Ceramic Fuels, Properties and Technology," Nuclear Engineering, August 1958.

28. "Atomic Energy of Canada Limited, Progress Report Chemistry and Metallurgy Division, Jan. 1, 1959 to March 31, 1959," pp. 80–84, PR-CM-17.

29. "Atomic Energy of Canada Limited, Progress Report Chemistry and Metallurgy Division, April 1, 1959 to June 30, 1959," pp. 84–85, PR-CM-18.

30. J. D. Eichenberg, "An In-Pile Measurement of the Effective Thermal Conductivity of UO_2," WAPD-200 (Sept. 1958).

31. "Technical Progress Report, Pressurized-Water Reactor (PWR) Project, April 24, 1959 to June 23, 1959," p. 58, WAPD-MRP-80.

32. J. A. L. Robertson, "$\int k d\theta$ in Fuel Irradiations," CRFD-835 (April 1959).

33. J. Belle and B. Lustman, "Properties of UO_2," pp. 18–26, 112 ff, WAPD-184 (Sept. 1957).

34. "Atomic Energy of Canada Limited, Progress Report Chemistry and Metallurgy Division, Jan. 1, 1959 to March 31, 1959," pp. 40–46, PR-CM-17.

35. "Atomic Energy of Canada Limited, Progress Report Chemistry and Metallurgy Division, April 1, 1959 to June 30, 1959," pp. 36–41, PR-CM-18.

36. J. A. L. Robertson et al., "Irradiation Behavior of UO_2 Fuel Elements, Nuclear Metallurgy Vol. VI, A Symposium of Effects of Irradiation on Fuel and Fuel Elements," November 1959.

37. O. J. C. Runnals, "Uranium Dioxide — A Promising Nuclear Fuel," CRL-51 (Jan. 1958).

38. J. Belle, "Properties of Uranium Dioxide," A/Conf.15/P/2404 (June 1958).

39. L. Tomlinson, "Measurement of Powder Surface Areas by Krypton Adsorption," IGR-TN/S 1032 (1959).

40. "GCR Semiann. Prog. Rep. June 30, 1959," ORNL-2767, p. 157 ff.

41. P. Murray, AERE Harwell Seminar at Oak Ridge National Laboratory, November 20, 1959.

42. O. J. C. Runnalls, "Uranium Dioxide Fuel Elements," CRL-55 (Jan. 28, 1959).

43. A. R. Hall, R. Scott, and J. Williams, "The Plastic Deformation of Uranium Oxides Above 800°C," AERE-M/R-2648.

44. P. Murray, S. F. Pugh, and J. Williams, "Uranium Dioxide as a Reactor Fuel, Paris Fuel Elements Conference," TID-7546 (Nov. 18–23, 1957).

45. J. L. Bates and W. E. Roake, "Irradiation of Fuel Elements Containing UO_2 Powder," Nuclear Engineering and Science Conference, Cleveland, Ohio, April 6–8, 1959, Preprint V-90.

46. "Technical Progress Report, Pressurized-Water Reactor (PWR) Project, April 24, 1959 to June 23, 1959," WAPD-MRP-80, p. 66.

47. "GCR Quar. Prog. Rep. Sept. 30, 1959," ORNL-2835, p. 80 ff.

48. T. N. Centinkale and M. Fishenden, "Thermal Conductance of Metal Surfaces in Contact," Institution of Mechanical Engineers, General Discussion on Heat Transfer, Proceedings, Sept. 11–13, 1951, p. 271.

49. W. G. Morrison, "Thermal Conductivity of Gas Mixtures in UO_2 Fuel Elements," NEI-88.

50. "GCR Quar. Prog. Rep. Sept. 30, 1959," ORNL-2835, p. 109 ff.

51. A. J. Taylor, ORNL, personal communication, January 1960.

52. J. D. Eichenberg et al., "Effects of Irradiation on Bulk UO_2," pp. 24–42, WAPD-183 (Oct. 1957).

53. "GCR Semiann. Prog. Rep. June 30, 1959," ORNL-2767, p. 147.

54. J. C. Lachman, "Calibration of Tungsten-Rhenium Thermocouples to 4000°C," APEX-365 (May 30, 1958).

55. "Atomic Energy of Canada Limited Chemistry and Metallurgy Division Progress Report, Jan. 1, 1957 to March 31, 1957," p. 52, PR-CM-9.

56. "Atomic Energy of Canada Limited, Progress Report Chemistry and Metallurgy Division, April 1, 1957 to June 30, 1957," p. 54, PR-CM-10.

57. "Atomic Energy of Canada Limited, Progress Report Chemistry and Metallurgy Division, Oct. 1, 1957 to Dec. 30, 1957," pp. 22–50, PR-CM-12.

58. D. B. Trauger, ORNL, personal communication.

59. "Atomic Energy of Canada Limited, Progress Report Chemistry and Metallurgy Division, Jan. 1, 1958 to March 31, 1958, pp. 21–45, PR-CM-13.

60. "Atomic Energy of Canada Limited, Progress Report Chemistry and Metallurgy Division, April 1, 1958 to June 30, 1958," pp. 18–43, PR-CM-14.

61. "Atomic Energy of Canada Limited, Progress Report Chemistry and Metallurgy Division, July 1, 1958 to Sept. 30, 1958," pp. 16–40, PR-CM-15.

62. "Atomic Energy of Canada Limited, Progress Report Chemistry and Metallurgy Division, Oct. 1, 1958 to Dec. 31, 1958," pp. 17–43, PR-CM-16.

63. "GCR Semiann. Prog. Rep. Dec. 31, 1958," ORNL-2676, pp. 105–137.

64. "GCR Semiann. Prog. Rep. June 30, 1959," ORNL-2767, pp. 131–171.

65. "GCR Quar. Prog. Rep. Sept. 30, 1959," ORNL-2835, pp. 104–120.

66. J. L. Scott and D. F. Toner, "The Study of Fission-Product Release from Ceramic Fuels," ORNL CF-59-12-82 (Dec. 23, 1959).

67. J. M. Markowitz, R. C. Koch, and J. A. Roll, "An Apparatus for the Measurement of Fission Gas Elimination from Fuel Materials During Pile Irradiation," WAPD-180 (1957).

68. A. H. Booth et al., "Collection and Measurement of Stable Xenon in Sheath Puncture Experiments," AECL-CRDC-719 (1957).

69. E. J. Shibbs and G. A. Walton, "The Release of Fission Product Rare Gas from Uranium-Zirconium Alloy During Neutron Irradiation," AERE-CM-372 (1958).

70. A. B. Auskern, WAPD, personal communication, April 1959.

71. W. Bostrom, WAPD, personal communication, April 1959.

72. J. Clayton, WAPD, personal communication, April 1959.

73. W. C. Thurber, ORNL, personal communication, June 1959.

74. "Experimental Gas-Cooled Reactor Preliminary Hazards Summary Report," ORO-196 (May 1959).

75. G. Samuels, ORNL, personal communication, Dec. 1959.

76. W. L. Albrecht, ORNL, personal communication, Dec. 1959.

77. "GCR Quar. Prog. Rep. Dec. 31, 1959," ORNL-2888, pp. 99–126.

78. W. K. Barney, "The Swelling of UO_2 at High Burnup," Nuclear Metallurgy Vol VI, AIME, 71 (1959).

79. O. Sisman, ORNL, personal communication.

80. O. Sisman and R. M. Carroll, ORNL, personal communication.

81. T. G. Godfrey, ORNL, personal communication.

82. M. T. Morgan, ORNL, personal communication.

ORNL-2935

Reactors – Power
TID-4500 (15th ed.)

INTERNAL DISTRIBUTION

1. G. M. Adamson
2. M. Bender
3. D. S. Billington
4. E. P. Blizard
5. C. J. Borkowski
6. G. E. Boyd
7. R. B. Briggs
8. F. L. Carlsen
9. C. E. Center (K-25)
10. R. A. Charpie
11. R. S. Cockreham
12. T. E. Cole
13. J. H. Coobs
14. J. A. Conlin
15-19. W. B. Cottrell
20. J. A. Cox
21. F. L. Culler
22-26. H. N. Culver
27. J. H. DeVan
28. L. M. Doney
29. D. A. Douglas
30. L. B. Emlet (K-25)
31. E. P. Epler
32. R. B. Evans
33. A. P. Fraas
34. J. H. Frye, Jr.
35. G. A. Garrett (K-25)
36. J. M. Googin (Y-12)
37. W. R. Grimes
38. E. Guth
39. W. O. Harms
40. R. F. Hibbs (Y-12)
41. T. Hikido
42. A. Hollaender
43. A. S. Householder
44. H. Inouye
45. W. H. Jordan
46. C. P. Keim
47. M. T. Kelley
48. R. B. Korsmeyer
49. P. G. Lafyatis
50. J. A. Lane
51. R. S. Livingston
52. H. G. MacPherson
53. W. D. Manly
54. H. C. McCurdy
55. H. F. McDuffie
56. A. J. Miller
57. R. S. Miller
58. J. G. Morgan
59. K. Z. Morgan
60. J. P. Murray (Y-12)
61. F. H. Neill
62. M. L. Nelson
63. L. G. Overholser
64. P. Patriarca
65. F. S. Patton (Y-12)
66. A. M. Perry
67. M. E. Ramsey
68. M. W. Rosenthal
69. A. F. Rupp
70. G. Samuels
71. H. W. Savage
72. A. W. Savolainen
73-77. J. L. Scott
78. E. D. Shipley
79. O. Sisman
80. M. J. Skinner
81. G. M. Slaughter
82. A. H. Snell
83. C. D. Susano
84. J. A. Swartout
85. E. H. Taylor
86. D. F. Toner
87. D. B. Trauger
88. C. S. Walker
89. A. M. Weinberg
90. J. R. Weir
91. J. C. White
92. E. A. Wick
93. C. E. Winters
94-98. M. M. Yarosh
99. J. Zasler
100-173. Laboratory Records Department
174. Laboratory Records Department, ORNL, R. C.

175-178. ORNL — Y-12 Technical Library
Document Reference Section
179-181. Central Research Library

EXTERNAL DISTRIBUTION

182-184. W. F. Banks, Allis-Chalmers Mfg. Co.
185-187. P. D. Bush, Kaiser Engineers
188. E. Creutz, General Atomic
189-191. R. B. Duffield, General Atomic
192. T. Jarvis, Ford Instrument Co.
193. Richard Kirkpatrick, AEC, Washington
194-195. H. Lichtenburger, General Nuclear Engineering Corp.
196. J. P. McGee, Bureau of Mines, Appalachian Experiment Station
197. S. G. Nordlinger, AEC, Washington
198. H. B. Rahner, Savannah River Operations Office
199. Corwin Rickard, General Atomic
200. S. T. Robinson, Sanderson & Porter
201. M. T. Simnad, General Atomic
202. Donald Stewart, AEC, Washington
203. Philip L. Walker, Pennsylvania State University
204. R. E. Watt, Los Alamos Scientific Laboratory
205-206. W. L. Webb, East Central Nuclear Group, Inc.
207. Division of Research and Development, AEC, ORO
208-784. Given distribution as shown in TID-4500 (15th ed.) under Reactors — Power category (75 copies — OTS)